

## N O T I C E

THIS DOCUMENT HAS BEEN REPRODUCED FROM  
MICROFICHE. ALTHOUGH IT IS RECOGNIZED THAT  
CERTAIN PORTIONS ARE ILLEGIBLE, IT IS BEING RELEASED  
IN THE INTEREST OF MAKING AVAILABLE AS MUCH  
INFORMATION AS POSSIBLE

CR-152376

**FINAL REPORT**  
**PART 1 - SYSTEM DESCRIPTION AND ANALYSIS**

**FEASIBILITY STUDY FOR HELICOPTER/VTOL  
WIDE-ANGLE SIMULATOR IMAGE GENERATION  
DISPLAY SYSTEM**

N80-27397

Unclas  
24229

NOR 77-102

OCTOBER 1977

G3/09

**PREPARED FOR:**

US Army Air Mobility Research  
And Development Laboratory And  
National Aeronautics and Space  
Administration, Under Contract  
NAS2-9351

Ames Research Center  
Mountain View, CA 94035

**PREPARED BY:**

Northrop Corporation  
Aircraft Group - Aircraft Division  
Aerosciences Laboratory  
Hawthorne, CA 90250

(NASA-CR-152376) SYSTEM DESCRIPTION AND  
ANALYSIS. PART 1: FEASIBILITY STUDY FOR  
HELICOPTER/VTOL WIDE-ANGLE SIMULATION IMAGE  
GENERATION DISPLAY SYSTEM Final Report  
(Northrop Corp.) 198 p HC A09/MF A01



# FINAL REPORT NAS2-9351

## TABLE OF CONTENTS

1.0	INTRODUCTION	
1.1	General	
1.2	Study Objective	
1.3	Study Approach	
1.3.1	Analysis and Tradeoff Studies	
1.3.2	Subcontractor Participation	
1.3.3	Visits to Simulation Facilities	
2.0	SYSTEM DESCRIPTION	
2.1	General Technical Requirements	
2.2	Overview Of The Proposed System	
2.3	Detailed Image Generation Subsystem	
2.3.1	General	
2.3.2	Terrain Modelboard and Support Structure	
2.3.3	Gantry and Probe/TV Camera Support	
2.3.4	Optical Probe	
2.3.5	Probe Protection	20
2.3.6	TV Camera	
2.3.7	Model Lighting	
2.3.8	Gantry and Probe Servos	
2.4	Peripheral Image Generation Subsystem	
2.4.1	General	
2.4.2	Raster Graphics	
2.4.3	Interface	
2.5	Projection Screen	
2.5.1	General	
2.5.2	Screen Construction	
2.5.3	Screen Finish	
2.6	Detailed and Peripheral Display Subsystem	
2.6.1	General	
2.6.2	Projector Roll and Yaw System	
2.6.3	Projector Roll Servo	

- 2.6 Detailed and Peripheral Display Subsystem (continued)
  - 2.6.4 Detailed and Peripheral TV Projectors
  - 2.6.5 Projection Optics
  - 2.6.6 Variable Visibility Generation
  - 2.6.7 Head Slaved Yaw
- 2.7 Sky-Horizon Projector Subsystem
  - 2.7.1 General
  - 2.7.2 Sky-Horizon Projector Gimbals
  - 2.7.3 Transparency and Light Source
  - 2.7.4 Sky-Horizon Projector Servos
- 2.8 Test, Monitor, and Control Subsystem
  - 2.8.1 General
  - 2.8.2 Servo
  - 2.8.3 Video
  - 2.8.4 Interface
- 2.9 Cockpit and Visual Display Support Structure
  - 2.9.1 General
  - 2.9.2 Cockpit Support
  - 2.9.3 Screen and Sky-Horizon Projector Support Structure
  - 2.9.4 TV Projector Roll and Yaw Support
- 3.0 DEVELOPMENT PLAN
  - 3.1 Hardware Breakdown
  - 3.2 Cost Estimates
  - 3.3 Schedules
- 4.0 ANALYSIS AND TRADEOFF STUDIES
  - 4.1 Terrain Model and Probe Configuration
    - 4.1.1 General
    - 4.1.2 Modelboard Construction
    - 4.1.3 Model Surface Detail
    - 4.1.4 Probe Configuration
  - 4.2 Control System and Structural Analysis
    - 4.2.1 Gantry and Probe Servos
    - 4.2.2 Projector Roll Mechanism
    - 4.2.3 Sky-Horizon Projector Kinematics
  - 4.3 Probe Protection Design Analysis

59

73

79

125

- 4.4 Video System Tradeoffs
  - 4.4.1 Requirement For A Color Display
  - 4.4.2 TV Camera System Selection
  - 4.4.3 TV Projection System
- 4.5 Field-Of-View, Resolution and Display Brightness 163
  - 4.5.1 Field-Of-View
  - 4.5.2 Resolution
  - 4.5.3 Brightness
  - 4.5.4 Relative Illumination
- 4.6 Cockpit Related Visibility Studies
  - 4.6.1 Cockpit Configuration
  - 4.6.2 Visibility and Occlusions
- 4.7 Head Slaved Yaw
- 4.8 Conclusions and Recommendations 190
- 5.0 SUPPORTING DATA
  - 5.1 Design Data
  - 5.2 Subcontract Study Reports
    - ER580 Study of wide angle, multi-sensor, optical scanning probes for Helicopter Flight Simulation - Farrand Optical Company, Inc.
    - ER601 Optical Design Study 5.16" f/1.0  $\pm$  31.5° Projection Lens for Helicopter Simulator - Pacific Optical Division of Bourns, Inc.
  - 5.3 Conceptual Drawings\*
    - PD-100 General Arrangement
    - PD-101 Visibility Plot - Layout
    - PD-102 Cockpit Frame Occlusions - Layout
    - PD-200 Dome, 20 ft. AMRDL Helicopter Simulator Study
    - PD-300 Cockpit General Arrangement
    - PD-301 Cockpit Positioner Assembly
    - PD-400 Terrain Projector Assembly
    - PD-500 Projectors Support & Drive Mechanics Assembly

---

\* PD-702 and PD-703 are included in Section 4.0. All other drawings are provided as a separate data package.

PD-700 Terrain Model Gantry Assembly  
PD-701 Camera Carriage Assembly  
PD-702 Model Contour Map  
PD-703 Model Surface Detail  
PD-800 Sky/Horizon Projector  
PD-900 Image Generation and Display Electronics

#### References

#### Appendices

Appendix 1 Variable Visibility Specification  
Appendix 2 Component Data Sheets  
Appendix 3 Liquid Crystal Light Valve  
Appendix 4 Model Specification - J. Piper

### References

- (1) Feasibility Study for Helicopter/VTOL Wide Angle Simulator Image Generation Display System, Contract NAS2-9351.
- (2) Technical Proposal, Feasibility Study for Helicopter/VTOL Wide Angle Image Generation Display System, NB-76-14, Northrop Corporation.
- (3) Memorandum , Motion System Design Parameters, Memo No. SAVDL-AM-T, US Army Air Mobility Research and Development Laboratory.
- (4) Vought Systems of I V Aerospace Company. Study to Analytically Derive External Vision Requirements for U.S. Army Helicopters. U.S. Army AVSCOM Technical Report 73-1 November 1973.
- (5) Systems Research Laboratories Inc., Visual Simulation Video Processing Techniques, Technical Report AFHRL-TR-74-76, December 1974.
- (6) Farrand Optical Company, Inc., Wide Angle Infinite Depth-of-Field Optical Pickup for Visual Simulation, Technical Report AFHRL-TR-71-41, 1971.

## 1.0 INTRODUCTION

### 1.1 General

This report represents the results of Northrop's study and a conceptual preliminary design of a simulator for helicopter research and development. The study was performed for the United States Army Air Mobility Research and Development Laboratory under NASA Contract NAS2-9351.

### 1.2 Study Objectives

The objective of the study was to obtain a preliminary design for a Helicopter/VTOL Wide-Angle Simulator Image Generation Display System. It is understood that the visual system is to become part of a simulator capability to support Army Aviation Systems Research and Development within the near term (3 to 5 years). As required for the Army to simulate a wide range of aircraft characteristics, versatility and ease of changing cockpit configurations were primary considerations of the study. Also, because of the Army's interest in low altitude flight (5 - 10 feet above the terrain) and descents into and landing in constrained areas, particular emphasis was given to wide field-of-view, resolution, brightness, contrast, and color.

The visual display study includes a preliminary design, demonstrated feasibility of advanced concepts, and a plan for subsequent detail design and development.

### 1.3 Study Approach

The focal point of the study approach was a baseline concept to satisfy the general overall objectives. The baseline concept, founded on current technology consistent with Northrop's continuing interest in visual simulation, was considered obtainable in the near term (3 to 5 years).

The following major study activities were applied to elements of the baseline concept to produce a visual display system preliminary design.

### 1.3.1 Analysis and Tradeoff Studies

Analysis and tradeoff considerations for various visual system elements are outlined and discussed in Section IV. Isolation of major problem areas and feasibility demonstrations were part of the criteria for making tradeoff decisions.

### 1.3.2 Subcontractor Participation

Subcontractor reports and supporting data are included in Section V. Study subcontracts were let to Farrand Optical Company and Pacific Optical Company for the purpose of obtaining specifications and cost data. Specifications and data from other major visual display system suppliers are included in the appendices.

### 1.3.3 Visits to Simulation Facilities

During the course of the study the following simulator facilities were visited for the purposes listed:

#### Facility Visited

#### Purpose Of Visit

- |                        |  |
|------------------------|--|
| o Singer               | To discuss DIG system capabilities and observe demonstrations.   |
| o Evans and Sutherland | To evaluate deliverable Lufthansa CGI display system.  |
| o Farrand              | To evaluate contents of probe study<br>To evaluate chalricon TV camera and variable visibility system manufactured by SRL.<br>To discuss terrain model technology with Independence Scale Model. |
| o CAE Electronics      | Fly CH-47 simulator to evaluate non-tilt corrected probe.<br>Discuss probe protection techniques.  |
| o Fort Rucker          | To evaluate 2 B-31 and 2 B-33 model-boards and ARI model sections<br>To make NOE flight in UH helicopter   |

#### 1.3.4 In-depth Analysis and Preliminary Design Of The Proposed System

The conceptual design and analysis of the proposed visual display system is outlined and discussed in Sections II and IV respectively. The purpose of the analysis and design activity was to produce, within the allotted manhours, technically competent specification and preliminary design drawings. Together with backup data, design data, and basic assumptions, these specifications and drawings will define a feasible visual display concept. The concept and these criteria and specifications will provide a suitable basis for preparation of a program plan for the phased hardware development.

#### 1.3.5 Phased Plan For Development

A development plan is outlined and discussed in Section III. The plan includes a budgetary and planning estimate of direct charge labor hours, unburdened material costs, and schedules for the phased development of the visual display concept.

#### 1.3.6 Reporting

Monthly and oral progress reports were submitted as required. This document is the final report and summarizes all study related activity.

## 2.0 SYSTEM DESCRIPTION

### 2.1 General Technical Requirements

The basic aim of this study was to define performance specifications at the subsystem level with particular attention to display and motion performance of image generation and display devices.

This approach was taken because definition and measurement of quantitative criteria for overall system performance are difficult in terms of the integrated visual scene. In particular the end-to-end display position cannot be accurately specified. This is primarily because in the past the absolute accuracy of optical probes has not been critical and therefore has not been specified. Another parameter is end-to-end display resolution in terms of Modulation Transfer Function, (MTF), where it is difficult to design individual components that will combine to satisfy the requirements of a specified end-to-end MTF.

Major subsystem concepts have been established; motion characteristics and dynamic performance requirements have been defined; and system arrangement, location and gross sizing of components has been determined. In addition to performance specifications, some firm requirements for physical envelopes, mechanisms, components, arrangement, subsystem configurations, structural criteria, and visual display characteristics have been defined.

The results of this study do not establish a fully verified design. During the design phase (Phase II) a preliminary design period will be required to refine the analysis and integration of the configuration and concept covered in this study.

## **2.2 Overview Of The Proposed System**

The proposed Helicopter Simulator Visual System shown in Figure 2.2-1 is comprised of subsystems designed to provide a wide-angle, full color, high fidelity display of detailed terrain and background information. Two crew members are provided with an accurate analog of real-world type terrain generated by a Model-Probe-Camera system. The pilot's field-of-view for this display is  $120^{\circ}$  horizontal by  $60^{\circ}$  vertical. The total field-of-view is extended to  $200^{\circ} \times 60^{\circ}$  with synthetic terrain imagery generated by a computer graphics system.

A dual scale terrain model system shown in Figure 2.2-2 is utilized to provide an optimized gaming area for NOE and high altitude flight simulation applicable to Helicopter Research and Development. The sythetic imagery provides attitude, altitude, and motion cues in the pilot's peripheral field-of-view.

Imagery generated by the terrain model system and the computer graphics system are displayed to the crew members on a 20 foot diameter dome type projection screen. The display system general arrangement is shown in Figure 2.2-3. The imagery is projected on the screen by five identical television projectors mosaicked to provide a  $200^{\circ} \times 60^{\circ}$  field-of-view. The three central projectors receive information from three mosaicked television cameras viewing the terrain model. The two peripheral projectors receive information generated by the computer graphics. A synthetic blue sky is generated by video special effects circuitry included in the television projector electronics.

A background display comprised of a blue sky and continuous horizon is provided by a gimbaled point light projection system. This provides an extended horizon when flying over relatively flat terrain, and attitude cues for high altitude flight simulation.

Simulation of Helicopter motions in the visual scene are produced by a servo driven gantry, optical probe, and projection heads. Translational and altitude motions are provided by the gantry with pitch and yaw motion being provided by the probe. Roll motion is produced by combining roll of the probe with roll

# AIR MOBILITY SIMULATOR BASELINE CONCEPT

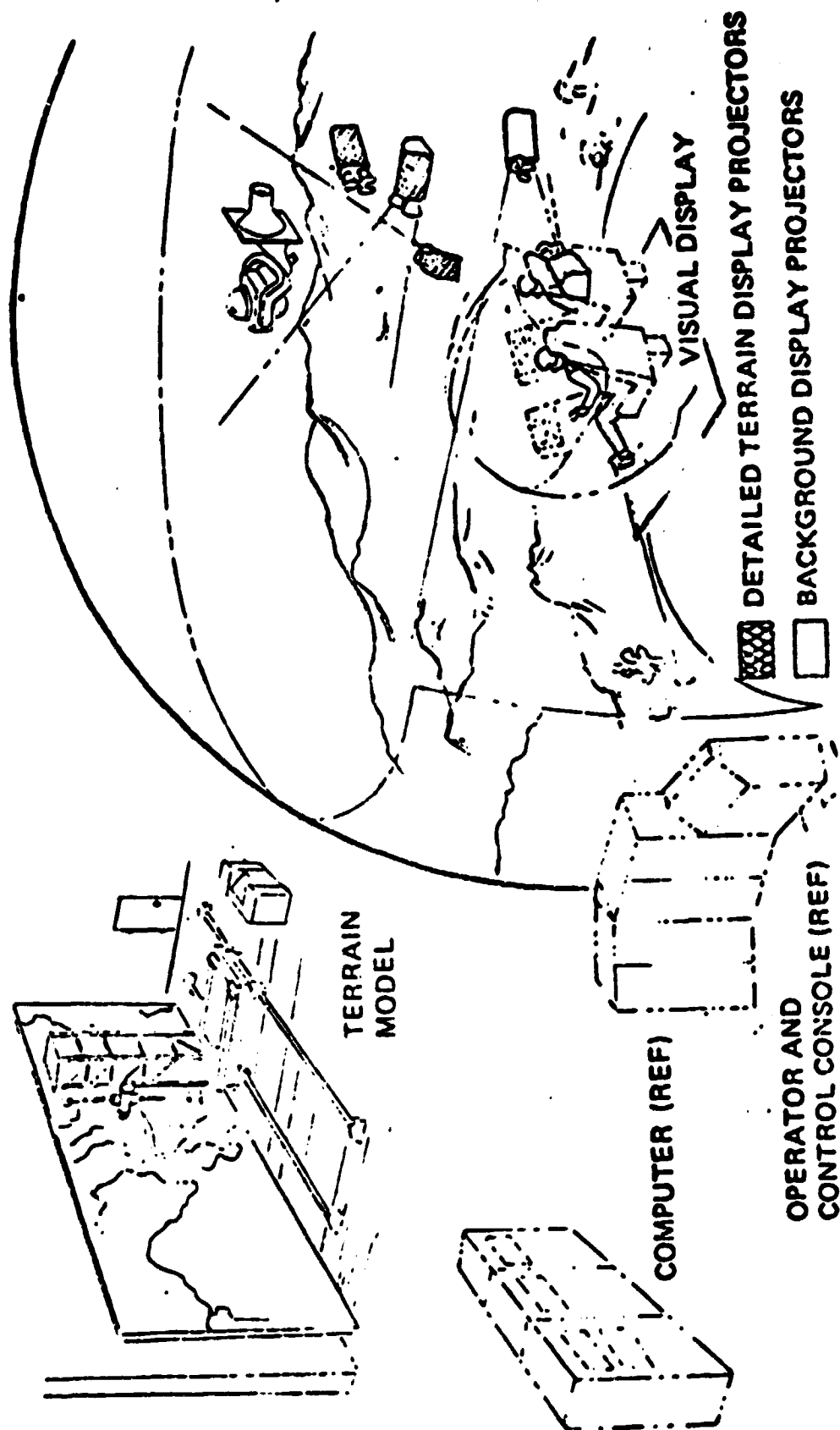


FIGURE 2.2-1 VISUAL SYSTEM BASELINE CONCEPT

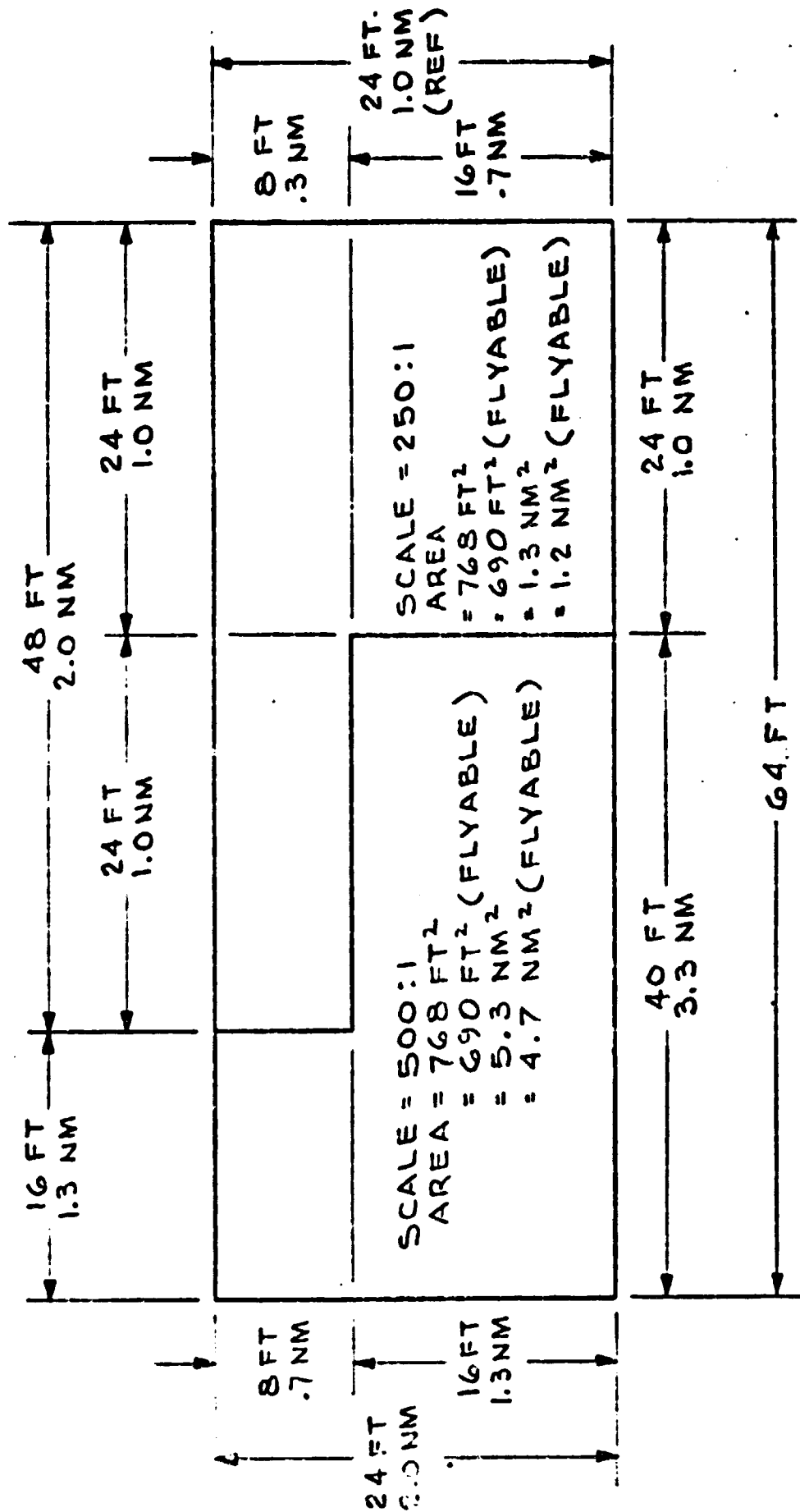


FIG 2.2-2 TERRAIN MODEL GENERAL ARRANGEMENT

- SIZE
- SCALE
- AREAS

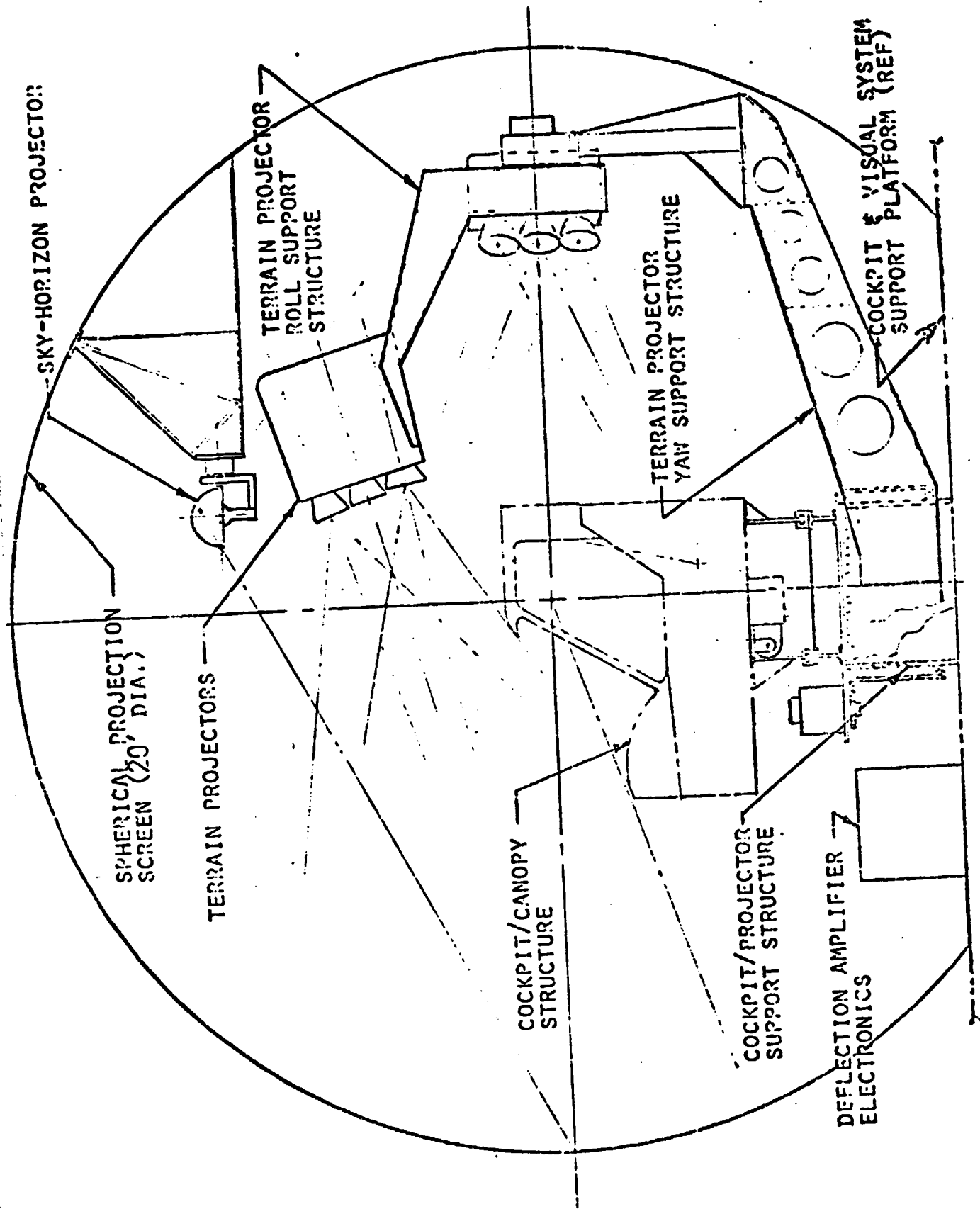


FIGURE 2.2.3 DISPLAY SYSTEM GENERAL ARRANGEMENT

of the television projector heads. Projector roll is utilized to increase the vertical field-of-view in roll maneuvers for low altitude and NOE flight simulation. In this configuration aircraft roll is limited to  $\pm 90^\circ$ . For tasks requiring continuous aircraft roll, the roll motion is produced solely by the optical probe.

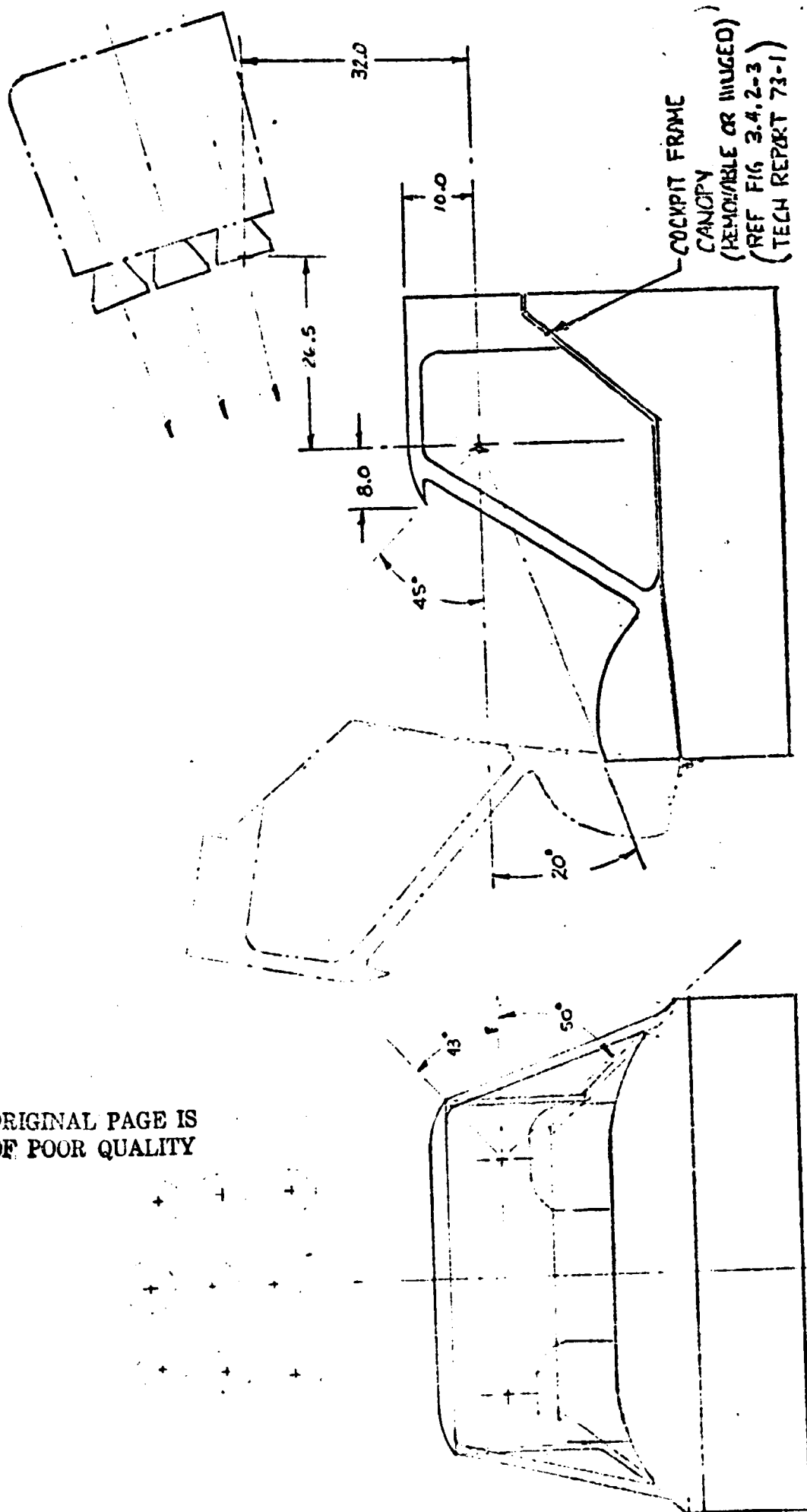
An Area-Of-Interest (AOI) system tracks the pilots head motion in azimuth and slaves the detailed imagery to the pilots line of sight. This technique permits viewing of detailed information out to  $\pm 100^\circ$ .

The cockpit and visual display support system is designed to accomodate two crew members in a side-by-side seating arrangement shown in Figure 2.2-4. An automatic cockpit positioning mechanism is used to position the viewpoint of either crew member to the screen center. The cockpit, screen, and projector support structures are mounted on a base structure designed to interface with a simulator motion base.

A test, monitor, and control console provides for rapid daily checkout, fault isolation, and local control of the Video and Servo equipment.

The following tables summarize the overall system performance characteristics. Table 2.2-1 compares the display system performance goals of the statement of work with the predicted performance of the conceptual system. Table 2.2-2 compares the desirable aircraft flight performance envelope from the statement of work with predicted system performance. Table 2.2-3 summarizes the nominal motion base performance established by USAAMRDL, and Table 2.2-4 summarizes the display system weights and inertias.

ORIGINAL PAGE IS  
OF POOR QUALITY



(PD-102 REF.)

COCKPIT FRAME - GENERAL ARRANGEMENT

FIGURE 3.2-1

TABLE 2.2-1 DISPLAY SYSTEM PERFORMANCE

PERFORMANCE PARAMETERS	SOW DESIGN GOAL	PREDICTED END-TO-END PERFORMANCE
<b><u>DETAILED DISPLAY</u></b>		
Resolution		
o Center (Arc Min/OLP)	4	9 Limiting On Axis
o Edge (Arc Min/OLP)	4	11 Limiting At $\pm 60^\circ$
Field-Of-View (Deg)	180H x 60V	120H x 60V
Luminance (Ft.-L) (*)	8	5.5/8 Average Scene Highlight
Contrast Ratio	20:1	15:1 Probe Limit
Color	Yes	Yes, RGB Color
Refresh Rate (No/Sec)	60	30 TV/Frames (60 Fields)
Lag (Sec)	.05	.05 @ 20% (Camera Tube)
Position Accuracy (Deg)	0.3	0.3 Final Design Goal
Geometric Distortion (%)	<1.0	<2.0
<b><u>BACKGROUND DISPLAY</u></b>		
Field-Of-View (Deg)	240H x 160V	200H x 60V Peripheral TV >240H x 160V Sky-Horizon
Luminance (Ft-L) (*)	8	5.5/8 Peripheral TV 0.5 Sky-Horizon
Contrast	10:1	>10:1 Peripheral TV N/A Sky-Horizon
Refresh Rate (no./Sec)	30	30 Raster Graphics 30 TV Frames (60 Fields)
Lag (Sec)	0.1	<0.1
Position Accuracy (Deg)	1.0	<1.0 Design Goal Raster Graphics <1.0 Sky-Horizon

\* Minimum highlight luminance is 5.5 ft. lamberts using an f/1.2 projection lens and 8 ft. lamberts using an f/1.0 projection lens.

7.2-14 147

TABLE 2.2-2 AIRCRAFT FLIGHT PERFORMANCE ENVELOPE

Parameter	SOW Desirable Performance	Predicted Performance
Altitude, Min/Max (Ft.)	5/1000	7.1/1000 scaled 250:1. 14.2/2000 scaled 500:1
Maneuvering Area	3NM x 2NM = 6NM <sup>2</sup>	1.17NM <sup>2</sup> scaled at 250:1, 4.67NM <sup>2</sup> scaled at 500:1. Total area = 5.8NM <sup>2</sup>
Velocity Horizontal (knots)	250	250 kts scaled at 250:1. 500 kts scaled at 500:1
Velocity Vertical (Ft./Sec.)	50	50 Ft./Sec scaled at 250:1, 100 ft/sec scaled at 500:1
Acceleration (G's)	3	3g's scaled at 250:1, 6g's scaled at 500:1.
Pitch Excursion (degrees)	+ 90	Sky-Horizon proj. + 70°, Optical probe + 30°, -60°, Graphics +75°
Pitch Velocity (degrees/sec)	+ 60	+ 60
Pitch Acceleration (degrees/sec <sup>2</sup> )	+ 100	+ 100
Roll Excursion (degrees)	Continuous	+ 45° with proj. roll only, + 90° with combined proj. roll and probe roll, continuous with probe roll only +180° for sky-horizon proj.
Roll Velocity (deg/sec)	+ 100	+ 100
Roll Acceleration (deg/sec <sup>2</sup> )	+ 150	+ 150
Heading Excursion (degrees)	Continuous	Continuous
Heading Velocity (deg/sec)	+ 100	+ 100
Heading Acceleration (deg/sec <sup>2</sup> )	+ 100	+ 100

TABLE 2.2-3 MOTION BASE NOMINAL PERFORMANCE

	SURGE $x_c$	SWAY $y_c$	HEAVE $z_c$	PITCH $\theta_c$	ROLL $\phi_c$	YAW $\psi_c$
Displacement Ft - Rad	$\pm 4$	$\pm 12$	$\pm 8$	$\pm 0.3$	$\pm 0.3$	$\pm 0.4$
Velocity Ft/Sec-Rad/Sec	$\pm 4$	$\pm 8$	$\pm 6$	$\pm 0.5$	$\pm 0.5$	$\pm 0.6$
Acceleration Ft/Sec <sup>2</sup> -Rad/Sec <sup>2</sup>	$\pm 10$	$\pm 10$	$\pm 10$	$\pm 1.0$	$\pm 1.0$	$\pm 1$
Dynamic Response	The dynamic response of each axis will approximate that of a second-order system with an undamped natural frequency of 3 Hz and a damping ratio of 0.7.					

TABLE 2.3-4 VISUAL DISPLAY SYSTEM WEIGHTS &amp; INERTIAS

VISUAL DISPLAY SYSTEM COMPONENTS	WEIGHT (POUNDS)	INERTIAS AT THE SCREEN CENTER (SLUG. FT. <sup>2</sup> )		
		$I_x$	$I_y$	$I_z$
Sphere	1400	2560	2560	2900
Other (*)	f/1.2 Lens	3100	4580	2970
	f/1.0 Lens	3655	5270	3465
TOTAL	f/1.2 Lens	4500	7140	5870
	f/1.0 Lens	5055	7830	6365

(\*) Does not include cockpit or cockpit and visual system support platform. Individual components are tabulated in section 5.1.

## 2.3 DETAILED IMAGE GENERATION SUBSYSTEM

### 2.3.1 General

The detailed terrain image generation subsystem is comprised of a dual scale three dimensional modelboard, gantry, wide angle multiple sensor optical probe, and a multiple TV camera system. The image from the probe is split off to three high resolution color TV cameras. The gantry is servo controlled to translate the probe/camera package over the modelboard.

The following paragraphs describe the major components of the detailed image generation subsystem.

### 2.3.2 Terrain Modelboard and Support Structure

#### Terrain Modelboard

The Terrain Modelboard, as required to simulate missions involving low altitude nap-of-the-earth (NOE) flight and descents into and landing in constrained sites, is required to be an accurate analog of the real world. The recommended modelboard is the type produced by John Piper, Ltd.

The proposed modelboard is comprised of forty-eight (48) 4 X 8 foot panels joined and edge-matched to form a continuous 24 X 64 foot terrain scene. The contour intervals and scene detail are shown on drawings PD702 and PD703 respectively. The modelboard surface is equally divided into two primary gaming areas: a 1:250 scale (rough terrain) and a 1:500 scale (smoother) general terrain area. The general arrangement, in terms of scale, area and size, is shown in Figure 2.2-2.

The boundary of the 1:250 scale NOE area is formed by utilizing higher elevations. Three saddle type passes are included to allow continuous flight between the two areas. A reflective aluminized mylar surface extends around the outer perimeter of the 1:500 scale general terrain area to a height of approximately 12 inches for the purpose of providing the illusion of extended terrain.

The scene detail provides the pilot with realistic velocity, altitude, attitude, and range cues. The scenery, particularly around very low altitude flight areas (NOE routes, stage fields, confined landing areas, pennacle, etc.) is to be modeled to maintain proper perspective relative to general terrain features and objects of known size.

The terrain scene depicts a generalized rural countryside and includes both rough and rolling terrain, wooded areas, a river, roads, a railroad, and buildings. The trees are to be modeled as highly realistic individual free-standing units. The ground texture is to be modeled with particular attention paid to scale and realism. The scene also includes scrub fields, cultivated plowed fields, and fields with crops. The buildings are to be modeled with special attention paid to scale and realism. The scene includes liberal use of fences, telephone poles, water towers, etc.

In addition, the following general requirements apply:

- (1) Seams - All seams to be indistinguishable at the final display.
- (2) Gradient - The maximum terrain gradient of any hard object is 45 degrees.
- (3) Altitude - The maximum altitude of any object on the terrain board is 1.2 feet above the minimum probe altitude.
- (4) Material - The modelboard is to be constructed of materials which provide a coefficient of linear expansion/ $^{\circ}$ C of less than  $10 \times 10^{-6}$  (i.e. epoxy/filler and glass layup).

The overall quality of the modelboard is to be established by two quality standards (250:1 and 500:1). These standards will become part of the criteria for the modelboard acceptance tests.

#### Support Structure

The modelboard structure, shown on drawing PD704, is approximately 26.5 X 66.0 foot overall, and is designed to permit a free-standing vertical installation with minimum interface with the facility. The support structure is comprised of eight (8) similar weldments - approximately 12.0 X 26.5 foot each. The weldments are constructed primarily of 5.0 X 5.0 inch and 2.5 X 5.0 inch steel tubing interlaced with 3.0 X 3.0 inch steel angle. The support structure has sufficient strength and rigidity to ensure that no perceptible movements or vibrations, or changes in alignment occur.

The structure is designed to be compatible with the eight point modelboard attachment described in the above paragraphs and allows free access to all modelboard edges for seaming.

### 2.3.3 Gantry and Probe/TV Camera Support

#### Gantry

The gantry, shown on drawing PD700, is a rigid steel tubular weldment structure (approximately 30 feet high) designed to support and translate the Probe/TV Camera package over the vertically mounted terrain modelboard. The required gantry translations are as follows (overtravel not included):

- . Longitudinal (X-axis)      60 feet
- . Lateral (Y-axis)            23 feet
- . Altitude (Z-axis)          4 feet

The gantry is supported from beneath by a pair of round way bearing assemblies on a single 65 foot long ball bushing shaft, and from above (and to the rear of the modelboard) on a single round way bearing assembly (tilted 30 degrees from the vertical) on a second parallel 65 foot long ball bushing shaft. A dc-torque motor/tachometer package, supported at the base of the gantry, provides longitudinal (X-axis) gantry translation by driving a spur gear against a gear rack mounted to the ball bushing shaft support structure.

The probe/camera package, mounted to a carriage on the side of the gantry, is mechanized for vertical (y-axis) translation (lateral across the modelboard). The carriage is supported on vertical shafts by pairs of ball bushings and cam follower assemblies. A dc-torque motor/tachometer package, mounted on the top of the gantry, drives the probe/camera carriage and counterbalance weight (located on the opposite side of the gantry) by a sprocket and closed-loop chain system.

Tachometers and gear driven potentiometers are mechanized in each axis to provide feedback inputs to the servo control system.

### Probe/TV Camera Support

The probe/camera carriage assembly is shown on drawing PD701. A platform, supported on the gantry vertical (Y-axis) translation system, provides support for both the altitude(Z-axis) translation system and the probe quick retract mechanism. The support structure is primarily a welded aluminum structure.

The platform is supported by four ball bushings on a pair of ball bushing shafts. A dc-torque motor/tachometer package, supported from the platform, provides altitude (Z-axis) carriage translation by driving a spur gear against a gear rack mounted to the ball bushing support structure. The tachometer of the drive package and a gear driven potentiometer provide feedback inputs to the servo control system.

The probe quick-retract mechanism utilizes an air cylinder drive and solenoid actuated release concept to operate in a fail-safe mode. Retraction of one foot is achieved in .065 seconds, and is compatible with probe protection requirements.

#### 2.3.4 Optical Probe

The Optical Probe will be a modification of a current design having a circular FOV of 120 degrees. The probe will be the non-tilt corrected type with the circular field-of-view expanded to 140 degrees. The probe will provide pitch, roll and yaw scanning and slant range focus. The single 140 degree circular field will be divided, by a single beamsplitter, to provide each of the three television cameras with an equal portion of the input field of view.

The probe characteristics are described in the following paragraphs.

##### Optical Characteristics

- (1) Field-Of-View - The input field-of-view will be 140 degrees circular and will be unobstructed and unvignetted.
- (2) Entrance Pupil Diameter - Diameter will be 1.0  $\pm$  0.05 mm.
- (3) Entrance Pupil-to-Modelboard Distance - 6.2 mm altitude at zero degrees pitch with a prism to modelboard clearance of 2.0 mm.
- (4) Slant Range Focus - 20 mm (or 32 feet at 500:1 scale) to infinity.
- (5) Relay Optics - Compatible with 17.1 mm sensor diagonal or approximately 8% overscan of a 15.9 mm standard sensor diagonal.
- (6) Relative Aperture - Approximately f/13.
- \* (7) Resolution (MTF) - 5 Arc Min/OLP at 50% relative amplitude on axis and 10 Arc Min/OLP at 50% over  $\pm$  35 degrees. Limiting resolution will be better than 7 Arc Min/OLP at 10% over  $\pm$  70 degrees.
- (8) Contrast Ratio - 15:1
- (9) Transmission - 45% for the basic optical probe and 47% for the multi-sensor beamsplitter to provide a total transmission of 21%.
- \* (MTF) refers to Modulation Transfer Function  
(OLP) refers to Optical Line Pairs

### Physical Characteristics

- (1) Size - The probe head diameter will not be greater than 1.5 inches measured along the pitch axis. Configuration of the probe head will be consistent with the outline profile shown in Figure 13 of the Farrand probe report ER-580 included in Section V.
- (2) Scan System - The scan system will have continuous roll and yaw and a pitch range of +30 and -60 degrees.
- (3) Visibility Limit - Up visibility of the probe will be limited to +15 degrees to insure that the sensors do not see the model lights.

### 2.3.5 Probe Protection

Probe protection is accomplished by using a computer modeling approach. The system design uses a small computer system designed to provide the needed protection while intruding very little on desired simulator operating characteristics. The computer memory can store the maximum elevations of a great many partitions. In fact, two to five hundred thousand partition elevations may be reasonably stored in memory. This would permit mapping down to grid spacing in the neighborhood of one-half to one inch. Close spacing can be used in areas of high relief and looser spacing can be used in relatively flat areas. In addition the model can be built with dual scaling to provide one area suitable for nap of the earth flight and a larger area suitable for more extended operations.

A system can be designed following this approach which would give full protection in normal operation and foreseeable abnormal operation or gantry drive hardware failure.

The conceptual design is shown in block diagram form in Figure 2.3.5-1. The gantry drive subsystem would provide translational position and rate information to the probe protect subsystem. This would be provided in parallel analog form by scaling and buffering the gantry servo linear position and rate feedback elements. The signals would then be multiplexed and converted from analog to digital form. The CPU would then use this current position and velocity data to predict the probe flight path for the next few tenths of a second. The CPU would compare this extrapolated flight path with a finely quantized elevation map of the terrain model to determine if any interference could occur. The program would take into account the various uncertainties of measurement, quantization effects, servo failure effects, and terrain board stability to give worst case protection. The computer memory is shown divided between program and data. This was done to highlight the relative storage requirements. The program would require at most a few thousand (16 bit) words of memory, certainly not more than 8K. The data memory, however, to map the terrain adequately in terms of resolution should store at least five hundred thousand (8 bit) bytes. This is based on storage of the elevation of each square in the grid in a single byte. This is desirable to keep the data memory size within reasonable bounds. Bulk core in 256K Byte modules is considered the best current compromise for the data memory. Disks or drums, although much larger and less expensive per bit, must be ruled out as having grossly

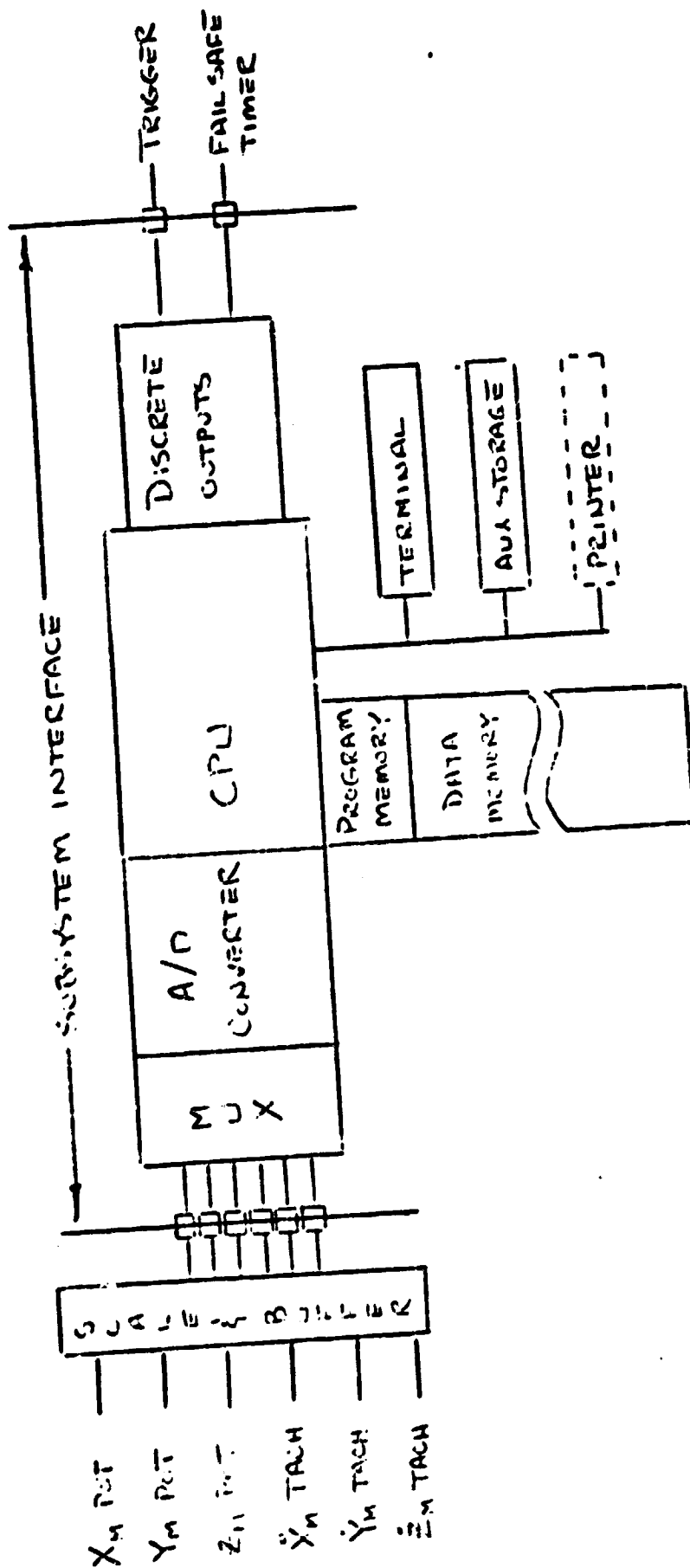


Figure 2.3.5-2

Probe Protection Conceptual Design Block Diagram

inadequate random access response times. OCDs and bubbles are also currently too slow and not available in large modules easily interfaced to existing minicomputers. Depending on the time frame of hardware selection, there is a small chance that one of these technologies might prove useable for the data memory.

The CPU would upon discovery of an incipient crash, set a discrete control line to activate the trigger release for the retract mechanism. Reasonable steps should be taken to fail-safe the protect subsystem itself for the most likely failures. The computer could integrate the rate signals each frame and compare them to increments of position inputs to detect most failures of the gantry transducers and associated electronics. Also two trigger lines driven by different parts of the program with coding appropriate for use with a fail-safe watchdog timer would protect against foreseeable computer failures. Some small auxiliary storage would be required to reload either program or data memory in the event of computer hardware failure. A terminal and perhaps a printer would be required for program development, terrain data editing, subsystem testing and troubleshooting. An overview of the basic program structure, without embellishments such as fail-safing, is given in flowchart form in Figure 2.3.5-2. A performance analysis was performed and is included in Section 4.3. This analysis was done to assure adequate worst case performance by providing design information on tradeoffs of computer program frametime, trigger release time, and maximum terrain gradient against minimum terrain clearance allowable before retract. Assumed system design parameters and the effect of scaling are given in Table 4.3-1.

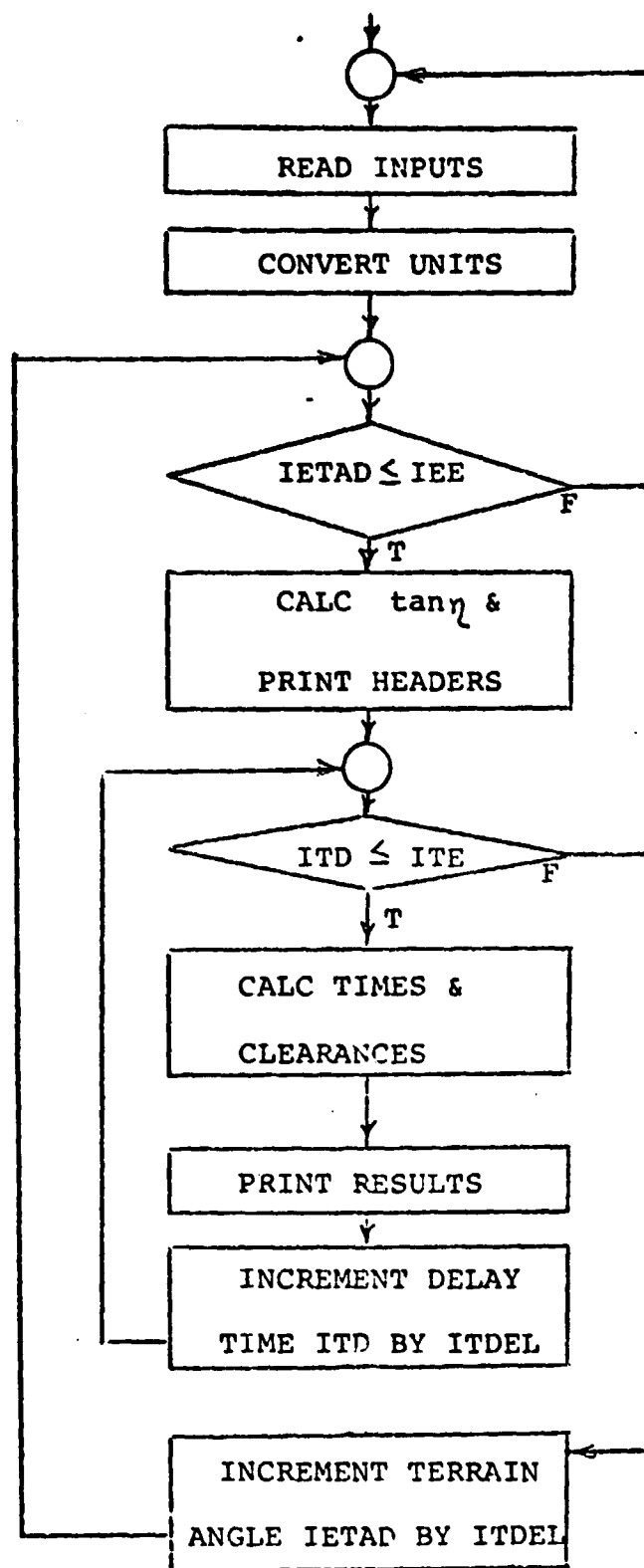


Figure 2.3.5-2

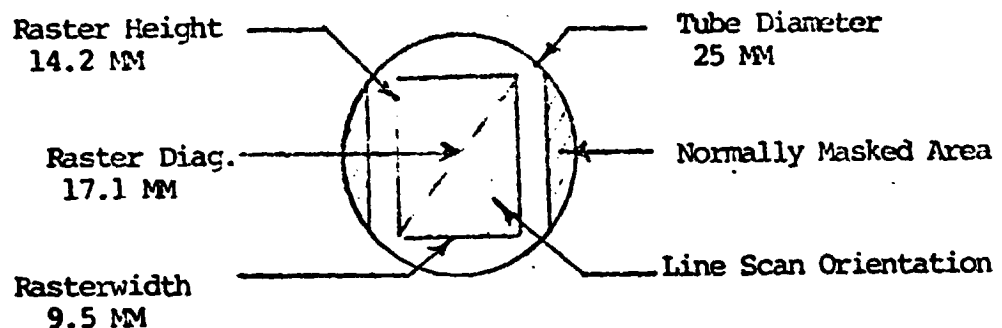
Probe Protection - Basic Program Structure Flowchart

### 2.3.6 TV Camera

Each color camera will view a segment of the wide angle image picked up by the optical probe. The image is converted to three parallel channels of red, green and blue (RGB) video. Color separation is accomplished with beam splitting dichroics and relay optics contained in the camera head.

#### Camera Performance

- (1) **Raster Scan** - The camera will be capable of operating at a line rate of 1023 line/frame to 1225 lines/frame, 30 frames/second at 2:1 interlace. The camera tube assemblies will be oriented such that the scan lines are perpendicular to the horizon in level flight.
- (2) **Aspect Ratio** - The raster height nominally will be approximately 1.5 times the raster width and will be adjustable to provide a 1:1 aspect ratio.
- (3) **Camera Tube and Format** - The camera tube will be a 25 mm Chalnicon which has a specified format of 9.5 X 12.7 X 15.9 mm. The diagonal will be expanded to have the format shown below.



- (4) **Resolution** - Limiting center resolution will be 800 TV lines/display width and 1200 TV lines/display height when operating at the nominal line rate of 1023 lines/frame.

- (5) Video Response - Bandwidth of the video amplifiers will be 27 MHz  $\pm$  1DB with a signal to noise ratio of 40 DB peak signal to RMS noise.
- (6) Grey Scale - 10 shades will be discernible
- (7) Shading - less than 10%
- (8) Video Outputs - One non-composite output for each color channel of 1.0 VPP into 75 ohms, with each output level being adjustable.
- (9) Sync Generation - A single multi-line rate sync generator will generate H drive, V drive, mixed sync and mixed blanking in accordance with EIA specification RS-343. Each output of the sync generator will be applied to a pulse distribution amplifier (PDA) and each camera will be provided with isolated sync outputs from the PDA.
- (10) Color Registration and Raster Shaping - Color registration will be accomplished by applying independent sweep correction signals to the linear sweep circuits of each color channel. In addition, raster correction signal adjustment will be provided in each camera, and will have sufficient range to correct for the F $\theta$  mapping distortion introduced by the optical probe. Typical adjustment ranges, expressed as a percentage of picture width relative to a linear raster, are as follows:
 

Size	$\pm$ 5%
Position	$\pm$ 5%
Linearity	$\pm$ 5%
Linearity Offset	$\pm$ 20%
Pincushion/Barrel	$\pm$ 5%
Pincushion/Barrel Offset	$\pm$ 10%
Curvature	$\pm$ 2%
Curvature Offset	$\pm$ 2%
Keystone	$\pm$ 2%
Orthogonality	$\pm$ 2%
"S"	$\pm$ 2%

- (11) Registration Accuracy - Registration of the three color channels will be within 0.1% over the picture width. Long term stability after warmup will be 0.1% with a goal of 0.05%.
- (12) Color Separation Optics - The dichroic beamsplitters and relay optics will be contained within the camera head. Efficiency and stability of the optical components will be a critical design requirement. A design goal for transmission of white light through the beamsplitting optics will be 40%.
- (13) Physical Camera Size - The size of each camera head will be 5.25 x 8 x 15 inches. The camera control unit and raster correction control panel will mount in a standard 19 inch equipment rack.

### 2.3.7 Model Illumination

The model illumination to be provided will be consistent with the probe transmission of 21% and camera tube sensitivity of  $0.25 \text{ lm/ft}^2$  after color separation. With an average model reflectance of 50% the model illumination required is  $1375 \text{ lm/ft}^2$ .

#### Model Lamps

A total of 96 lamps will be placed in a 6 x 16 matrix with equal spacing between the lamps. The lamp assemblies will be located 20 feet from the model surface, and each assembly will contain a 2000 watt 750 hour tungsten-Halogen lamp. The reflector assembly will have a 40 degree beamwidth at 50% light intensity, and a center illumination of  $125 \text{ lm/ft}^2$ . The total illumination provided by the lamp bank will be  $1380 \text{ lm/ft}^2$  for the 24 x 64 foot modelboard.

#### Probe Fill Lighting

Fill lighting will be accomplished with four 2000 hour 75 watt tungsten-halogen lamps. At specified wattage they will provide a total light output of 6400 lumens at a color temperature of  $3000^\circ\text{K}$ . Lamp voltage will be adjustable such that light output can be varied between 4800 and 11,000 lumens with a color temperature of  $2800^\circ\text{K}$  to  $3200^\circ\text{K}$  respectively.

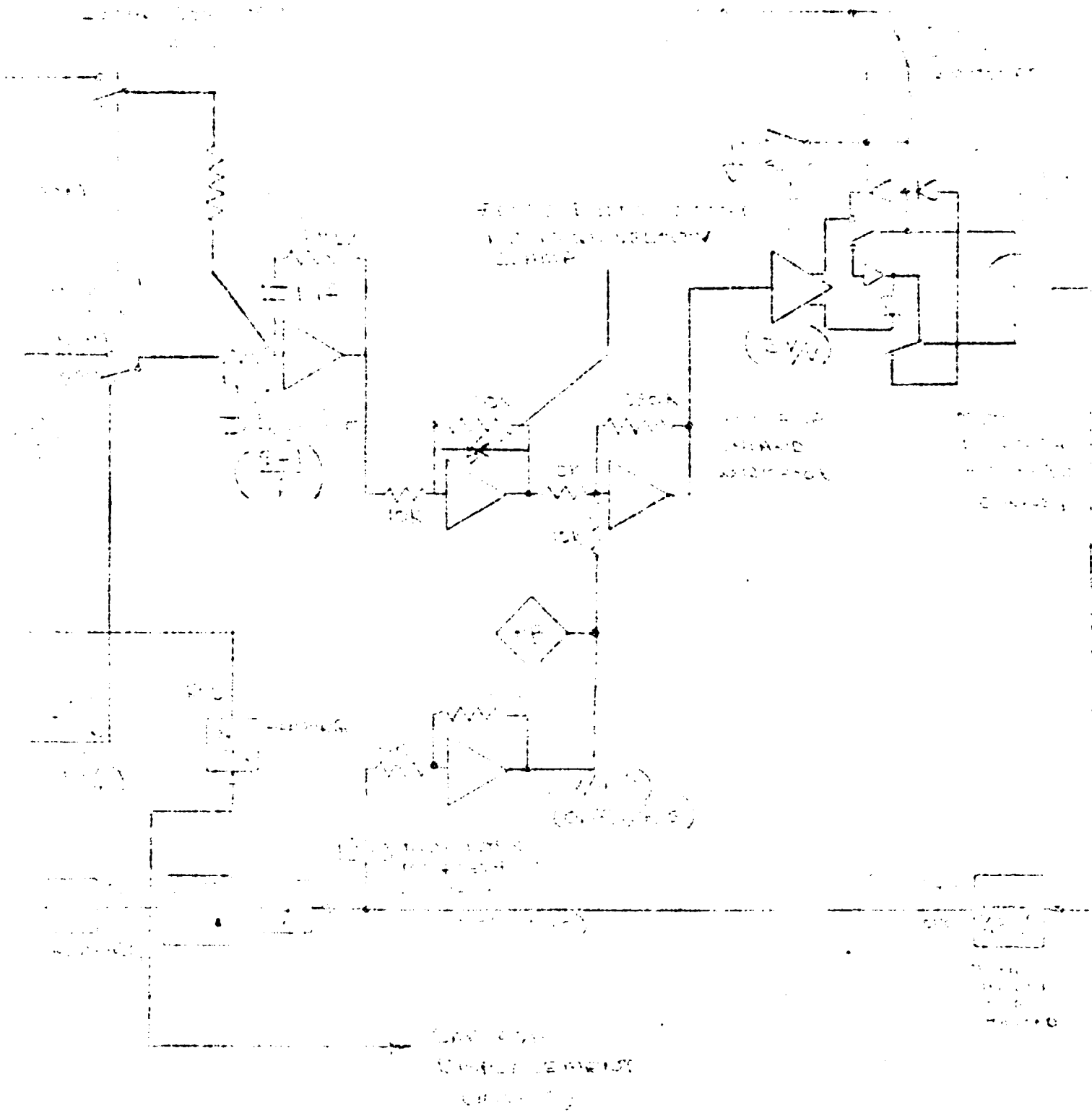
### 2.3.8 Gantry and Probe Servos

#### Gantry Servos

The gantry servos position the optical scanning probe over the terrain model in a rectilinear coordinate system. The servos and the corresponding motions are identified successively in order  $X_M$ ,  $Y_M$ , and  $Z_M$  proceeding from the fixed floor axis to the optical probe.

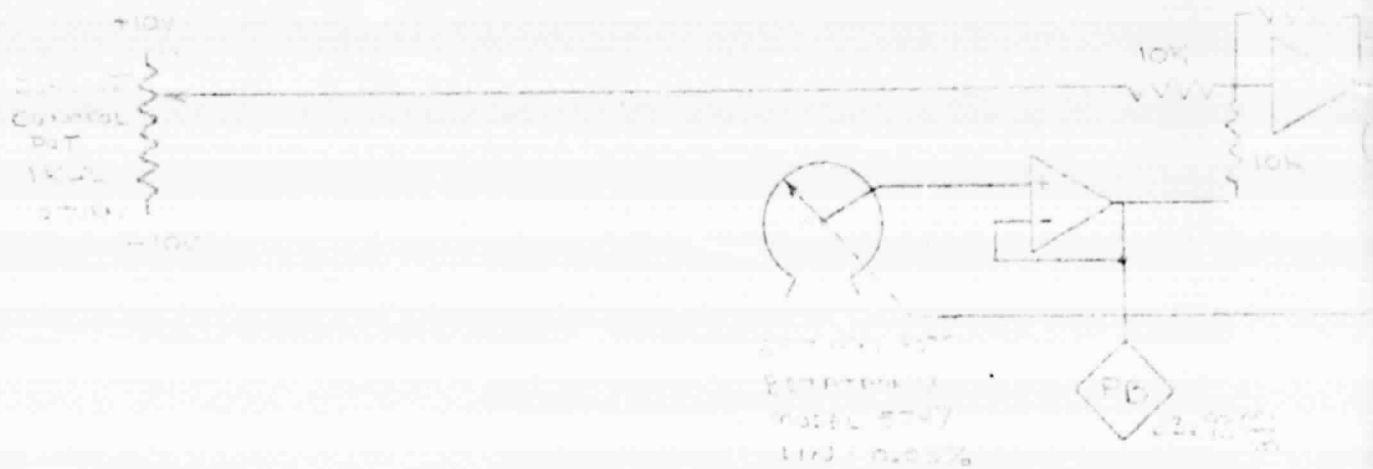
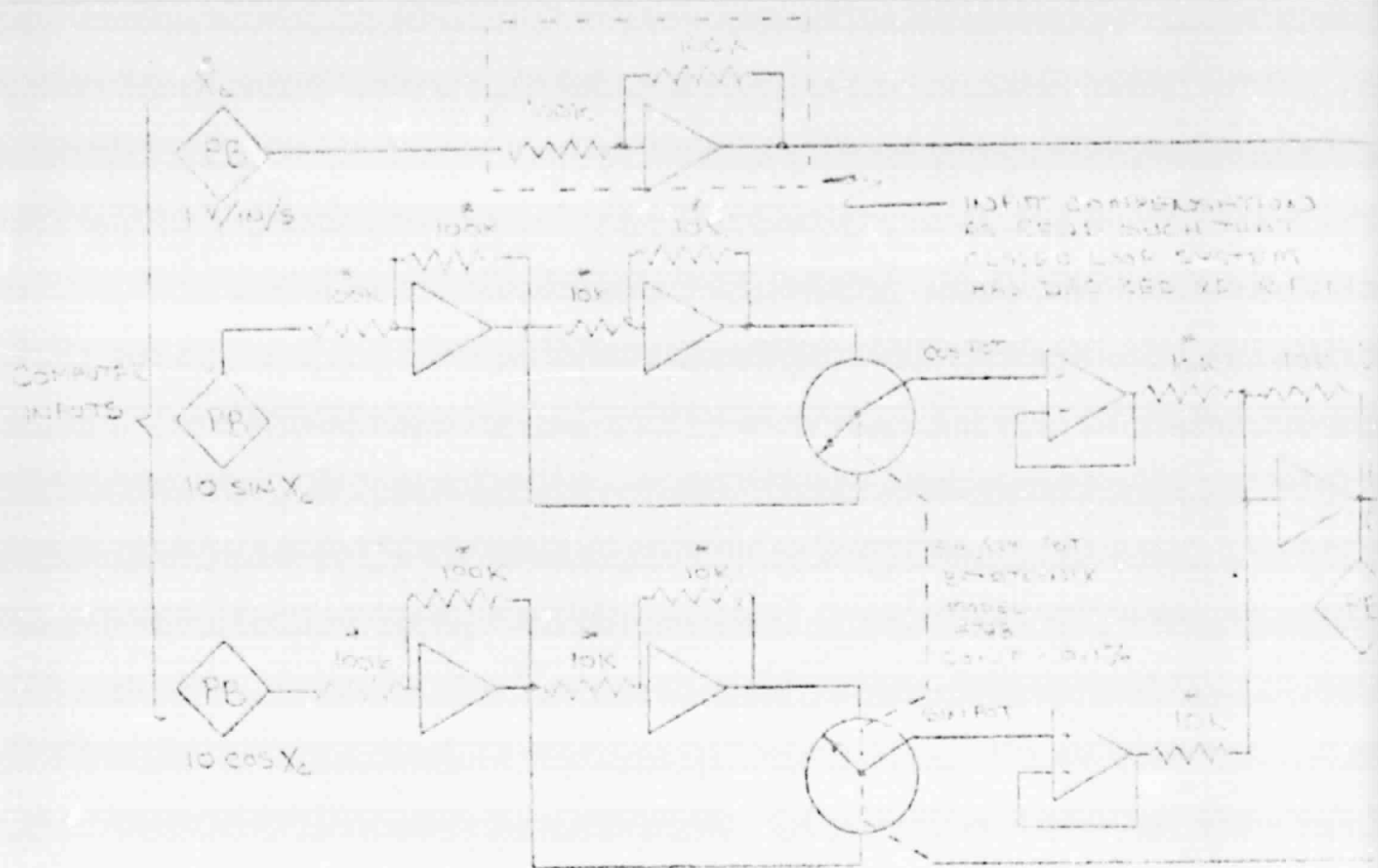
The inputs to each X, Y, or Z servos is a continuous sine/cosine voltage command from the computer. High quality rate commands are also provided for velocity feed-forward connections. The output of the X-servo is the relative motion along the X-axis between the X-carriage and the fixed floor structure. The output of the Y-servo is the relative motion along the Y-axis between the Y-carriage and the X-carriage. The output of the Z-servo is the relative motion along the Z-axis between the Z-carriage and the Y-carriage. Each gantry servo will be capable of achieving simultaneously aircraft maximum velocity and maximum acceleration shown in Table 2.2-2 ratioed by the terrain model scale of 250:1. The design of each gantry servo will incorporate electronics such that these maximums can not be exceeded. This provision is required so that the probe protection system (paragraph 2.3.5) does not have to contend with excessive probe translational motions. The ability to hold the maximum acceleration up to the maximum velocity is necessary so that the system does not transverse too much terrain in obtaining initial simulation velocity conditions. The basic closed loop system for the gantry servos is shown in Figure 2.3.8-1. The servo consists of two alternate position loop closures. A sine/cosine position closure is used in the computer mode of operation for increased accuracy performance. A standard linear multiturn feedback potentiometer closure is used in the local control mode of operation. Initial gantry positioning, at the beginning of a simulation run, is performed in the computer mode by commanding the computer to apply zero input to the sine/cosine potentiometer and driving the system with the rate command. When the gantry is near the desired position (monitoring the linear multiturn potentiometer) the correct sine/cosine commands are applied and the velocity command removed.

A single electric torque motor on each axis is capable of providing the required gantry power. Each motor is sized for twice the required velocity and twice the torque required to accelerate the gantry at its maximum and to overcome friction. The power amplifier driving the torque



100-1  
 100-1000-1-10000  
 100-1000

ORIGINAL PAGE IS  
 OF POOR QUALITY



All resistors are 0.05% ; 10 ppm/°C

All amplifiers are Burr Brown 3500C

FIGURE

X-RAY GAMMA 2500

ORIGINAL PAGE IS  
OF POOR QUALITY

motor is then current limited to a torque which is needed to overcome friction and produce the maximum required acceleration.

The gantry velocity will be limited to the maximum required velocity. This velocity clamp is achieved by clamping the voltage out of the amplifier summing the output of the integrator and the computer velocity command (see Figure 2.3.8-1). When the output of this amplifier becomes clamped the system becomes a velocity servo with a fixed input. The value of the clamped voltage is set by selected zener diodes.

1. Output operating envelope.

- |                          |                                      |
|--------------------------|--------------------------------------|
| a. Displacement:         | 60 feet ( $X_M$ -servo)              |
|                          | 23 feet ( $Y_M$ -servo)              |
|                          | 4 feet ( $Z_M$ -servo)               |
| b. Maximum velocity:     | 20 in/sec ( $X_M$ & $Y_M$ -servo)    |
|                          | 2.4 in/sec ( $Z_M$ -servo)           |
| c. Maximum acceleration: | 4.6 in/sec <sup>2</sup> (all servos) |

\* 2. Static performance.

- |                    |                           |
|--------------------|---------------------------|
| a. Static accuracy | 0.015 inches (all servos) |
| b. Repeatability   | 0.005 inches (all servos) |

3. Dynamic performance.

- |                   |   |
|-------------------|---|
| a. Dynamic range  | 1000:1  |
| b. Tracking error | The actual servo position error for step velocity input will be equal to or less than the position error of an ideal system with a transfer function of a 0.7 damped 12.5 rad/sec second order lag and 18 rad/sec first order lead. |

\* Measured position accuracy of Northrop owned Farrand Optical Probe.

### Probe Servos

The type of probe to be used in this application is described in Section 2.3.4. The probe contains four servos. Three of these servos provide line-of-sight image rotations in pitch ( $\theta_M$ ), roll ( $\phi_M$ ) and yaw ( $\psi_M$ ). The fourth servo provides image focus ( $F_M$ ).

The focus servo will be capable of dynamically focussing the image along the line-of-sight to within the specifications of paragraph 4.5.2 for any slant range down to 20 mm. This focussing ability will be achievable for the slant range changes caused by the combined motion of the probe pitch and yaw servos along with the below listed probe vertical motions.

Altitude (mm)	Vertical Velocity (mm/sec)	Vertical Acceleration (mm/sec <sup>2</sup> )
16.0	0	64.4
16.4	7	
17.5	14	
19.4	21	
22.0	28	
25.4	35	
29.6	42	
34.5	48	64.4
40.0 (above)	50	0

The probe manufacturer in earlier probe designs has put the design emphasis on repeatability of the line-of-sight and not on absolute position accuracy. The probe selected for this application will have improved position accuracy performance, however, at this time the magnitude of the improvement is not known. The Northrop owned Farrand probe position accuracy has been measured and is included herein for specification completeness.

The inputs to the  $\phi_M$  and  $\psi_M$  servos are continuous sine/cosine voltage commands from the computer. A high quality rate command will also be provided for velocity feed-forward connections. Inputs to the  $\theta_M$  and  $F_M$  servos are each a single computer command which is proportional to the combined position and rate commands. The output of the  $\theta_M$ -servo is the relative angular motion between the pitch optical element support shaft and the adjacent  $\psi_M$  supporting structure. The output of the  $\psi_M$ -servo is the relative angular motion between the center hub of the  $\theta_M$  axis and the adjacent fixed support structure. The output of the  $\phi_M$ -servo is

the relative angular motion between the roll optical element support and the adjacent fixed support structure. It should be noted that the roll optical element has an optical roll gain such that one rotation of the element yields two image rotations.

1. Output operating envelope.

- |                           |  |
|---------------------------|--|
| a. Displacement:          | Continuous ( $\psi_M$ & $\beta_M$ servos)<br>+30 degrees, -60 degrees ( $\theta_M$ -servo)   |
| b. Peak no-load velocity: | 2 rad/sec ( $\theta_M$ -servo)<br>9 rad/sec ( $\beta_M$ -servo)<br>7 rad/sec ( $\psi_M$ -servo)  |
| c. Stall acceleration:    | 3.5 rad/sec <sup>2</sup> ( $\theta_M$ -servo)<br>25 rad/sec <sup>2</sup> ( $\beta_M$ -servo)<br>20 rad/sec <sup>2</sup> ( $\psi_M$ -servo) |

2. Static performance.

- |                     |  |
|---------------------|--|
| a. Static accuracy: | 0.53 degrees ( $\theta_M$ -servo)<br>0.27 degrees ( $\beta_M$ -servo)<br>0.43 degrees ( $\psi_M$ -servo) |
| b. Repeatability:   | 0.1 degrees (all servos)   |

3. Dynamic performance (all servos).

- |                        |  |
|------------------------|--|
| a. Dynamic range:      | 1000 to 1  |
| b. Frequency response: | The actual servo phase characteristics at any frequency shall match within 10% that of an ideal 0.7 damped 25 rad/sec second-order system over a frequency band of 0 to 3 cps. |
| c. Time response:      | The actual servo time response at any time shall match that of an ideal 0.7 damped 25 rad/sec second-order system within 10% of the step amplitude.                            |

## 2.4 Peripheral Image Generation Subsystem

### 2.4.1 General

Images for the two peripheral displays are generated by a modified off-the-shelf raster graphics system designed for low cost trainer applications. The system generates patterns that provide attitude and motion cues in the pilots peripheral vision. This system is capable of generating color presentations for multiple displays.

### 2.4.2 Raster Graphics

The raster graphics system output is capable of generating a six degree of freedom synthetic terrain pattern simultaneously with a runway or target presentation. Outputs are provided for up to three displays with variable visibility capability for all displays.

The performance characteristics of an off-the-shelf design, such as the type produced by Operational Displays of Tector Ltd, are listed below.

Ground Speed	-	0 to preset maximum (Mach 2 max.)
Heading	-	Continuous
Roll	-	Continuous
Pitch	-	$\pm$ 75 degrees
Altitude	-	0 - 1500 feet for visible terrain
Travel	-	Unlimited X and Y
Terrain	-	Regular array of three tone patterns in color
Cloud Base	-	Variable from 0 - 1500 feet
Visibility	-	Variable 0.1 mile to infinity
Runway/Target Position Store	-	Internal up to 25 miles from origin
Runway/Target Size	-	Runway variable up to 1000 x 10,000 feet; target variable from 0 to 100 feet
Scan System	-	1023 line, 30 frames, 2:1 interlace

The recommended raster graphics system configuration is one which provides an output capability for three displays. The synthetic terrain information will normally be displayed by the peripheral projectors when the full display capability of the simulator is required. For selected tasks such as target tracking, weapon delivery, landing, and takeoff the three central projectors can be provided with computer generated information from the three outputs of the raster graphics.

#### 2.4.3 Interface

##### Simulation Computer Interface

The raster graphics system is capable of accepting D.C. voltages, synchro signals, digital data or a mixture of these signals as driving input commands. Generally the simulation computer outputs are available in D.C. form, therefore, the D.C. voltage option is recommended.

##### Video Interface

The raster graphics system is capable of generating RGB video at scan rates up to 1023 lines/frame, 30 frames/second at 2:1 interface. The scan rate is primarily dependent on the sync generator option specified. The two interface requirements are first that the display system sync generator can be locked to the raster graphics sync generator, and secondly that the display is capable of accepting RGB video. The display system design satisfies both of these requirements.

## 2.5 PROJECTION SCREEN

### 2.5.1 General

The following paragraphs describe the spherical projection screen for the visual display system. The recommended projection sphere is the type produced by Spitz Space Systems, Inc. The weight and inertia characteristics of the sphere are as follows:

WEIGHT (pounds)	INERTIAS ABOUT THE SPHERE CENTER (slug - ft <sup>2</sup> )		
	I <sub>pitch</sub>	I <sub>roll</sub>	I <sub>yaw</sub>
1400	2560	2560	2900

The projection screen, shown on drawing PD100, is a 20-foot I.D. (20.5 foot O.D. max.) sphere with a truncated mounting base (280° elevation - 360° horizontal) which is adaptable to being supported from beneath by a platform type support structure. The truncated base will be designed to provide adequate rigidity to maintain a steady viewing surface and to achieve stability in operating the motion system servos.

An existing Spitz projection screen design, shown on drawing PD200, could be adapted to meet the requirements of the proposed visual display system.

### 2.5.2 Screen Construction

The sphere consists of an outer frame of arcuate aluminum rectangular members spaced 20° in the plan and approximately 20° in the elevation dividing the total spherical area into 112 bays. The projection surface is attached directly to the inner frame surface. The frame contains total structural integrity and does not rely on the sheath (projection surface) to maintain its shape. The arcuate frame members are rectangular aluminum tubes (1 1/4 X 1 3/4 X 3/32 inch) arced to 120 inch inside radius, so that the 1 1/4 inch dimension becomes the width and the 1 3/4 inch dimension becomes the depth. All gore and circumferential members have the same cross section.

The inner panel sheath is 0.040 aluminum sheet stretch formed to a 120 inch radius. The panels are cut undersized producing a gapped area between all edges upon attaching to the frame. Countersunk blind rivets, recessed approximately 20 mils below the surface on 3.0 to 4.0 inch spacing, are used to attach the sheaths. A two-part polyester filler is applied to fillet the panel gaps and rivet head recesses. After curing, the filler is sanded flush to the panel surface producing a continuous surface from panel to panel.

An entry door (approximately 36.0 inches wide X 78.0 inches high) is located in the rear left quarter of the spherical screen. The door is a side swinging (hinged) type opening outward. When the door is closed and latched, the inner surface will be smooth and well matched to the surrounding screen. The aft section of the screen (approximately 140.0 inch wide X 160.0 inch high) is removable for equipment installation and removal.

#### 2.5.3 Screen Finish

The display surface panels will be cleaned, etched, and irradiated for priming before erection. The inner screen surface finish coat will be flat white (3M Nextel) with a minimum reflectance for "white light" of 90%. All areas of the screen where images cannot be displayed will be painted with a low reflectance flat black paint. The exterior finish paint is optional.

## 2.6 Detailed and Peripheral Display Subsystem

### 2.6.1 General

The general arrangement of the Detailed and Peripheral Display Subsystem is shown on drawing Pd-100 and in Figure 2.2 - 3. The detailed display, comprised of three color projectors, presents the pilot(s) with a wide-angle ( $120^{\circ}$  - horizontal x  $60^{\circ}$  - vertical) detailed terrain scene generated by the terrain model. The peripheral display, comprised of two identical color projectors, extends the detailed display horizontal field-of-view to  $200^{\circ}$  with imagery generated by the computer raster graphics image generation system.

### 2.6.2 TV Projector Roll and Yaw System

The TV Projector Roll and Yaw System shown on drawing PD-500, provides support, alignment and rotation capability for the five TV projectors. The yaw and roll structures rotate the projected scene about the sphere center to preclude introducing changes in the projection geometry which would result in the individual displays being mosaicked incorrectly.

Aircraft roll is accomplished by combining the servo controlled probe and projector roll to increase the vertical field-of-view for the low altitude roll maneuvers by rotating the field-of-view window.

The projectors will be gear driven by an electric motor and locked at discrete yaw positions (up to  $\pm 40^{\circ}$  maximum) consistent with specific simulation tasks. The imagery within the total field-of-view window will be switched from display to display as required to be consistent with the pilot's line-of-sight.

#### Projector Yaw

The projector yaw structure is a tapered lightweight aluminum weldment weighing approximately 620 pounds. The structure is supported from the cockpit support pedestal on

angular contact bearings designed to rotate the projectors about the vertical screen center. The upper yaw structure is designed to support the projector platform and roll structure pivot on the longitudinal sphere center.

### Projector Roll

The projector roll structure is a tapered lightweight aluminum weldment, weighing approximately 320 pounds. The structure is supported on angular contact bearings at the roll pivot of the yaw structure. The roll mechanism is servo driven through a 40:1 gearing system (10:1 planetary gearhead followed by 4:1 spur gearing) by a WSI hydraulic motor to  $\pm 50^\circ$  ( $\pm 45^\circ$  useable). A potentiometer and tachometer are gear driven to provide high quality position and velocity feedback signals to the servo control system.

Two sets of limit switches are located at the travel extremes. Contact with the first set smoothly returns the roll system to the initial start position by means of a reset voltage command at the normal input to the servo system. The reset will not shut down hydraulic power to the servos. Travel past the first set of switches activates a second set of limit switches which abruptly shuts down hydraulic power to the servos and removes the drive signal to the servo control valve. Controlled deceleration at the travel limit is provided by external snubbers to limit the force of deceleration which may occur due to inadvertent overtravel. The travel stop design considers the kinetic energy produced by the maximum velocity at the instant contact is made with the stop.

The weight of the projectors is approximately 1200 pounds (240 pounds each).

### 2.6.3 Projector Roll Servo

The projection roll servo precisely controls the motion about the roll axis in a manner to correctly roll the projected image about the pilots eye.

The input to this servo is single computer command which is proportional to the combined angular position and angular rate command. The output of the projection roll servo is the relative rotation between the yaw support structure and the roll support structure. Hydraulic drive is suggested for this servo.

#### 1. Output operating envelope.

- |                           |                                |
|---------------------------|--------------------------------|
| a. Displacement:          | $\pm 45$ degrees               |
| b. Peak no-load velocity: | $\pm 2.9$ rad/sec              |
| c. Stall acceleration:    | $\pm 5.8$ rad/sec <sup>2</sup> |

#### 2. Static Performance.

- |                     |              |
|---------------------|--------------|
| a. Static accuracy: | 0.2 degrees  |
| b. Repeatability:   | 0.08 degrees |

#### 3. Dynamic performance.

- |                        |  |
|------------------------|--|
| a. Dynamic range:      | 1000 to 1  |
| b. Frequency response: | The actual servo phase characteristics at any frequency shall match within 10% that of an ideal 0.7 damped 25 rad/sec second-order system over a frequency band of 0 to 3 cps. |
| c. Time response:      | The actual servo time response at any time shall match that of an ideal 0.7 damped 25 rad/sec second-order system within 10% of the step amplitude.                            |

#### 2.6.4 Detailed and Peripheral TV Projectors

Five (5) identical projectors are used to provide the viewer with a 200° continuous display. Each projector displays a nominal 40 degree wide by 60 degree high segment of the total display field-of-view. A CRT/lens triad is converged at the screen to produce a high brightness color display.

##### Projector Head

The projector contains a projection lens, 6 inch diameter CRT assembly and video amplifier electronics, for each color channel. The CRT assembly is comprised of the CRT, CRT cooling manifold, deflection coils, and focus coils. The assembly is adjustable to provide tilt-focus correction for off axis projection. All other electronics not required to be near the CRT will be located remotely.

##### Deflection Amplifier Electronics

The deflection amplifiers will be located within the sphere and as close to the heads as practicable. This is required to minimize lead inductance ensuring minimum retrace time. High voltage linear deflection amplifiers are also required to insure minimum retrace time. In addition, the unit will contain video controls and raster shaping controls. This control capability permits final registration to be performed within the sphere area.

##### Projector Electronics

The projector electronics equipment racks are located remotely from the sphere. These racks house the sweep chassis raster correction circuitry, and low voltage and high voltage power supplies. This equipment can be located up to 150 feet from the sphere electronics.

##### Video System Performance

- (1) Scan Format - The projectors are designed to operate at any line rate between 525 and 1225 lines/frame, 2:1 interlace, and at any frame rate between 15 and 30 frames/second.
- (2) Sync Input - Horizontal and vertical drive pulses with an amplitude of -3 to -5 volts.
- (3) Video Amplifiers - The video amplifiers for each color channel will have a bandwidth of 27 MHz  $\pm$  1DB. Provisions

will be made to optimize video bandwidth by inserting fast roll-off filters in the blue and red channels, and a delay line in the green channel. The amplifiers will be capable of providing full output to the CRT cathode with a video input of 0.5 VPP.

(4) Projection CRT's - The three (3) CRT's (one for each color channel) are 6 inch diameter tubes with a usable diameter of 5.3 inches. Faceplate flatness is maintained within 0.004 inches to be compatible with wide angle low f/number refractive optics. The CRT uses electromagnetic deflection and focus, and is capable of producing a line width of 0.003 to 0.004 inches depending on the drive requirements.

(5) CRT Electrical Focus - Electromagnetic focus is used to focus the CRT beam. A static focus regulator and dynamic focus modulator will be provided to insure optimum focus over the entire raster.

(6) CRT Cooling - CRT faceplate and phosphor cooling is provided to increase tube life and luminous efficiency. Uniform cooling will be provided with filtered and dried high pressure air.

(8) D.C. Restoration - Black level is controlled by a balanced key clamp which is keyed to the horizontal drive pulses.

(9) Phosphor Protection - Sweep, and power supply failure sensing is provided which will cut off the CRT beam and high voltage in the event of failure. In addition, a slow start circuit applies the high voltage gradually at turn on.

(10) Personnel Safety - Interlock switches interrupt the high voltage if any access door in the projector head is opened. Lead shielding is provided to limit X-Ray radiation to a safe level.

(11) Raster Shaping - Linear deflection amplifiers are provided to permit shaping of the CRT Raster. Raster shaping is required to provide accurate matching of each image segment and registration of each color channel. The corrections, correction adjustment range, and registration accuracy requirements are the same as for the TV camera described in paragraph 2.3.6.

### 2.6.5 Projection Optics

The projection lens design is a compromise between physical size and optical performance. The optical design is optimized to provide higher contrast at spatial frequencies consistent with those encountered in television systems. The optical design discussed in section 5.2 is for an f/1.0 lens providing optimum size and performance. Characteristics of this lens design are listed below:

Magnification Ratio:	29.8x
Projection Angle	+ 31.5° (120" radius spherical screen)
Object Size:	5.3 Inch diameter
Track Length:	170.2 Object to image distance
Back Focal Distance:	4.726"
Front Vertex to Object Distance:	150.0"
Focal Length:	5.16"
f/# at Infinity:	1.0
Color Correction:	Photopic
Distortion:	2% (Barrel at screen)
Resolution:	4 C/MM @ 50%
Relative Illumination:	30% at 31.5°
Transmission:	80% nominal
Coating:	Magnesium Fluoride
Physical:	
Diameter:	10.5 inches
Length:	16.75 inches
Weight:	77 lbs.

The f/1.2 lens discussed in paragraph 4.4.3 provides essentially the same optical performance as the lens previously described, however, the higher f/no. results in lower screen brightness. Physical characteristics of this lens are as follows:

Diameter:	8.5 inches
Length:	12.9 inches
Weight:	40 pounds

#### 2.6.6 Variable Visibility Generation

Generation of variable visibility conditions will be accomplished with special effects video equipment. A modified off-the-shelf design will be used to provide each of the three detailed displays with variable visibility effects. This is accomplished by processing video from each camera and providing the display with the modified video. The following are the special effects simulated:

##### (1) Cloud Top

Simulation of flying above clouds, below clouds, and in clouds (zero visibility) will be provided. Roll capability during cloud top simulation will be +30 degrees.

##### (2) Variable Visibility

Visibility will be variable from 0 to 100% by introducing a haze signal into the video. Variation in visibility with range is achieved by varying the haze intensity from the bottom to the top of the scene.

##### (3) Day-Dusk-Night

Simulation of day-dusk-night operation will be accomplished with video and will be independent of model illumination. Change from day to night operation will be simulated by changing the brightness and contrast of the display video.

##### (4) Selective Lighting Intensification

During dusk and night operation simulation of selective lighting, such as beacons and stagefield lights, will be provided by video intensification. This requires that the discrete lights on the modelboard have a higher intensity than that of the general lighting.

##### (5) Helicopter Landing/Search Lights

Simulating landing lights during dusk or night flight is accomplished by high lighting the video signal in a pattern

representing the light beam. The video intensity will be variable as a function of altitude.

Control of the special effects video system will be from a local control panel or the simulation computer. Signal inputs required to vary the video as a function of aircraft motions will be  $\pm 10$  VDC with sin and cos required for roll. Logic signals required to initiate changes in the scene will be 0 and +5 VDC.

The video special effects system will operate at scanning standards compatible with the camera and display system (1023 line, 60 fields, 2.1 interlace). Frequency response of the system will be 27 MHz  $\pm 1$  DB with a signal to noise ratio of at least 52 DB.

### 2.6.7 Head Slaved Yaw

A head slaved area-of-interest (AOI) system will track the pilots head motion in azimuth and displace the detailed display window  $\pm 40$  degrees. This provides the pilot with the capability of viewing detailed information to  $\pm 100$  degrees. To accomplish this, azimuth head position is sensed, and a discrete signal is generated at approximately  $\pm 40$  degrees of head displacement. At this time probe roll and heading are slewed at maximum velocity one field-of-view width of 40 degrees, and simultaneously the video to each individual display is switched left or right one display. Slew rate of the roll and heading servos will be matched, and displacement of the image will be accomplished in less than 200 ms or 6 frames of video. This capability has been demonstrated with an existing probe design.

Matching of the maximum velocity of heading and roll servos will be accomplished in the simulation computer. The probe drives must decouple roll from pitch and heading during normal simulator operation. An additional computation will be made to decouple roll from heading (yaw) as function of heading position.

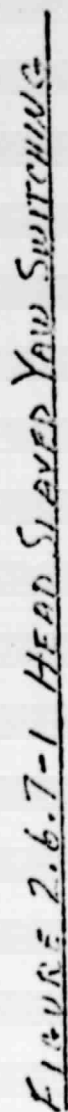
The probe heading and display video switching commands will be initiated concurrently. At this time the probe will be slewed accurately one display width (40 degrees) and all display video will be switched left or right one display. Information normally displayed in the outer detailed display is now displayed in the peripheral display. The detailed display information is now displayed from 20 degrees to 100 degrees when the pilot's line-of-sight (LOS) exceeds a displacement of  $\pm 40$  degrees. Hysteresis will be provided to preclude unwanted switching when the pilot's LOS is at the switch point. Hysteresis will be typically 10 degrees. This will return the display to center when the pilot's LOS is 30 degrees. Both the switch point and hysteresis will be adjustable.

Video switching will be accomplished electronically through wide band switching amplifiers included in the test monitor

and video interface section (refer to paragraph 2.8.3). The switching arrangement is shown schematically in Figure 2.6.7-1.

Head position sensing will be provided by the position sensing section of a GFE Helmet mounted sight. This unit will measure the angular position of the pilot's head with respect to the X Y Z axes of the cockpit. The output will be processed to provide a discrete command initiating probe slewing and video switching.

VINCE WALKER TO SWITZERLAND.



## 2.7

### Sky/Horizon Projector Subsystem

#### 2.7.1 General

The Sky/Horizon (S/H) Projector, shown on drawing PD-800 and in Figure 6.2.1-1, will be used primarily for higher altitude flight. The S/H projector presents a full-screen display giving the pilot(s) an attitude reference as well as a representation of a horizon on a featureless blue sky with clouds. The S/H projector utilizes a point light source - colored transparency projector technique.

The S/H projector, located above and behind the screen center to allow approximately 110° maximum up vision, is mounted in a 3-axis gimbal support structure which allows the scene to be rotated in roll, pitch, and yaw to simulate the required aircraft attitude.

All axes of the S/H projector are to be aligned to within  $\pm 1/4$  degrees. Precision high quality gearing is required to insure smooth operation.

The S/H projector lamp is mechanically counter-rotated with respect to the roll-axis to avoid image distortions associated with rolling the lamp and transparency as a unit. The position of the point-light source within the transparency must maintain the same 3-dimensional geometric relationship with respect to the center of the projector horizon plane as does the position of the S/H projector within the spherical display screen with respect to the sphere center. Since the transparency is rotated in pitch and yaw about the lamp, further corrections are not required.

The S/H projector rotations are as follows:

- . Pitch -  $\pm 75^\circ$  ( $\pm 70^\circ$  usable)
- . Roll -  $\pm 180^\circ$
- . Yaw - continuous

The weight of the S/H projector assembly is approximately 15 pounds.

#### 2.7.2 S/H Projector Gimbals

The S/H Projector Gimbals are designed to support and rotate the hemispherical sky/horizon transparency about the lamp to simulate aircraft roll, pitch, and yaw attitude.

The lamp is fixed with respect to pitch and yaw rotation (hemisphere rotates about the lamp), and is de-rotated in roll by a sprocket and chain drive system from the roll axis.

Mechanical lockouts, travel stops, and limit switches are incorporated in the roll and pitch systems. Potentiometers and tachometers are gear driven from each system (roll, pitch and yaw) to provide linear shaft angle and velocity feedback inputs to the servo controllers.

#### Roll

The S/H projector is supported and directly driven on the roll axis by a dc torque motor. The roll axis shaft supports the projector pitch and yaw gimbals, and the lamp support and de-roll mechanism, which are in turn supported from the main projector support structure. The roll structure is a rigid cradle-like aluminum weldment which supports the pitch axis and drive system.

#### Pitch

The roll structure, as described above, interfaces with the pitch axis pivots and provides support for the pitch axis dc torque motor/tachometer drive package and potentiometer. The projector yaw drive and support structure is gear driven in pitch by a motor mounted pinion driving a gear sector attached to the yaw structure. A similar sector drives the feedback potentiometer.

#### Yaw

The transparency and yaw drive gear are mounted to the outer race of a large diameter radial contact bearing. The inner race mounts to a hollow circular aluminum plate supported from the pitch axis pivots. The plate supports a dc torque motor, tachometer, and potentiometer which are geared to the large diameter yaw drive gear.

### 2.7.3 Transparency and Light Source

The Transparency and Light Source are the primary components of the sky/horizon projection system. Images are formed and rotated on the projection screen surface by rotating the transparent hemisphere about the light source.

#### Transparency

The sky/horizon transparency is vacuum formed from a clear sheet of Plex-55 (.25 inch thick) to a 12-inch diameter hemisphere. The transparency is decorated by applying a blue acrylic hot dip dye to the inner surface.

### Light Source

The sky/horizon projector light source will be a dimmable miniature tungsten - halogen lamp. The light flux output will be 2100 lumens, and the screen brightness will be approximately 0.5 Foot Lamberts, depending on the transmission characteristics of the sky/horizon transparency.

#### 2.7.4 Sky-Horizon Projector Servos

The (3) three gimbal servos of the sky-horizon projector precisely controls the motions of the individual gimbals in a manner to orient and dynamically project the sky-horizon scene onto the spherical screen. Deroll of the light is accomplished by a mechanical coupling to the roll gimbal.

The inputs to the yaw ( $\psi_s$ ) servo is a continuous sine-cosine voltage command from the computer. A high quality rate command will also be provided. Inputs to the roll ( $\theta_s$ ) and the pitch ( $\phi_s$ ) servos are each a single computer command which is proportional to the combined angular position and the angular rate commands. The output of the  $\psi_s$  servo is the relative rotation, about the  $\psi_s$ -axis, between the main support of the  $\psi_s$ -gimbal and the adjacent supporting structure of the  $\theta_s$ -gimbal. The  $\theta_s$ -servo output is the relative rotation, about the  $\theta_s$ -axis, between the main support shaft of the  $\theta_s$ -gimbal and the adjacent support structure of the  $\phi_s$ -gimbal. The output of the  $\phi_s$ -servo is the relative rotation, about the  $\phi_s$ -axis, between the main support shaft of the  $\phi_s$ -gimbal and the fixed adjacent support structure.

##### 1. Output operating envelope.

a. Displacement:	+ 180 degrees ( $\phi_s$ -servo)
	+ 70 degrees ( $\theta_s$ -servo)
	Continuous ( $\psi_s$ -servo)
b. Peak no-load velocity:	7.4 rad/sec ( $\phi_s$ -servo)
	2.0 rad/sec ( $\theta_s$ -servo)
	6.0 rad/sec ( $\psi_s$ -servo)
c. Stall acceleration:	28 rad/sec <sup>2</sup> ( $\phi_s$ -servo)
	18 rad/sec <sup>2</sup> ( $\theta_s$ -servo)
	9.3 rad/sec <sup>2</sup> ( $\psi_s$ -servo)

##### 2. Static performance.

a. Static accuracy:	0.5 degrees (all servos)
b. Repeatability	0.2 degrees (all servos)

##### 3. Dynamic performance (all servos)

a. Dynamic range:	1000 to 1
-------------------	-----------

b. Frequency response:

The actual servo phase characteristics at any frequency shall match within 10% that of an ideal 0.7 damped 25 rad/sec second-order system over a frequency band of 0 to 3 cps.

c. Time response:

The actual servo time response at any time shall match that of an ideal 0.7 damped 25 rad/sec second-order system within 10% of the step amplitude.

## 2.8 Test, Monitor and Control Subsystem

### 2.8.1 General

The test, monitor and control subsystem will provide simulator maintenance personnel with sufficient test and monitor equipment to perform rapid daily checkout and alignments required to insure high simulator utilization.

The monitor and control console will provide an operator with the capability of controlling the operation of the simulator independent of the simulation computer for check-out and alignment purposes. Full time monitoring of video signals and servo position feedback signals will be provided. This equipment arrangement is shown on PD-900.

### 2.8.2 Servo

The monitoring and control station will include local controls for all servo systems. This will include controls for positioning the individual servos. Full time monitoring of the position feedback will be provided to insure correct positioning. In addition, local controls will provide the capability of transferring control between the control station and the simulation computer. A fade circuit will be included to provide smooth transfer of control regardless of the differential between the local control commands and computer commands.

A switching matrix is provided and permits any servo input command, feedback signal, and error signal to be monitored with a digital voltmeter or oscilloscope. A servo analyzer is provided to permit frequency response measurements required for troubleshooting and to validate performance of the servos.

### 2.8.3 Video

Full time monitoring of the display video for each display channel will be provided. Monochrome multiline rate monitors will be used to provide full time monitoring of the luminance (green) channel of each display. A 20 x 20 video

### 2.8.3 (continued)

switching matrix is provided to permit monitoring by oscilloscope and a 1023 line color TV monitor, the video from all cameras and projectors. A video signal generator provides the signals essential for camera and projector setup and maintenance. The test signals can be inserted into any channel through the switching matrix. The signal generator will be an RGB color test pattern generator capable of providing the grating, resolution, and color signals necessary to setup the video equipment.

Remote control of all projectors and auxillary video equipment is included in the monitoring and control station. All camera control units are located in a separate bay adjacent to this station.

### 2.8.4 Interface

#### Servo Interface

The primary interface between the simulator hardware is through the analog patch board located in the display servo electronics station. All commands from the simulation computer are routed through the patch board to the appropriate probe, gantry, and display servos. All servo feedback signals and position error signals are routed through the patchboard to the computer. These signals are listed below:

- (1) Linear position feedback - all servos
- (2) Sin and Cos Feedback -  $Y_m$ ,  $Y_M$ ,  $Z_M$  of the gantry,  $\psi_s$  of the sky-horizon projector, and  $\psi_m$ ,  $\phi_m$ , of the probe
- (3) Position Error - all servos
- (4) Tachometer Feedback - all servos

#### Video Interface

The video switching electronics and pulse distribution amplifiers act as the primary video and sync interface. The video switch amplifiers provide switching and line driving capability. All camera video signals are inputs to the switching input amplifiers and all projectors receive their input from the switching output amplifiers. In addition, video test signal and monitoring equipment interfaces with switching electronics.

Sync signals from the sync generator are distributed to the TV camera, TV projector, and auxillary video equipment through pulse distribution amplifiers. The video and pulse distribution amplifiers provide isolated and buffered outputs to all video equipment.

## 2.9 COCKPIT AND VISUAL DISPLAY SUPPORT STRUCTURE

### 2.9.1 General

The cockpit and visual display support platform, although shown in Figure 2.6.1-1 and drawing PD100 and described in section 2.9.2 and 2.9.3 in terms of interfacing with elements of the visual display (cockpit positioner, cockpit support pedestal, and projection screen support), are not considered part of the visual system. The cockpit was considered in terms of general arrangement for the purpose of defining cockpit frame occlusions to the projectors and is described in section 4.6.

### 2.9.2 Cockpit Support

The cockpit support includes the cockpit positioner mechanism and the cockpit support pedestal which interface with the TV projector yaw support structure and the cockpit and visual display support platform of the motion system. These structures are described as follows:

(1) Cockpit Positioner - The cockpit is attached to the lateral T-shaped slide supports of the positioner mechanism as shown on drawing PD301. The slide supports are aluminum weldments (approximately 8.75-inch deep X 58.5-inch long) machined at the base to accommodate anti-friction type bearing plates. The slides are supported and retained in lateral machined aluminum tracks (approximately 1.25 X 3.00 X 93.5-inches) attached to the top surface of an 8.0-inch aluminum I-beam/base plate structure which mounts directly to top of the cockpit pedestal. The cockpit is gear driven laterally by an electric motor/lead screw drive system. Three cockpit lockout positions are provided as follows:

- . Center
- . 14.0-inches left
- . 18.0-inches right

(2) Cockpit Support Pedestal - The Cockpit Support Pedestal, shown on drawing PD500, interfaces with the cockpit positioner, the projector yaw support structure, and the cockpit and visual display support platform of the motion system. The pedestal is a cylindrical welded aluminum structure (approximately 34.0-inch O.D. X 32.0-inch I.D. X 28.25-inches high) with machined surfaces as required for the projector yaw support bearings and the upper and lower pedestal attach surfaces.

### 2.9.3 Screen and Sky/Horizon Projector Support Structure

The screen and sky/horizon projector are supported from common structure to the cockpit and visual system support platform (\*), and are described as follows:

(1) Screen Support - The screen support structure is described in terms of screen construction in section 2.5.1.

(2) Sky/Horizon Projector Support - The sky/horizon projector support structure, shown on drawing PD100, is a lightweight, monocoque sheet aluminum type structure suspended from the upper rear projection screen support frame members. This type structure satisfies the rigidity and strength requirement and is compatible with the low inertia requirement of a sphere (screen) supported load.

(\*) References:

The recommended shape for the support platform (considered part of the motion system) is octagonal - measuring 16-foot between flats. The platform is required to provide attachment points with adequate rigidity and strength for supporting the screen and cockpit pedestal.

### 2.9.4 TV Projector Roll and Yaw Support

The TV projector roll and yaw support structure interfaces with the cockpit support pedestal as shown on drawing PD500 and described in section 2.6.2.

### 3.0 DEVELOPMENT PLAN

This section of the final report presents the program plan and schedule, work breakdown structure, and cost estimates for the proposed Helicopter Simulator System.

#### 3.1 Program Plan and Schedule

The recommended plan for accomplishing the objectives of the Helicopter Simulator Program is illustrated in Figure 3.1-1. The program, as shown, is divided into five phases as follows:

- I. Design, procurement, and fabrication.
- II. Completion of major assemblies and set-up development test areas.
- III. Subsystem development tests, checkout, and performance optimization.
- IV. In-plant acceptance tests.
- V. On-site installation, and functional and final acceptance tests.

The calendar relationship of the phases to each other and to the total program is shown as a function of months after go-ahead. The phases vary in length from 5 to 7 months. The overall program length is estimated to be 30 months.

A major long-lead (over six months) procurement schedule is shown in Figure 3.1-2.

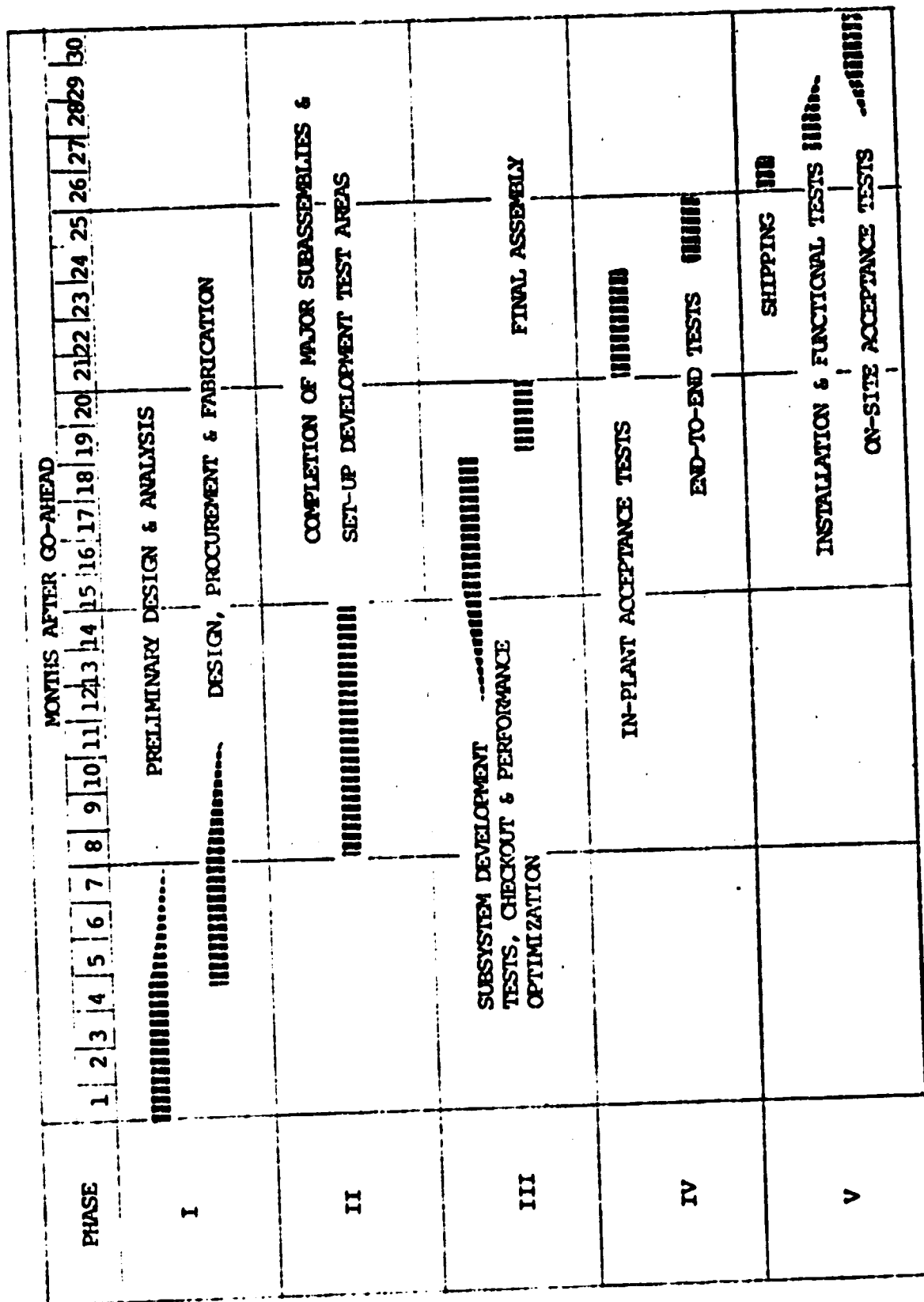


FIGURE 3.1-1 PROGRAM SCHEDULE BY PHASES

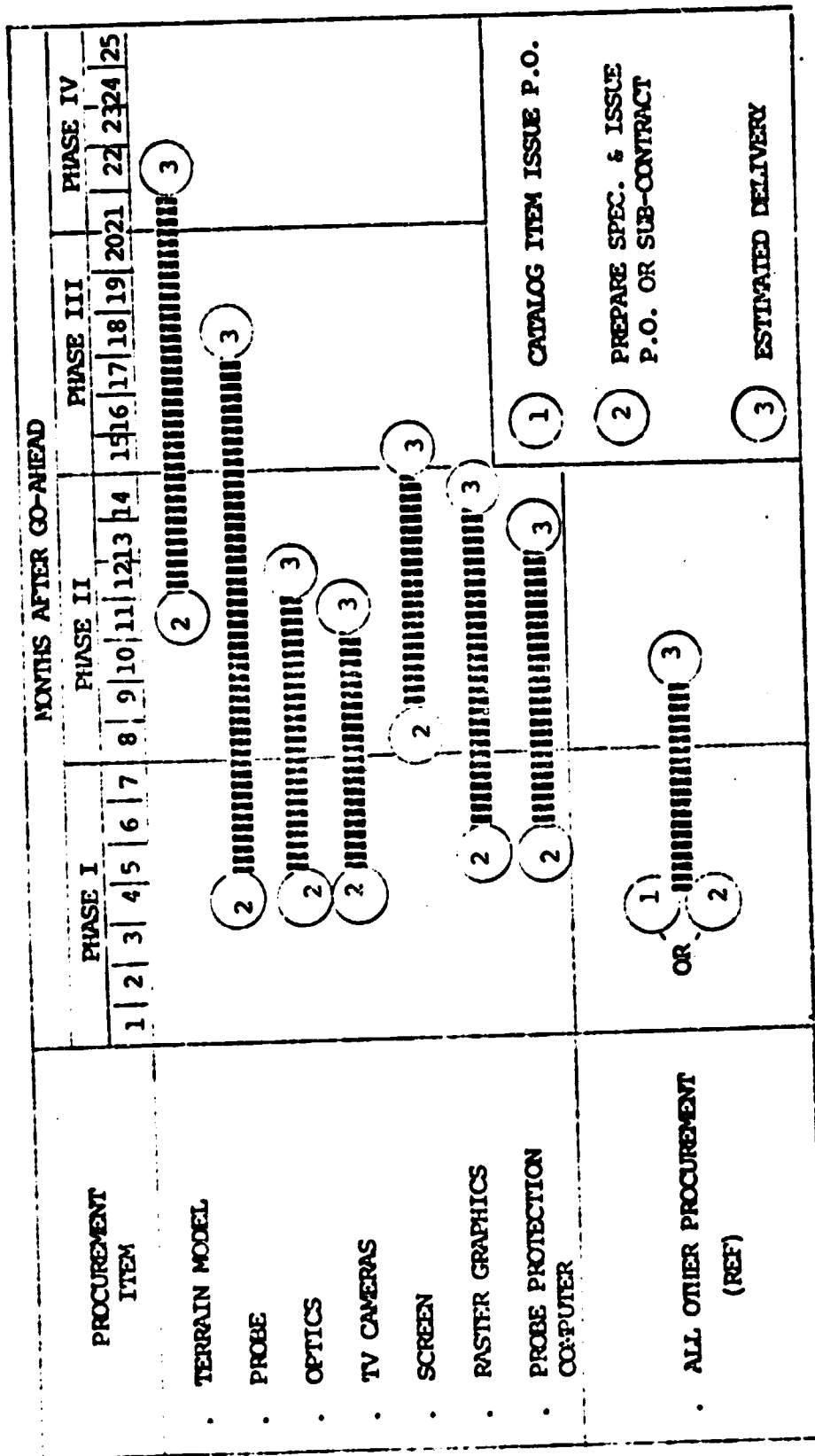


FIGURE 3.1-2 MAJOR LONG-LEAD PROCUREMENT SCHEDULE

### 3.2 Work Breakdown Structure

The Helicopter Simulator Program work breakdown is shown in Figure 3.2-1. The four-digit number over the upper right hand corner of each element in the breakdown is the Work Breakdown Structure (WBS) number assigned for identification and planning purposes. The 1000 - series elements comprise essentially the simulator hardware items, while the 2000 through 5000 - series consist of the integrating and supporting services and end-items provided during the course of the program. The WBS elements are defined to the third level in Figure 3.2-2 and 3.2-3. The WBS 1000 - series includes preliminary and detailed design, analysis and engineering, procurement, and fabrication and assembly for each element of the helicopter simulator.

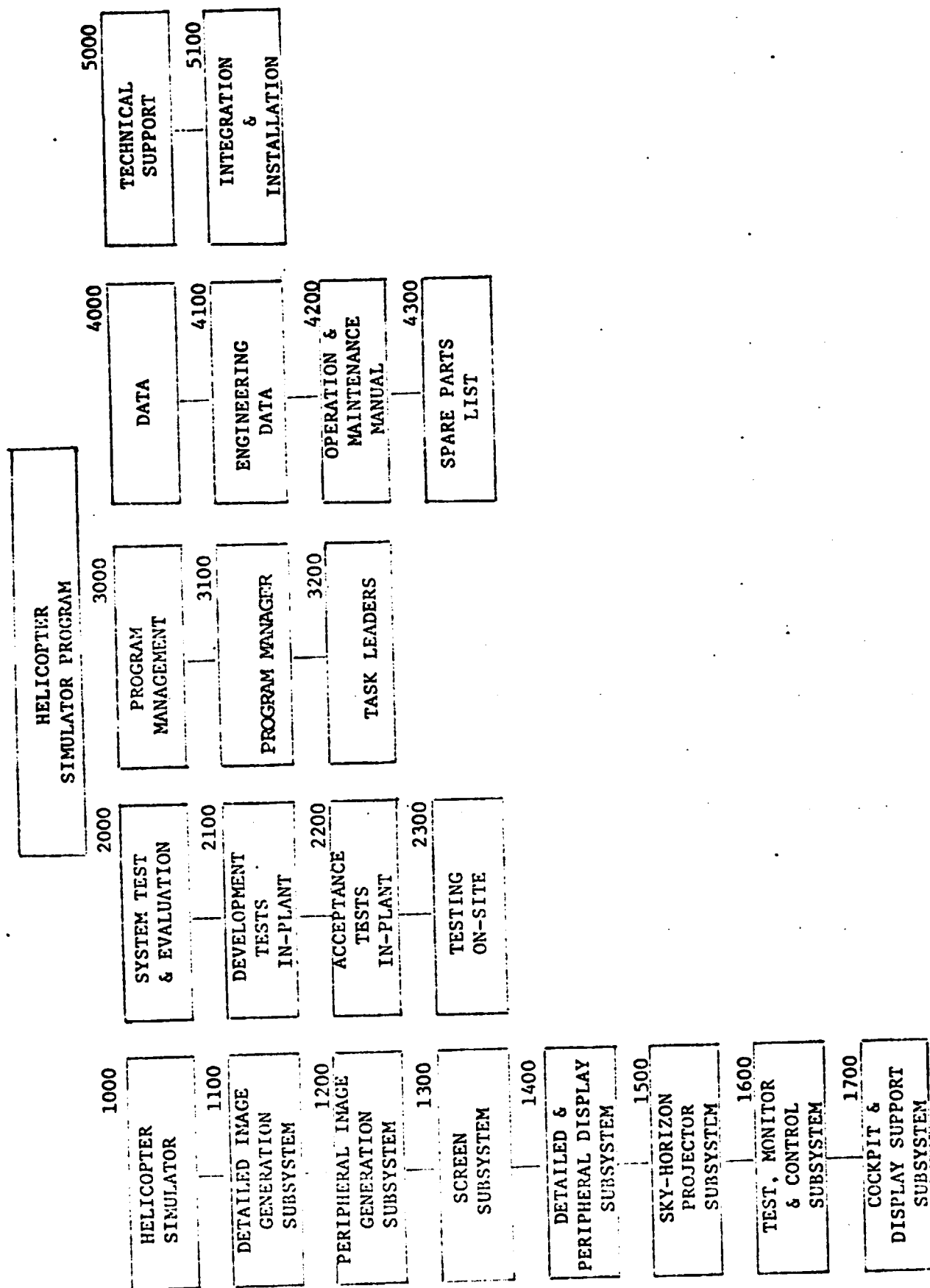


FIGURE 3.2-1 HELICOPTER SIMULATOR PROGRAM BREAKDOWN STRUCTURE

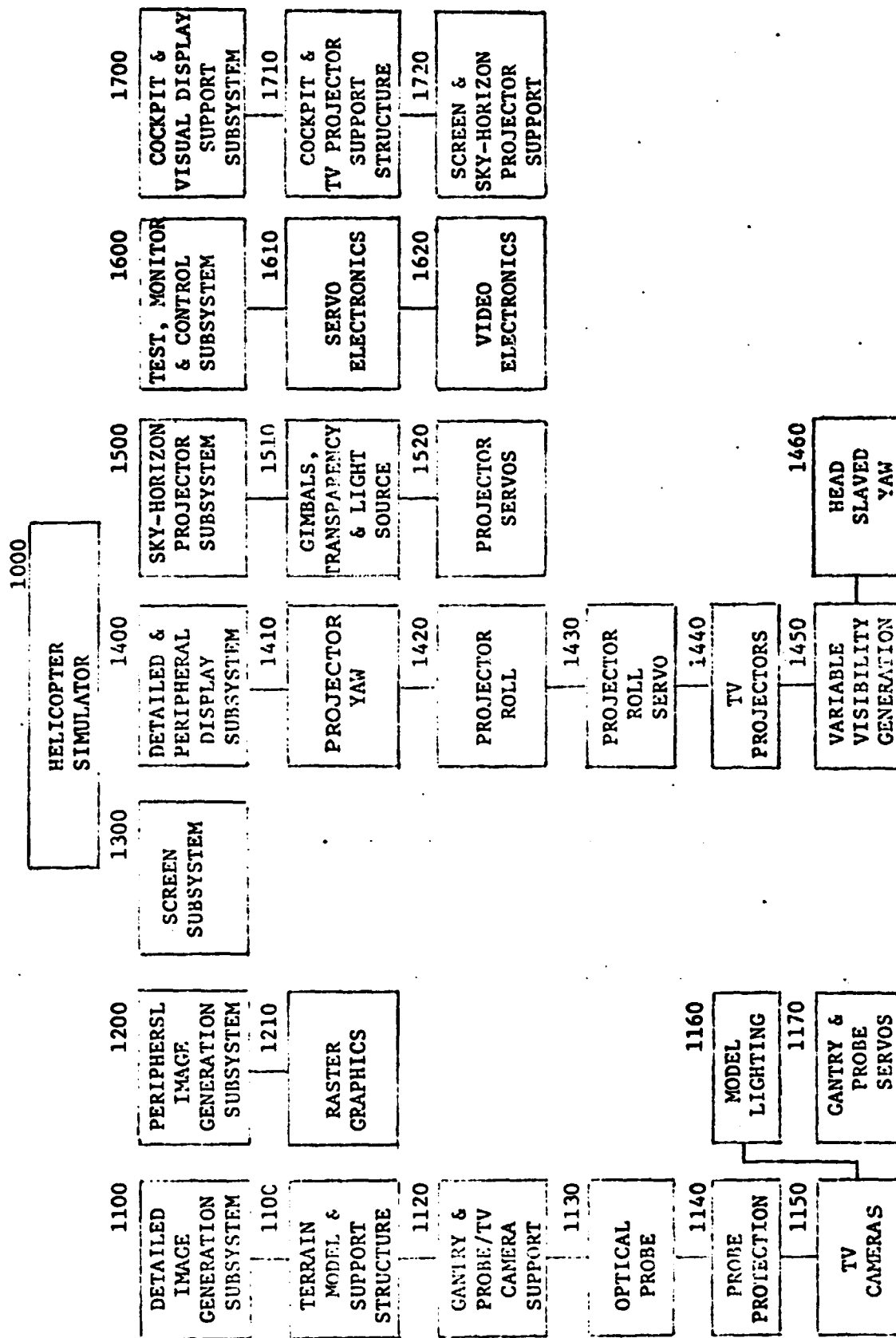


FIGURE 3.2-2 HELICOPTER SIMULATOR  
SYSTEMS BLOCK BREAKDOWN STRUCTURE

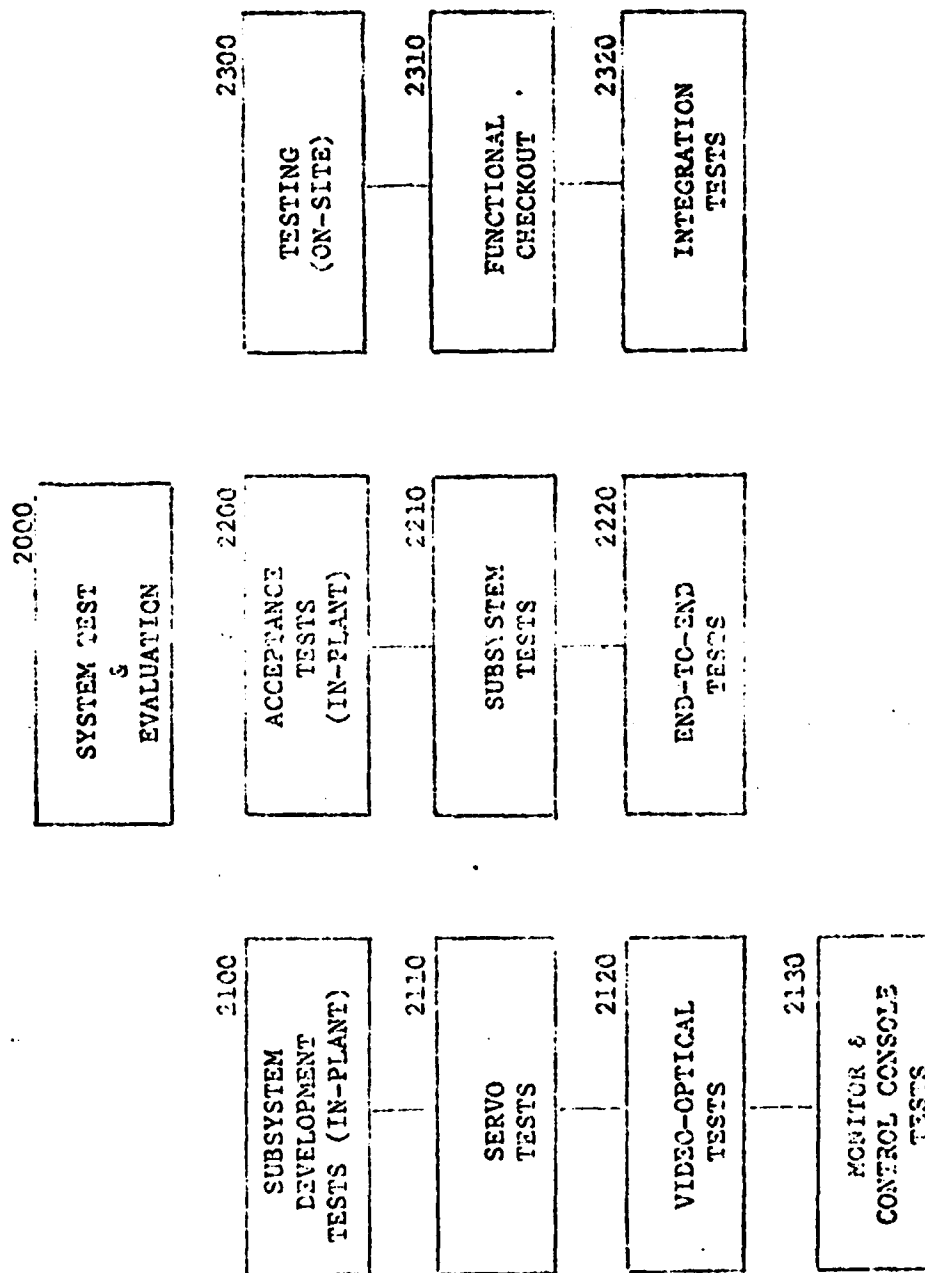


FIGURE 3.2-3 HELICOPTER SIMULATOR TEST AND EVALUATION WORK BREAKDOWN STRUCTURE

### 3.3 Cost Estimates

The following (rough) budgetary cost estimates are presented for government planning purposes in terms of direct charge man-hours and unburdened material costs associated with WBS 1000 and 3000 elements. Manhour estimates for WBS 2000, 4000, and 5000 elements are included in WBS 1000. Table 3.3-1 presents the estimated manhours in terms of engineering and shop/technician costs per development phase. Table 3.3-2 presents the estimated unburdened material costs in terms of 1977 dollars per development phase. Table 3.3-3 presents a description of the material in terms of dollars per WBS element.

TABLE 2.3-1  
MANHOUR ESTIMATES

ORIGINAL PAGE IS  
OF POOR QUALITY

A ENGINEERING  
B SHOP AND TECHNICIAN

WBS	TOTAL MANHOURS		MANHOURS PER PHASE				
			I	II	III	IV	V
1110	A	800	350	330	40	-	80
	B	1540	260	410	-	-	870
		2340	610	740	40	-	950
1120	A	1850	770	590	130	130	230
	B	1270	290	620	50	50	260
		3120	1060	1210	180	180	490
1130	A	720	120	160	200	80	160
	B	300	-	-	150	40	110
		1020	120	160	350	120	270
1140	A	1300	-	200	160	840	100
	B	170	-	-	-	100	70
		1470	-	200	160	940	170
1150	A	670	250	90	200	40	90
	B	170	-	-	90	20	60
		840	250	90	290	60	150
1160	A	660	-	320	180	100	60
	B	780	-	120	310	230	120
		1440	-	440	490	330	180
1170	A	670	400	270	Servo electronics checkout & tests are included in the above hardware elements.		
	B	950	290	660			
		1620	690	930	---	---	---
1100	A	6670	1890	1960	910	1190	720
	B	5180	840	1810	600	440	1490
		11850	2730	3770	1510	1630	2210
1200	A	380	160	40	40	40	100
	B	230	-	-	130	20	80
		610	160	40	170	60	180
1300	A	560	400	80	40	20	20
	B	180		20	60	10	90
		740	400	100	100	30	110
1410	A	800	480	200	40	20	60
	B	860	170	310	250	10	120
		1660	650	510	290	30	180

TABLE 2.3-1  
MANHOUR ESTIMATES (Continued)

A ENGINEERING  
B SHOP AND TECHNICIAN

WBS	TOTAL MANHOURS	MANHOURS PER PHASE				
		I	II	III	IV	V
1420	A 1090	490	340	100	40	120
	B 840	150	380	120	30	160
	1930	640	720	220	70	280
1430	A 160	100	60	Servo electronics checkout & tests are included in the above hardware elements		
	B 240	60	180			
	400	160	240	-	-	-
1440	A 2440	1110	990	160	60	120
	B 4190	1200	2500	170	90	230
	6630	2310	3490	330	150	350
1450	A 290	80	60	40	30	80
	B 140	-	-	80	20	40
	430	80	60	120	50	120
1460	A 270	80	40	40	30	80
	B 140	-	-	80	20	40
	410	80	40	120	50	120
1400	A 5050	2340	1690	380	180	460
	B 6410	1580	3370	700	170	590
	11460	3920	5060	1080	350	1050
1510	A 1100	390	410	100	100	100
	B 1110	280	610	70	80	70
	2210	670	1020	170	180	170
1520	A 570	300	270	Servo electronics checkout & tests are included in the above hardware elements		
	B 950	300	650			
	1520	600	920	---	---	---
1500	A 1670	690	680	100	100	100
	B 2060	580	1260	70	80	70
	3730	1270	1940	170	180	170
1610	A 2100	880	880	80	80	180
	B 2450	690	1370	90	90	210
	4550	1570	2250	170	170	390
1620	A 560	220	180	40	40	80
	B 430	120	220	20	30	40
	990	340	400	60	70	120

TABLE 2.3-1  
MANHOUR ESTIMATES (Continued)

A ENGINEERING  
B SHOP AND TECHNICIAN

WBS	TOTAL MANHOURS	MANHOURS PER PHASE				
		I	II	III	IV	V
1600	A 2660	1100	1060	120	120	260
	B 2880	810	1590	110	120	250
	5540	1910	2650	230	240	510
1710	A 200	110	30	40	10	10
	B 180	40	90	10	-	40
	380	150	120	50	10	50
1720	A 410	370	40	-	-	-
	B 590	110	260	-	110	110
	1000	480	300	---	110	110
1700	A 610	480	70	40	10	10
	B 770	150	350	10	110	150
	1380	630	420	50	120	160
1000	A 17600	7060	5580	1630	1660	1670
	B 17710	3960	8400	1680	950	2720
	35310	11020	13980	3310	2610	4390
3010 (Ref)	1 Mgr	Full Time (Probably Indirect Charge)				
3020	3 Task Leaders	Full Time	Three-Quarter Time	Half Time		
	12375	3500	3500	2250	1875	1250

TABLE 3.3-2  
MATERIAL ESTIMATES  
(Unburdened Dollars)

WBS	TOTAL DOLLARS X 1000	DOLLARS X 1000 PER PHASE				
		I	II	III	IV	V
1110	232	10	220	2		
1120	30	15	15			
1130	352	350	2			
1140	51		50	1		
1150	276	275	1			
1160	38			33	5	
1170	9	4	5			
1100	988	654	293	36	5	
1200	51	50	1			
1300	73		47	20		6
1410	5		5			
1420	15	10	5			
1430	3	2	1			
1440	455	453	2			
1450	26	25	1			
1460	50	50				
1400	554	540	14			
1510	12	6	6			
1520	7	3	4			
1500	19	9	10			
1610	20	15	5			
1620	24	18	6			
1600	44	33	11			
1710	2	2				
1720	2	2				
1700	4	4				
1000	1733	1290	386	56	5	6

**TABLE 3.3-3**  
**MATERIAL DESCRIPTION**  
**(UNBURDENED DOLLARS)**

WBS	TOTAL DOLLARS X 1000	MATERIAL DESCRIPTION
1110	232	164 Modelboard and Seaming 56 Modelboard Mapping 2 Trip 10 Miscellaneous Parts and Raw Material
1120	30	8 Motors, Potentiometers and Tachometers 6 Ball Bushing Shafts 16 Ball bushings, roundway bearings, cam tracks, cams, gears, gear racks, cable supports, misc. parts and raw material
1130	352	350 Optical probe 2 Trip(s)
1140	51	50 Computer 1 Misc.
1150	276	275 TV Cameras (3) 1 Misc.
1160	38	33 Lamp Assemblies (96) 5 Facility Wiring
1170	9	9 Misc. Servo Electronics & Wiring
1200	51	50 Raster Graphics System 1 Trip
1300	73	73 Screen and Assembly
1410	5	5 Motor and Gearing, raw material and misc. parts
1420	15	7 Hydraulic Actuator, gears and bearings 8 Potentiometer, tachometer, and raw materials

TABLE 3.3-3  
MATERIAL DESCRIPTION (Continued)  
(UNBURDENED DOLLARS)

WBS	TOTAL DOLLARS X 1000	MATERIAL DESCRIPTION
1430	3	3 Misc. servo electronics
1440	455	247 CRTs, deflection components, deflection amplifiers, sweep chassis, power supplies, and misc. parts 208 Projection optics (15)
1450	26	26 Variable visibility generation system
1460	50	50 GFE type helmet mounted sight head position electronics
1510	12	12 Motors, potentiometers, tach- ometers, gears, bearings, raw material and misc. parts
1520	7	7 Misc. servo electronics and wiring
1610	20	20 Switching matrix, DVM, equip- ment racks, scope, patchboard and misc. hardware and electronics
1620	24	Switching matrix, monitors, scope, signal generators, equipment racks, and misc. hardware and electronics
1710	2	Misc. raw material
1720	2	Misc. raw material
1000	1733	Total Material

## 4.0 ANALYSIS AND TRADEOFF STUDIES

### 4.1 Terrain Model and Probe Configuration

#### 4.1.1 General

The terrain model and probe configuration are based on providing the following requirements:

- (1) Provide a field-of-view consistent with that of a helicopter.
- (2) Provide capability for low altitude nap-of-the-earth (NOE) flight in rough high relief areas.
- (3) Provide landing capability in confined areas.

Satisfying these requirements is highly dependent on the compatibility of the optical probe with the terrain model-board scale and terrain gradient.

The following considerations were instrumental to the selection of a dual scale terrain model:

- (1) The low altitude flight requirement in rough terrain (canyon areas) and the direct relationship between the probe field-of-view and head size to the minimum altitude, were primary reasons for selecting a relatively low scale terrain model.
- (2) Although a current probe design with a 140 degree field-of-view is reasonably compatible with a 300:1 scale model (as originally planned) providing a minimum pupil to modelboard distance of 6.2 mm (with 2mm Prism clearance), the modelboard required to provide a 2 x 3 NM gaming area would be very large - approximately 40 x 60 feet.

The dual scale modelboard (250:1 and 500:1) decision, based on evaluations of operational simulators utilizing dual scale modelboards and other criteria, led to the following conclusions and/or advantages:

- (1) Dividing the modelboard into two sections of equal area for each model scale reduces the model-board size to 24 x 64 feet without reducing the total gaming area.

#### 4.1.1 (continued)

- (2) Minimum eye height on the 250:1 model is reduced to 5 feet. Additional probe head clearance is provided for the same terrain gradient.
- (3) Model lighting requirements are reduced.
- (4) The dual scale reduces the modelboard and gantry heights and simplifies fabrication and assembly.
- (5) The requirement to drive probe focus is probably not required for either model scale.
- (6) A dual scale modelboard is thought to provide improved performance and a more cost effective and stable system.

#### 4.1.2 Modelboard Construction

Modelboard construction techniques were studied and optimized to be compatible with the dual scale model approach described above. Figure 4.1-1 compares the characteristics of three types of modelboard construction.

Configuration I - This configuration represents the lowest cost type construction. The soft polyurethane core material has an inherent advantage of providing a degree of secondary probe protection. The contoured foam/plywood base forms a fixed (unadjustable surface) rigid structure with a relatively high coefficient of linear expansion/ $^{\circ}\text{C}$  and is therefore not considered to be compatible with requirements for low altitude flight.

Configuration II & III - These configurations are similar shell-type structures with hard surfaces. The structures are compatible with being supported on studs (equally spaced across the modelboard) which provide very accurate model surface control. Configurations II and III, although slightly more expensive, are constructed of materials with significantly lower coefficients of linear expansion/ $^{\circ}\text{C}$  and are therefore considered more compatible with requirements for low altitude flight. Configuration III is recommended for the visual display system. A positive probe protection system is required and is described in Section 2.3.5.1.

# MODELBOARD FABRICATION & SUPPORT DATA

ORIGINAL PAGE IS  
OF POOR QUALITY



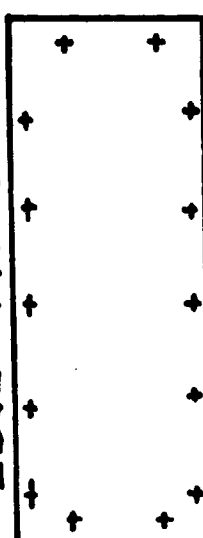

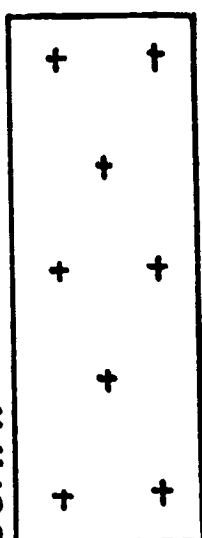
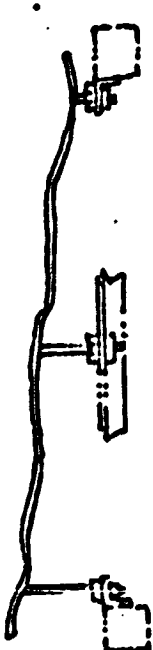
<u>CROSS SECTION</u>			<u>TYPE SUPPORT</u>	
I.			<u>EDGE - FIXED</u>	
II.			<u>SURFACE - CONTROLLED</u>	
III.				
<u>CONF</u>	<u>MATERIAL</u>	<u>COST FACTOR</u>	<u>COEF. OF LINEAR EXPANSION/C.</u>	
I	PLYWOOD BASE POLYURETHANE CORE POLYESTER SURFACE	70%	$55 \times 10^{-6}$	
II	POLYESTER & GLASS LAYUP SHELL	85%	$35 \times 10^{-6}$	
III	EPOXY/FILLER & GLASS LAYUP	100%	$10 \times 10^{-6}$	

FIGURE 4.1-1

#### 4.1.3 Model Surface Detail

The contour arrangement, shown on drawing Figure 4.1-2, was developed to provide optimized flight areas for FOL flight over both rough and smooth terrain. Saddles are provided to permit smooth transition from one model scale to the other. The 250:1 contour was optimized to provide a non-repeating flight path of approximately 6 to 7 NM.

The surface details, shown on Figure 4.1-3 provides terrain which is considered to be applicable for helicopter flight. The scene includes towns, rivers, airfields, stage fields, and confined landing areas.

#### 4.1.4 Probe Configuration

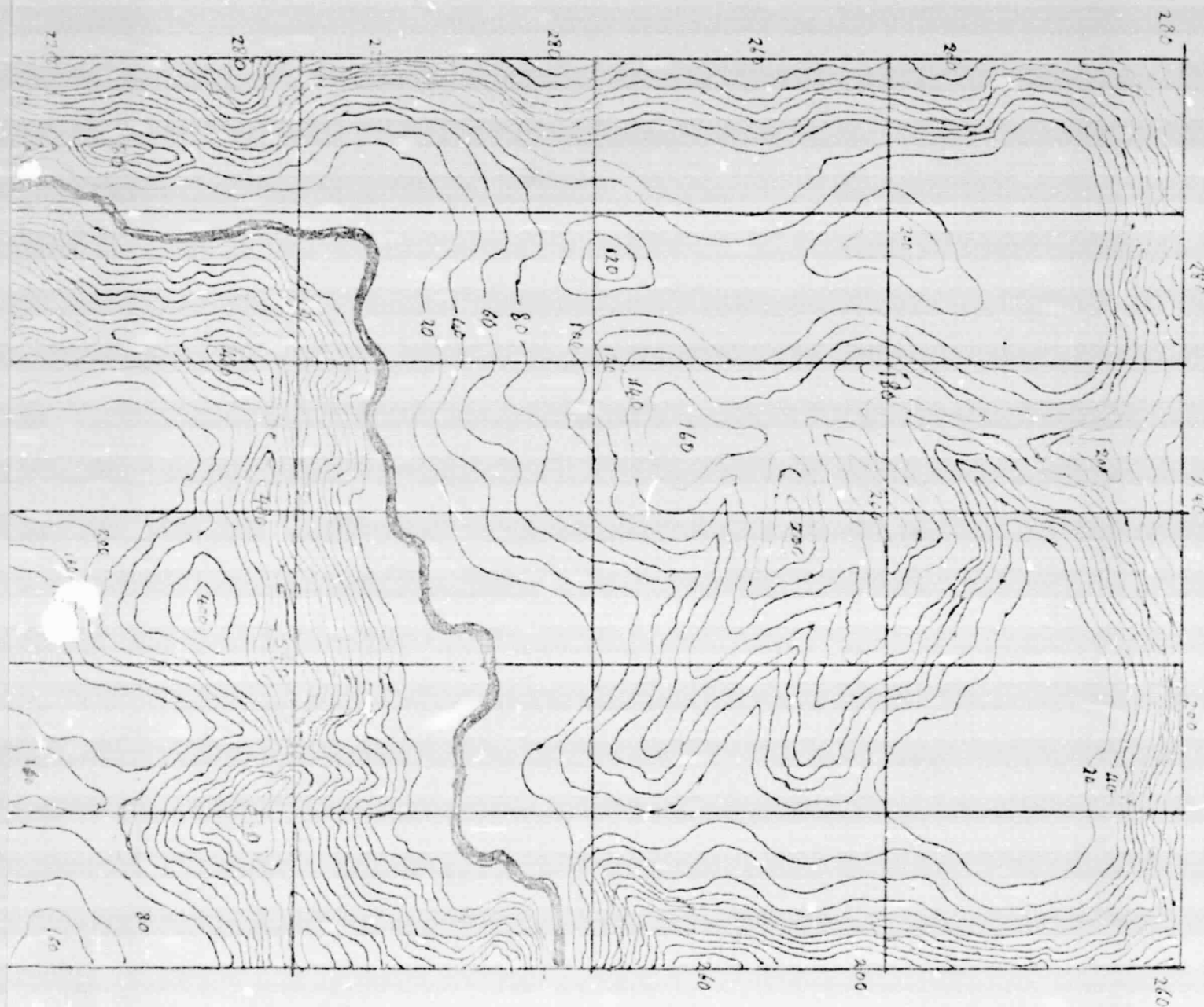
The probe configuration which provides the best compatibility with the model is shown in Figure 16 of the Farrand Report ER 580 included in section 5.2. This configuration is considered optimum for the following reasons:

- (1) The head diameter at the pitch axis (1.5 inch or approximately 32 feet scaled at 250:1) permits approaches to an eye height of 5 feet (with a flat terrain base of 32 feet) with terrain gradients up to 45 degrees.
- (2) The main probe body is approximately 7 inches from the pitch prism with a profile that varies from 4 inches to 1.5 inches below the body. The head profile represents minimum occlusions to the fill lighting. The area underneath the body is more than adequate to accomodate lighting fixtures.

1/2" = 40'  
1" = 20'

Sketch Design by John Piper Ltd  
Kingston-upon-Thames, Surrey U.K.

Issue 3/29/77 J. Piper.



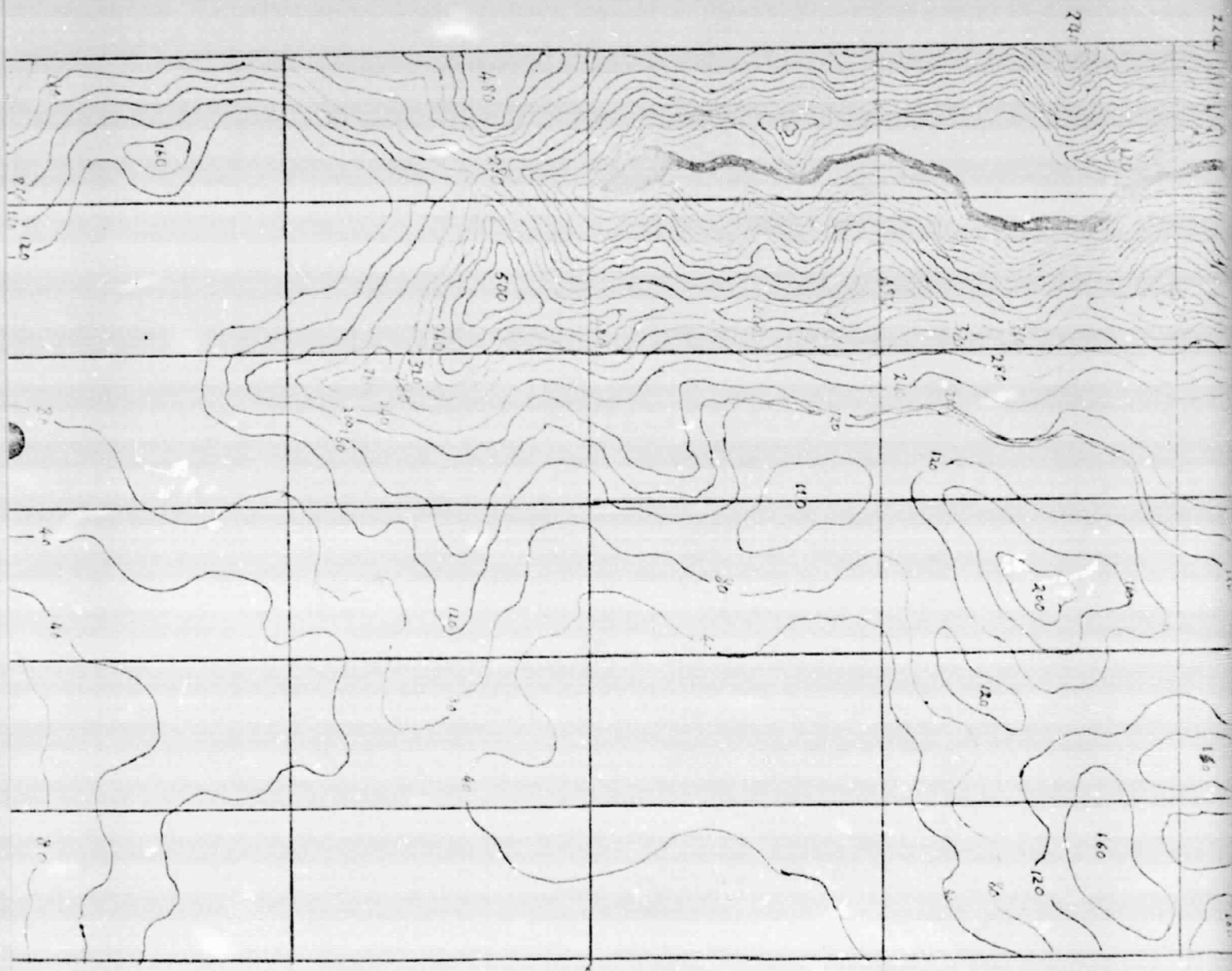
ORIGINAL PAGE IS  
OF POOR QUALITY

THESE PAGES CONTAIN  
FIGS 4.1-2

PD-702

Scale  $\frac{1}{4}$  Inch = 1 Ft

Contour Interval 1:500 Scale  
1:250 Scale



Scale  
cale

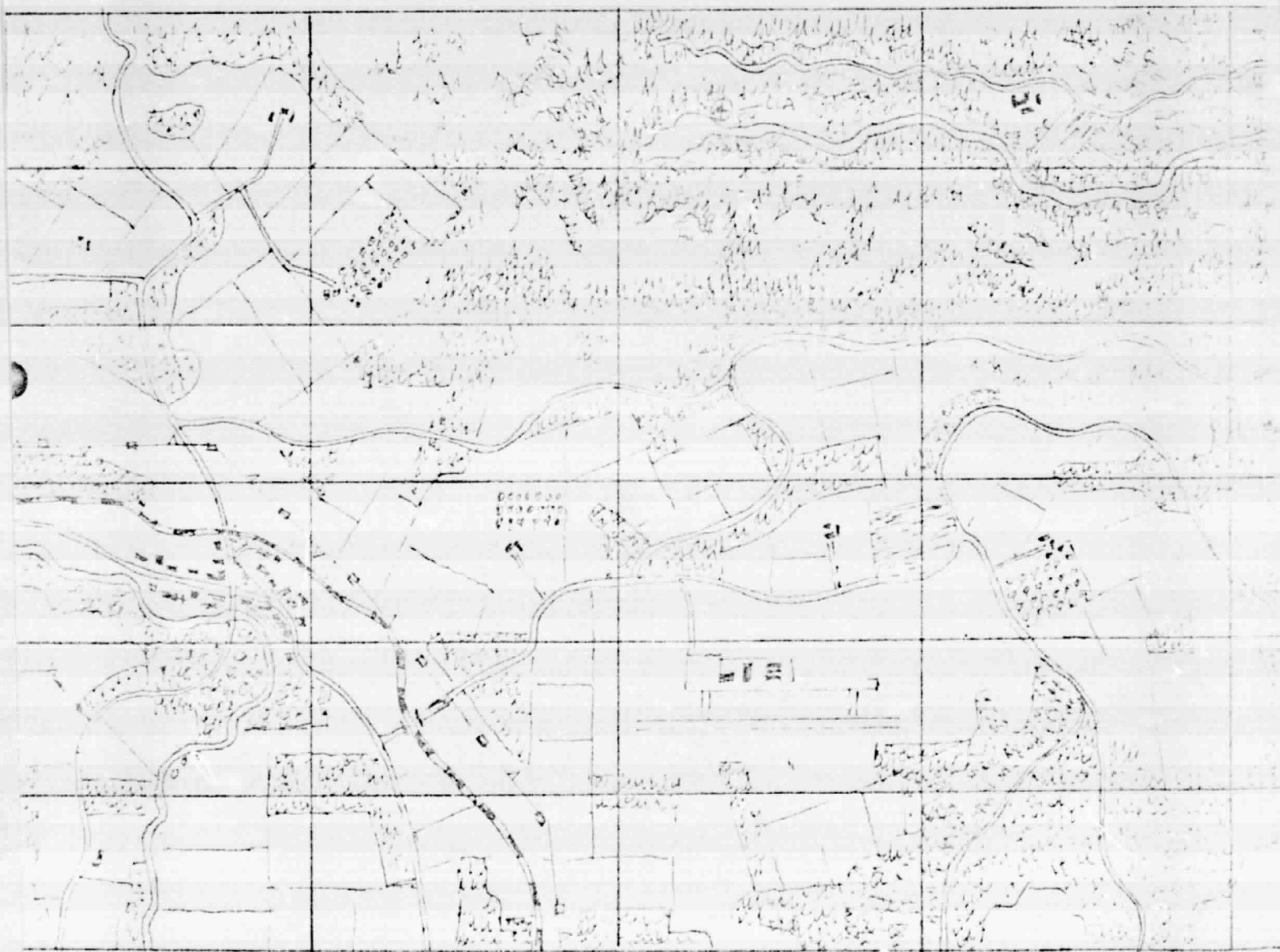
Sketch Design by John Piper Ltd.  
Kingston-upon-Thames Surrey U.K.

Issue 3/30/77 ~~John Piper~~.



Kingston-upon-Thames Surrey U.K.

PD-703    Scale  $\frac{1}{4}$  Inch = 1 Ft    Surface Detail    1:500 Scale  
1:250 Scale



ORIGINAL PAGE IS  
OF POOR QUALITY

General Servo Requirements

This section defines general design and performance criteria for the eleven servos of the proposed wide-angle image generation and display system. Sections of this report covering subsystem detail descriptions contain specifications and requirements of individual servos. Servo analytical results of the study are developed in 4.2.1 of this section.

(1) Servo Identifications - The servos which control motions of projection and image generation equipment of the system are listed in Table 4.2-1.

<u>Equipment Subsystem</u>	<u>Servo Name</u>	<u>Servo Symbol</u>	<u>Servo Type</u>
Detailed and Peripheral Display Projector:	Projector Roll	$\phi_P$	Noncontinuous
Sky-Horizon Projector:	Sky-Horizon Yaw	$\psi_S$	Continuous
	Sky-Horizon Pitch	$\theta_S$	Noncontinuous
	Sky-Horizon Roll	$\phi_S$	Noncontinuous
Probe:	Probe Heading	$\psi_M$	Continuous
	Probe Pitch	$\theta_M$	Noncontinuous
	Probe Roll	$\phi_M$	Continuous
	Probe Focus	$F_M$	Noncontinuous
Gantry:	Gantry X-Axis	$X_M$	See Discussion Below
	Gantry Y-Axis	$Y_M$	
	Gantry Z-Axis	$Z_M$	

TABLE 4.2.1 - SERVO IDENTIFICATION

The continuous servo types in Table 4.2-1 are servos which control continuous rotations, i.e. the capability for positional control over an unlimited range of displacement. Servos of this type are designed to accept voltage commands from the computer which are formulated in terms sine and cosine of the angle to be represented,

(1) Servo Identifications (continued) - instead of the angle.

The sine and cosine formulation of the command avoids angular limitations since these are bounded functions. Figure 4.2-1 provides a more detailed explanation of the feedback technique for these servos.

The noncontinuous servo types in Table 4.2-1 are servos which control mechanisms with limits on displacement. Servos of this type have a conventional position command provided by the computer.

The translational gantry servos,  $X_M$ ,  $Y_M$ ,  $Z_M$ , in Table 4.2-1 receive position feedback signals from angular feedback sensors driven by precision rotating drive gears from the main rack gears of the translating carriage drives. These feedback sensors therefore rotate many revolutions over the total translational displacements of these servos. As with the continuous servos described above, these rotating feedback sensors are designed to accept voltage commands from the computer which are sine and cosine functions of the sensor (and sensor drive gear) shaft angle. This approach results in very accurate positioning control of the gantry over the large displacements involved, since the feedback sensor is cycled many times over the total travel. The carriage positioning accuracy achieved with this technique is analytically developed in Section 4.2.1.

The gantry servos also incorporate multi-turn linear feedback potentiometers, geared to provide a linear signal proportional to the total travel. This signal is provided for computer monitoring during initial positioning control of the gantry carriages. Initializing is computer controlled by rate commands applied to the servos with the sine and cosine positioning commands held at zero. The actual-versus-desired initial position is monitored by the computer by means of the signal from the linear feedback potentiometer. Computer switching to the accurate control of the sine and cosine position commands completes the initializing when the desired position is approached. Section 2.3.8 gives a more detailed description of this gantry servo initializing technique.

(2) Servo Input Voltage Commands - Input signals for all servos are DAC voltages scaled to a  $\pm 10$ -volt range. A schedule identifying servo input signals for each of the servos is given in Table 4.2-2.

Servo	Servo Type	Computed Servo Input Signals	
		Position Command	Velocity Command
$\phi_P$	Noncontinuous	$(\theta_P)i$	$(\theta_P)vi$
$\psi_S$	Continuous	Sine $(\psi_S)i$	$(\psi_S)vi$
		Cosine $(\psi_S)i$	
$\theta_S$	Noncontinuous	$(\theta_S)i$	$(\theta_S)vi$
$\phi_S$	Noncontinuous	$(\theta_S)i$	$(\theta_S)vi$
$\psi_M$	Continuous	Sine $(\psi_M)i$	$(\psi_M)vi$
		Cosine $(\psi_M)i$	
$\theta_M$	Noncontinuous	$(\theta_M)i$	$(\theta_M)vi$
$\phi_M$	Continuous	Sine $(\theta_M)i$	$(\theta_M)vi$
		Cosine $(\theta_M)i$	
$F_M$	Noncontinuous	$(F_M)i$	
$X_M$		Sine $(\theta_{X_M})i$	$(X_M)vi$
		Cosine $(\theta_{X_M})i$	
$Y_M$	See discussion in this section	Sine $(\theta_{Y_M})i$	$(Y_M)vi$
		Cosine $(\theta_{Y_M})i$	
$Z_M$		Sine $(\theta_{Z_M})i$	$(Z_M)vi$
		Cosine $(\theta_{Z_M})i$	

TABLE 4.2-2 - SERVO INPUT VOLTAGE COMMANDS

As shown in Table 4.2-2, all servos of the display system (except the probe focus servo,  $F_M$ ) are supplied with positions inputs augmented by inputs proportional to the commanded velocity. These velocity commands serve to augment the position commands in the following respects:

. Synchronization - The availability of a velocity input command is useful in achieving accurate dynamic synchronization of the servo output response. Accurate dynamic synchronization is important between the three (3) rotational servos of the probe. Also

. Synchronization (continued) - synchronization is important between the probe servos and the servos that control the sky-horizon projector and the roll servo of the detailed and peripheral projector platform. The velocity input is especially useful in dynamically synchronizing the continuous rotational servos because the use of networks on sine/cosine input commands is not a feasible compensation method for these servos.

. Smoothness - The availability of a velocity input command permits a proportionally greater amount of velocity versus position feedback gain. Jitter-free projection of the optically and electronically magnified scene is improved by greater velocity feedback control.

. Dynamic Tracking Error - The velocity input commands are used in the gantry servos to limit the servo tracking errors during changes in steady-state velocity commands. This result is described in greater detail in Section 4.2.1. The velocity inputs to the gantry servos are also used in controlling the initial positioning of the gantry as described in Section 4.2(1).

The total required number of DAC input voltages from Table 4.2-2, is 23. This number assumes that the input position and velocity signals for the noncontinuous servos,  $\theta_P$ ,  $\theta_S$ ,  $\phi_S$ , and  $M$ , are combined in the digital computer so that only a single DAC voltage command is required for each of these four servos.

(3) Servo Control Power - Control power requirements of the servos are largely established by the inertias of the driven elements in conjunction with peak acceleration and velocity requirements of the servo motion envelopes. The final torque selections for each servo must therefore be made by an assessment of inertias from the final detail design.

Acceleration and velocity requirements for the servos have been developed and are covered in the general servo requirements Section 4.2(5)

Additional servo torque increments must also be considered which are imparted from accelerations of the motion base to the projector servos of the display system. These projector servos

(3) Servo Control Power (continued) - are subject to disturbance torques due to the external angular accelerations from the motion base. The magnitude of these torques also depend on the inertias of the driven elements of the servos. Accelerations of the motion base have been defined for the study by AMRDL memorandum. Nominal motion base acceleration levels from this memorandum are listed for reference in Table 2.2-3 of this report.

(4) Servomechanism and Structural Design Considerations -

. Smoothness - To achieve the necessary smoothness of servo response, it is essential to minimize all sources of small, discontinuous nonlinearities in the specification or design of components of the display servos. Specifically these nonlinearities include:

- . nonlinear friction in the servo drive (static and coulomb friction),
- . backlash,
- . poor smoothness quality in the output voltages of feedback sensors, and
- . threshold, deadband, or cogging in actuators (motors) of the servos.

. Structural Dynamics - The dynamics of structures are of concern primarily in the gantry and roll projector platform servos. These servos are required to move large inertia loads over large displacements, and structures are consequently large and heavy. The structural dynamics affect the response of projector or optical elements of these servos in the following ways:

- . the transmissibilities of the intermediate moving structural elements which transmit motion from the driving point of the servo to the controlled projector or probe directly affect the dynamic response of the projector or probe, and
- . the transmissibility of the backup structure, on which the driving point of the servo relies for support also appears in the output response of the servo.

The equations of motion of the gantry structures were not developed and analyzed as part of the study because in final detail design these structures were judged to be easy to brace and the loads to be well distributed. The moving and backup structures of the

. Structural Dynamics (continued) - roll projector platform servo present a more difficult design problem and the conceptual design of these structures were extensively studied. The analytical development and results are presented in Section 4.2.2 of this report.

. Travel Stops and Travel Limit Sensors - Soft travel stops with overtravel are specified to control and limit the deceleration forces on all non-continuous servos which may occur due to inadvertent overtravel.

Limit sensors are specified on all non-continuous servos to remove or limit control power to the servo actuators when the servo is inadvertently driven into the travel stops. Remote reset capability is specified to allow these servos to be restored to normal operation.

. Lockouts - Removable mechanical lockouts are specified for all continuous and non-continuous servos. These lockouts are specified to provide a means of securing moving mechanisms during handling and shipment and also to provide a precise, repeatable calibration reference for position sensor alignment.

(5) Servo Performance - This section discusses the servo performance specifications used in the subsystem descriptions of this report.

. Motion envelope - Required displacements, peak no-load velocities and peak stall accelerations are specified for each servo in the subsystem specifications. The specified stall accelerations and peak no-load velocities take into account expected simultaneous levels of both acceleration and velocity. The accelerations specified for the projector servos also account for accelerations imparted from the motion base.

Acceleration and velocity requirements have been studied by considering the following:

- . required peak aircraft motions,
- . order and orientation of the probe and sky-horizon projector gimbals, and
- . model scaling.

. Motion envelope (continued) - Peak aircraft motion requirements are from the Statement of Work and are listed for reference in Table 2.2-2 of this report. The gimbal motion analysis is presented in Section 4.2.3.

. Static Accuracy - Static servo positioning accuracy is one of the factors in the end-to-end accuracy of the placement of the projected image on the projection screen (others are T.V., optical probe and mechanical alignment errors). Required static positioning accuracies are specified for each servo in the subsystem descriptions of this report. The design goal positioning accuracy of the display from the Statement of Work is listed for reference in Table 2.2-1 of this report.

To achieve accurate servo static positioning, the following techniques are specified for the display servos:

- . Mechanizations are specified which contain an integrating amplifier in the forward path of the servo. This integrating amplifier acts to reduce the position error signal to virtually zero during static positioning. The action of the integration also makes the static positioning accuracy of the servo independent of static torques (or force) thresholds or loading on the output of the servo.
- . Servo mechanizations are also specified to include a unity voltage follower immediately following each feedback pot wiper output signal. This follower amplifier is physically located as near to the potentiometer as practical and the extremely high input impedance of this voltage follower, estimated to be 1000 megohms, serves to virtually eliminate errors due to pot loading.
- . The method by which the position error signal is generated in the continuous sine/cosine servos depends first upon exciting the sine/cosine feedback pots with the computer generated sine/cosine commands, and secondly, upon summing the output wiper voltages of the sine/cosine feedback pots.

• Static Accuracy (continued) -

- The overall positioning accuracy of these servos depends in part, on retaining the accuracy of the computed sine/cosine command up to the point where the excitation signals are applied to the sine/cosine pots, also upon the accuracy of the summation of the output sine/cosine feedback pot wiper voltages. For this reason matched and temperature compensated resistor pairs are specified in the amplifiers which handle these critical functions.

With the application of the techniques described above, remaining static positioning errors occur almost entirely from two sources:

- Feedback potentiometer linearity (or conformity) errors, and
- Gearing errors between the feedback pot shaft and the applicable controlled output of the servo.

These error sources are developed in the servo accuracy analyses of Section 4.2.1.

• Static Repeatability - Static repeatability accuracy is specified for each servo in the subsystem specifications. With the application of the servo design techniques specified above, backlash in gearing is the only significant error source in the determination of static repeatability accuracy.

• Static Compliance - An integrating amplifier is specified in the forward path of each visual display servo. The action of this integrating amplifier causes the closed loop dc sensitivity (gain) of each servo output displacement to disturbance torques or forces applied at the servo output, to be virtually infinite. This means that the servos are capable of resisting any externally applied output torque (or force) up to the peak motor torque, without having to hold a corresponding error in position. The result is a static servo compliance which is virtually zero.

• Dynamic Range - The capability of the visual system servos to smoothly control the movement of the projected image over a wide range of velocities, is a critical requirement. The dynamic range defines the ratio of the largest to the smallest velocity which the servo can smoothly control. The maximum velocity

. Dynamic Range (continued) - for each servo is defined by the motion envelope in the detailed servo specifications. The corresponding minimum velocity is thereby defined by the dynamic range. The dynamic range is specified for each servo in the subsystem specifications.

Smoothness of the servo output response is specified on the basis of the dynamic range by the requirement that velocity variation at the minimum velocity not exceed  $\pm 20\%$  of the commanded velocity. Compliance with the smoothness performance specifications is best demonstrated by using the tachometer signal for the evaluation, but with much of the higher frequency content of the signal attenuated by a second-order filter having dynamic characteristics set at the dynamic response selected for the angular visual system servos, i.e., by a second-order filter with a natural frequency of 25 rad/sec and a damping ratio of 0.7.

. Frequency Response - A critical requirement in achieving an accurate representation of the external visual scene is synchronization of all servos involved in projecting the scene. This requires that the servos have the same dynamic response (transient and steady state) as well as a high degree of smoothness. To accurately control the synchronization of the visual system servos, the dynamic response for all angular visual system servos is specified to accurately match that of a second-order system with a damping ratio of 0.7 and a natural frequency of 25 rad/sec. The steady-state time lag of this second-order model to a constant velocity command is 56.6 milliseconds. The accuracy of the synchronization is specified in the detail servo specifications by the requirement that the actual servo frequency response match that of the ideal second-order system, over the frequency range specified, within the stated tolerance, in terms of phase angle deviation.

The frequency response of the gantry servos and the probe focus servo are defined according to other criteria in the detail servo specifications.

. Time Response - Specification of time response is another means of assuring the dynamic match (synchronization) between the actual velocity step response of each angular visual system servo versus the step response of the 0.7 damped, 25 rad/sec, second-order

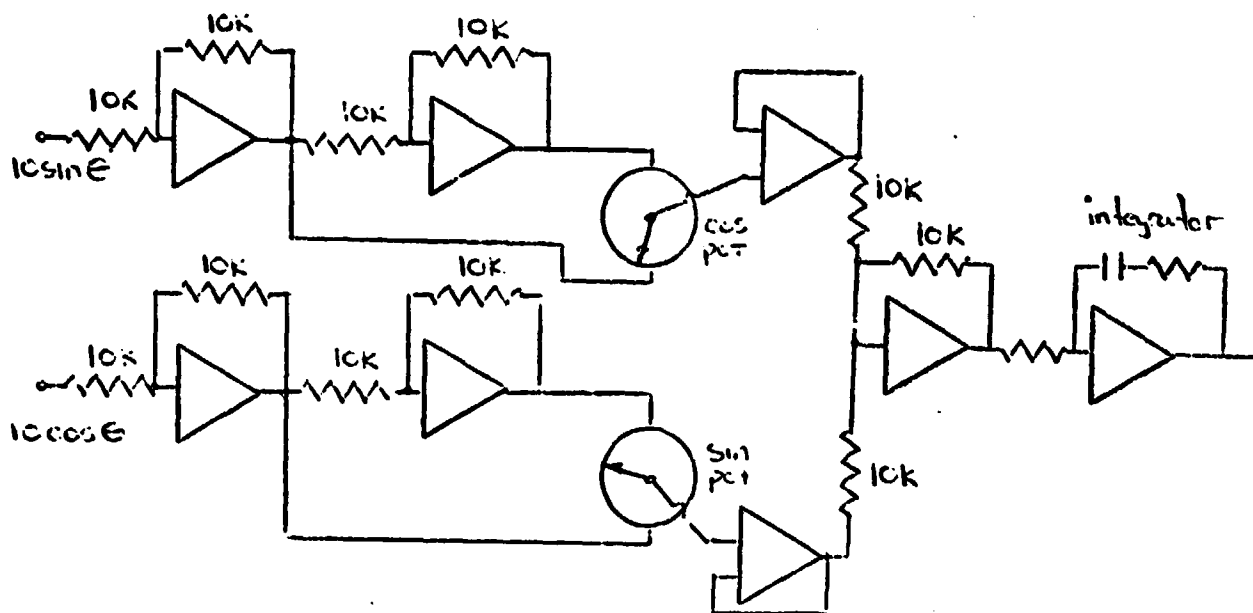
#### 4.2.1 Gantry and Probe Servos

The gantry and probe servos control the mechanical motion which position the probe camera relative to the terrain model. Translational motions ( $X_M$ ,  $Y_M$ , and  $Z_M$ ) are provided by the gantry servos. Rotational motions ( $\phi_M$ ,  $\theta_M$ , and  $\psi_M$ ) are provided by mechanisms inside the probe assembly. In addition, a focussing servo is provided to maintain optical focus as the slant range between the probe and terrain model varies.

In this section, details of the gantry translational servo performance are described. The requirements for the performance of the probe rotational servos and the focussing servo are derived. Information on implementation of these requirements was provided by the probe subcontractor (see Section 5.2).

### Gantry Accuracy

The X-axis is evaluated as typical of the three (3) gantry servos. A sketch of the X-axis servo front end is shown below:



Static Repeatability - The integrator shown in the above sketch provides near infinite dc open loop gain such that the static closed loop system becomes independent of forward loop non-linearities. All errors will be evaluated by superposition (errors of errors are significant). The position feedback sensors use antibacklash gearing such that the static repeatability depends only on the following elements:

- 1) Amplifier resistor drift as a function of temperature
- 2) Amplifier drift as a function of temperature
- 3) Rack and model length change as a function of temperature

### Resistor Temperature Drift

All resistors before the forward loop integrator have a matched temperature coefficient of 10 ppm/°C. It is assumed the maximum temperature change within the control console is  $\pm 10^{\circ}\text{C}$ .

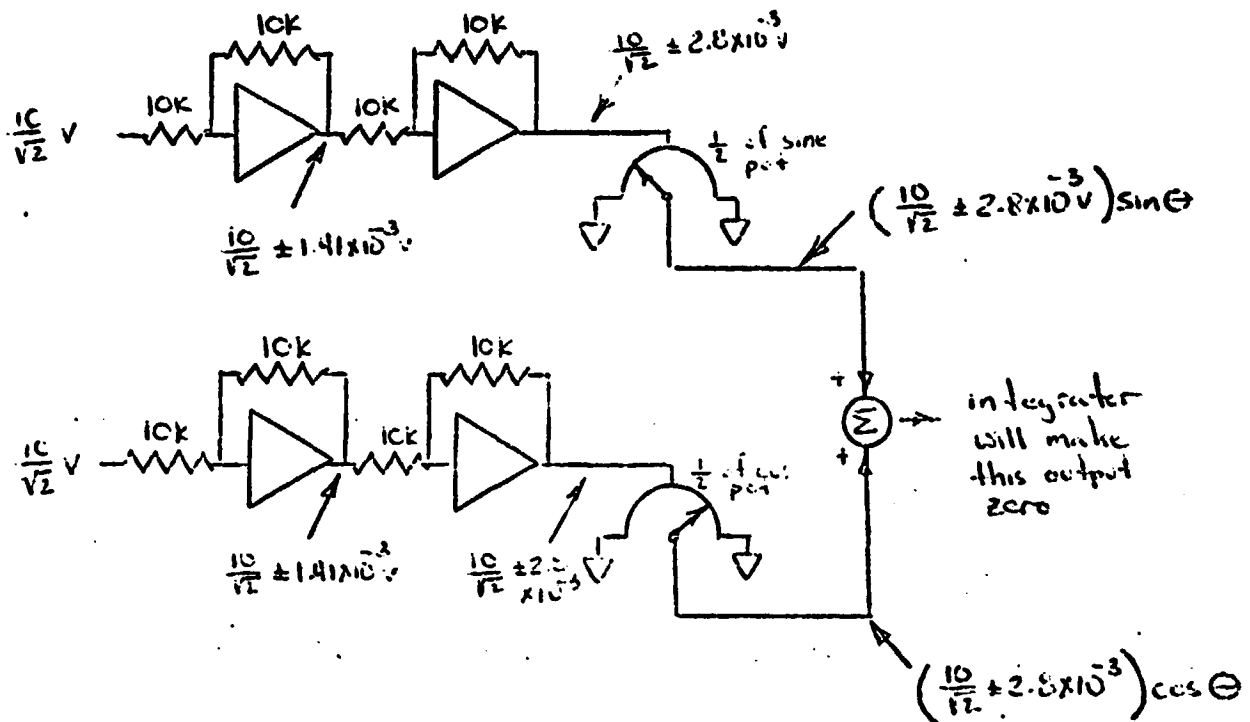
### Resistor Temperature Drift (continued)

The maximum resistor change then becomes:

$$\frac{10}{10^6} \times 20 = 20 \times 10^{-5} \text{ parts}$$

From paragraph 4.2.2 the worst case position for the sine/cosine pot is  $\pi/4$  radians. This position will give an input to the servos of  $\frac{10}{\sqrt{2}}$  volts. Each amplifier will then have an error at its output due to resistor change of:

$$\frac{10}{\sqrt{2}} (20 \times 10^{-5}) = 1.41 \times 10^{-3} \text{ volts}$$



The output of the sine pot must equal the output of the cosine pot

$$\left( \frac{10}{\sqrt{2}} \pm 2.8 \times 10^{-3} \right) \sin \theta = \cos \theta \left( \frac{10}{\sqrt{2}} \pm 2.8 \times 10^{-3} \right)$$

or for the worst case

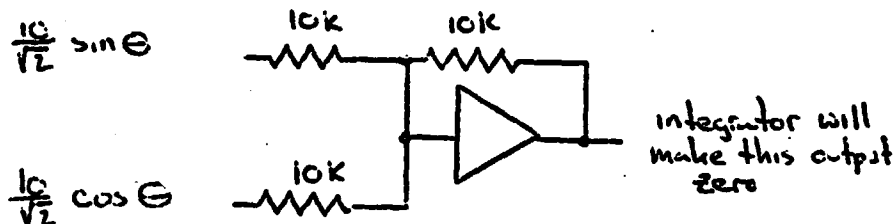
$$\tan \theta = \frac{\frac{10}{\sqrt{2}} + 2.8 \times 10^{-3}}{\frac{10}{\sqrt{2}} - 2.8 \times 10^{-3}}$$

$$= 45 \pm 0.0227 \text{ degrees}$$

### Resistor Temperature Drift (continued)

The position repeatability error is then  $\pm 0.0227^\circ$  for the amplifiers that drive the sine/cos pots.

The resistor repeatability error of the amplifier which sums the outputs of the sine and cosine pot is:



$$\text{Then } \frac{10}{\sqrt{2}} \sin \theta \left( \frac{10K}{10K + 20 \times 10^{-5} \times 10K} \right) = \frac{10}{\sqrt{2}} \cos \theta$$

$$\text{or } \tan \theta = 1 \pm 20 \times 10^{-5}$$

$$\theta = 45 \pm 0.0057 \text{ degrees}$$

The position repeatability error is then  $\pm 0.0057^\circ$  for the summing amplifier. The total repeatability error due to resistor drift then becomes:

$$E_R = \sqrt{\left( \pm 0.0227 \right)^2 + \left( \pm 0.0057 \right)^2} = \pm 0.023^\circ$$

The feedback pot is driven by a 4" diameter gear on a rack. The above resistor drift error referenced to the gantry motion then becomes:

$$\pm 0.023^\circ \times \frac{4 \text{ in.}}{360^\circ} = \pm 8.03 \times 10^{-4} \text{ inches}$$

### Amplifier Temperature Drift

All amplifiers up to and including the integrator are Burr Brown Model 3500C trim adjusted to zero at  $25^\circ\text{C}$ . The noninverting input of inverting amplifiers will be referenced to ground through a resistor equal to the parallel combination of the inverting input and feedback resistors. This will realize a minimum offset current effects. The temperature characteristics for this amplifier for a  $20^\circ\text{C}$  temperature change is shown on the next page.

### Amplifier Temperature Drift (continued)

$$\begin{aligned}\text{Input Offset Voltage} &= \pm 100\mu\text{v} = e_{os} \\ \text{Input Bias Current} &= \pm 6\text{ n a} = i_b \\ \text{Input Difference Current} &= \pm 2\text{ n a} = i_d\end{aligned}$$

The drift of any unity gain inverting amplifier with input and feedback ( $R_f$  &  $R_i$ ) resistors of 10K becomes:

$$\begin{aligned}E = \text{Error} &= \frac{R_f}{R_i} \left[ e_{os} \left( \frac{R_f + R_i}{R_f} \right) + i_b R_i + i_d R_i \right] \\ &= 2 e_{os} + 10^4 (i_b + i_d) \\ &= 2 \times 10^{-4} + 10^3 (6 + 8) \times 10^{-9} = 0.21 \times 10^{-3} \text{ volts}\end{aligned}$$

This amplifier temperature drift is less than 1/5 the resistor temperature drift and will, therefore, be neglected.

### Rack and Model Change With Temperature

The model lighting will cause a temperature rise in both the model and the feedback gear rack. Experiments on a Piper Ltd. polyester and glass model showed a temperature change of 60 degrees F with mercury arc lamps at ten feet and a power level of 188 watts/ft<sup>2</sup>. After one half hour the model stabilized at a steady state temperature of 115°F. It is assumed that the epoxy/filler and glass layup model material will have near identical heating and steady state temperature characteristics. An initial one half hour warmup will be required before system operation thereby eliminating the model growth during this period. The model and gear rack change with room temperature will, however, effect the system repeatability.

It is assumed the room temperature is controlled within  $\pm 5^\circ\text{F}$ . The model and rack have positive coefficient of linear expansion of

$$\text{Model } 10 \times 10^{-6} \text{ unit/unit}/^\circ\text{C} \quad (5.6 \times 10^{-6} \text{ unit/unit}/^\circ\text{F})$$

$$\text{Steel rack } 6.3 \times 10^{-6} \text{ unit/unit}/^\circ\text{F}$$

### Rack and Model Change With Temperature (continued)

If it is further assumed that both the model and gear rack change in length due to temperature from the center out the following repeatability may be determined.

$$\begin{aligned}\text{length change} &= (30 \text{ ft.}) \left(12 \frac{\text{in}}{\text{ft}}\right) (6.3 \times 10^{-6} - 5.6 \times 10^{-6}) / ^\circ\text{F} (+5^\circ\text{F}) \\ &= + 1.3 \times 10^{-3} \text{ inches}\end{aligned}$$

The total repeatability error then becomes the RSS sum of the resistor temperature drift and model/rack temperature change.

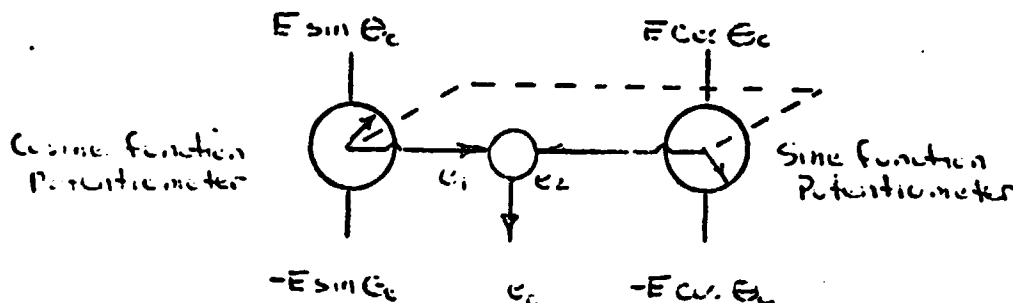
$$\begin{aligned}\text{Total Repeatability} &= + \sqrt{(+ 8.03 \times 10^{-4})^2 + (+1.3 \times 10^{-3})^2} \\ &= + 1.52 \times 10^{-3} \text{ inches}\end{aligned}$$

Static Accuracy -The static accuracy of the X-axis gantry is a function of the following items:

- 1) Static repeatability error
- 2) Sine/cosine feedback conformity error
- 3) Resistor accuracy
- 4) Gear error

### Sine/Cosine Feedback Error

The relationship between the potentiometer conformity specification and the corresponding servo positioning error is based on the following analytical derivation.



$E$  = voltage scaling of the sine/cosine functions of  $\theta_c$  volts.

### Sine/Cosine Feedback Error (continued)

Where:

- $\theta_c$  = command angle (radians)
- $\theta_f$  = potentiometer shaft position angle (radians)
- $e_1$  = voltage output of cosine function pot (volts)
- $e_2$  = voltage output of sine function pot (volts)
- $C$  = independent conformity of sine or cosine pot expressed as a percentage of the full pot excitation voltage

$$e_1 = E \sin \theta_c \cos \theta_f \pm 2E \left( \frac{C}{100} \right) \sin \theta_c$$

$$e_2 = E \cos \theta_c \sin \theta_f \pm 2E \left( \frac{C}{100} \right) \cos \theta_c$$

The electrical portion of the servos contains an integrator in the forward part of the servo loop which will provide infinite dc open loop gain thereby making  $e_1 - e_2 = 0$ .

Then:

$$\begin{aligned} E \sin \theta_c \cos \theta_f \pm 2E \left( \frac{C}{100} \right) \sin \theta_c - E \cos \theta_c \sin \theta_f \pm 2E \left( \frac{C}{100} \right) \cos \theta_c &= 0 \\ \pm 0.02 C \sin \theta_c \pm 0.02 C \cos \theta_c &= \sin \theta_c \cos \theta_f - \sin \theta_f \cos \theta_c \\ &= \sin(\theta_c - \theta_f) \\ &= (\theta_c - \theta_f) \text{ for small angles} \end{aligned}$$

The servo position error due to the sine/cosine feedback pot error is:

$$\epsilon = \theta_c - \theta_f$$

$$\epsilon = \pm 0.02 C \sin \theta_c \pm 0.02 C \cos \theta_c$$

The worst case error occurs at  $\frac{d\epsilon}{d\theta_c} = 0$

$$\frac{d\epsilon}{d\theta_c} = 0 = \pm 0.02 \dot{\theta}_c \cos \theta_c \pm 0.02 C \dot{\theta}_c \sin \theta_c$$

$$\theta_c \text{ worst case} = \pm \frac{\pi}{4} \pm \frac{\pi}{4}$$

Then:

$$\epsilon \text{ worst case} = \frac{\sqrt{2}}{100} C \pm \frac{\sqrt{2}}{100} C \text{ radians}$$

### Sine/Cosine Feedback Error (continued)

A sine/cosine feedback pot with a conformity of  $\pm 0.1\%$  has been selected for this application. Then:

$$\epsilon \text{ worst case} = \pm 0.081 \pm 0.081 \text{ degrees}$$

The feedback pot is driven by a 4" diameter gear on the rack. The pot error referenced to the gantry motion then becomes:

$$(\pm 0.081^\circ \pm 0.081^\circ) \frac{4 \pi \text{ in}}{360^\circ} = \pm 2.83 \times 10^{-3} \pm 2.83 \times 10^{-3} \text{ in.}$$

### Resistor Accuracy

All the  $10K\Omega$  resistors shown in the sketch of paragraph 4.2.1 are matched pairs to within 0.05% or  $50 \times 10^{-5}$  parts. This error is 2 1/2 times the resistor temperature error. The error due to resistor tolerance then becomes.

$$\pm 8.03 \times 10^{-4} \text{ (in)} (2.5) = \pm 2 \times 10^{-3} \text{ inches}$$

### Gear Error

The only gears which cause position errors are the four inch gear on the feedback sine/cosine pot and the long gear rack attached to the carriage rail.

In this application an antibacklash gear is used such that the gear teeth are loaded so as to track along one side of the backlash. From gear theory the angle  $\theta_m$  which gives the maximum position error is:

$$\frac{e}{E} \max = \frac{\sin \theta_m}{1 + \frac{PD_2}{PD_1}} \pm \tan \phi (1 - \cos \theta_m)$$

Where:

$e$  = position error

$E$  = total eccentricities

$\theta_m$  = rotation of antibacklash gear which gives maximum error

$PD_2$  = pitch diameter antibacklash gear = 4 inches

$PD_1$  = pitch diameter of rack =  $\infty$

$\phi$  = gear pressure angle =  $20^\circ$

### Sine/Cosine Feedback Error (continued)

Substituting in the above constants yields:

$$\begin{aligned}\frac{e}{E} \max &= \frac{\sin \theta_m}{1 + 4/\omega} \pm \tan 20^\circ (1 - \cos \theta_m) \\ &= \sin \theta_m \pm 0.182 (1 - \cos \theta_m)\end{aligned}$$

The maximum  $\frac{e}{E}$  max occurs at

$$\theta_m = \pm 79.7^\circ \text{ and } \pm 100.3^\circ$$

The value of  $e/E$  max for the maximum  $\theta_m$  is

$\theta_m$	$e/E$ max	
+ 79.7°	1.133;	0.834
- 79.7°	-0.834;	-1.133
+ 100.3°	1.198;	0.770
- 100.3°	-1.198;	-0.770

The maximum peak-to-peak error then becomes  $\frac{e}{E}$  max p-p  
= 1.198 + 1.133 = 2.33 or  $\pm 1.17$ .

For purposes of calculation it is more convenient to use concentricity rather than eccentricity.

$$\text{Concentricity} = C = 2 E$$

$$\text{Then } e_{\max \text{ p-p}} = \frac{1.17}{2} C = \pm 0.585C$$

Listed below are the anticipated gear and fabrication parameters:

SOURCE	CONCENTRICITY (Inches)
Sine/cosine pot runout	0.001
Rack parallel to rails	0.010
Total Composite Error (Gear)	0.005
Total Composite Error (rack)	0.007
Gear Bore to Pot Shaft	0.001
Rack To Rack Non-accumulative Error	0.010
(Rack made of 12, 60" segments)	

Since all the listed errors will not occur simultaneously, they are RSS together.

Sine/Cosine Feedback Error (continued)

$$C_{RSS} = \sqrt{(.001)^2 + (.01)^2 + (.005)^2 + (.007)^2 + (.001)^2 + (.01)^2}$$
$$= 0.0166 \text{ inches}$$

The gear error then becomes:

$$e_{\max p-p} = \pm 0.565 (.0166) = \pm 0.0097 \text{ inches}$$

The total X-axis gantry accuracy then becomes the RSS of the repeatability error, the sine/cosine pot error, the resistor error and the gear error.

$$X \text{ Gantry Accuracy} = \pm \sqrt{(\pm 1.52 \times 10^{-3})^2 + (\pm 2.83 \times 10^{-3})^2 + (\pm 2.83 \times 10^{-3})^2 + (\pm 2 \times 10^{-3})^2 + (\pm 9.7 \times 10^{-3})^2}$$
$$= \pm 0.0108 \text{ inches}$$

Referenced to the pilot this accuracy is  $\pm 2.7$  inches at a model scale of 250:1 and  $\pm 5.4$  inches at a model scale of 500:1.

### Gantry Dynamic Tracking Error

Of particular interest in the gantry servos is the ability of the servo to minimize the dynamic tracking error. The dynamic tracking error is defined as the position error with respect to varying velocity commands.

From Figure 2.3.8-1 it can be seen that the servo has two integrations in the forward path elements, the electrical integrator and the integration from velocity to position. The integration associated with the inertia is an interloop tachometer closure and is not a free forward path integrator. A system with double forward path integrations is a type 2 servo. This type of servo has the ability of producing a closed loop system which will have zero position error for a relatively constant or slowly varying velocity command. However, the transient position error with respect to varying velocity commands is of equal importance. Again referring to Figure 2.3.8-1 the addition of a velocity command will improve the transient behavior of the servo. The electrical compensation and gain in the velocity command are adjusted such that the resultant closed loop servo has the following transfer function:

$$\frac{X_p}{R(s)} = \frac{\frac{S + \omega_n/\zeta}{\omega_n/\zeta}}{\frac{S^2 + 2\zeta\omega_n S + \omega_n^2}{\omega_n^2}}$$

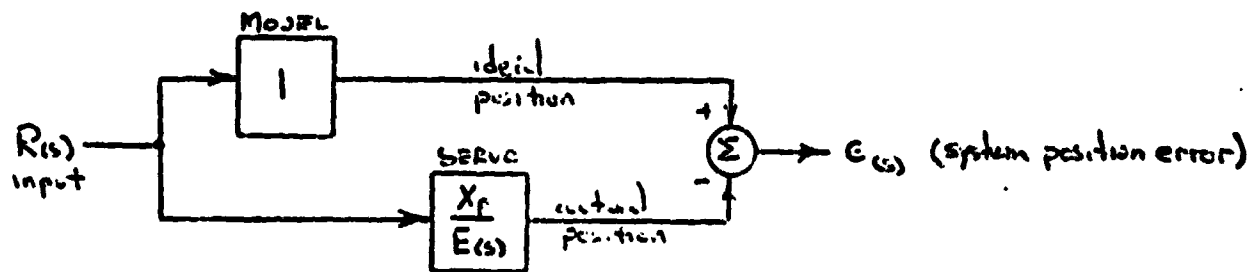
Where:  $R(s)$  = position input command

$X_p$  = Servo position

$\omega_n$  = natural frequency of a second order system

$\zeta$  = damping ratio

The dynamic response and system accuracy may be judged by evaluating the system error. The system error is found by taking the difference between the actual system and an ideal system.



The error as a function of the input becomes:

$$\begin{aligned}
 e(s) &= R(s) \left( 1 - \frac{X_p}{E(s)} \right) \\
 &= R(s) \left[ 1 - \frac{\frac{S + \omega_n/\zeta}{\omega_n/\zeta}}{\frac{S^2 + 2\zeta\omega_n S + \omega_n^2}{\omega_n^2}} \right] \\
 &= R(s) \frac{S^2}{S^2 + 2\zeta\omega_n S + \omega_n^2}
 \end{aligned}$$

For a step command in velocity (ramp command in position)

$$R(s) = \frac{A}{S^2} \quad \text{Where } A \text{ is the amplitude of the velocity step.}$$

The error for this type of command then becomes:

$$e(s) = \frac{A}{S^2 + 2\zeta\omega_n S + \omega_n^2}$$

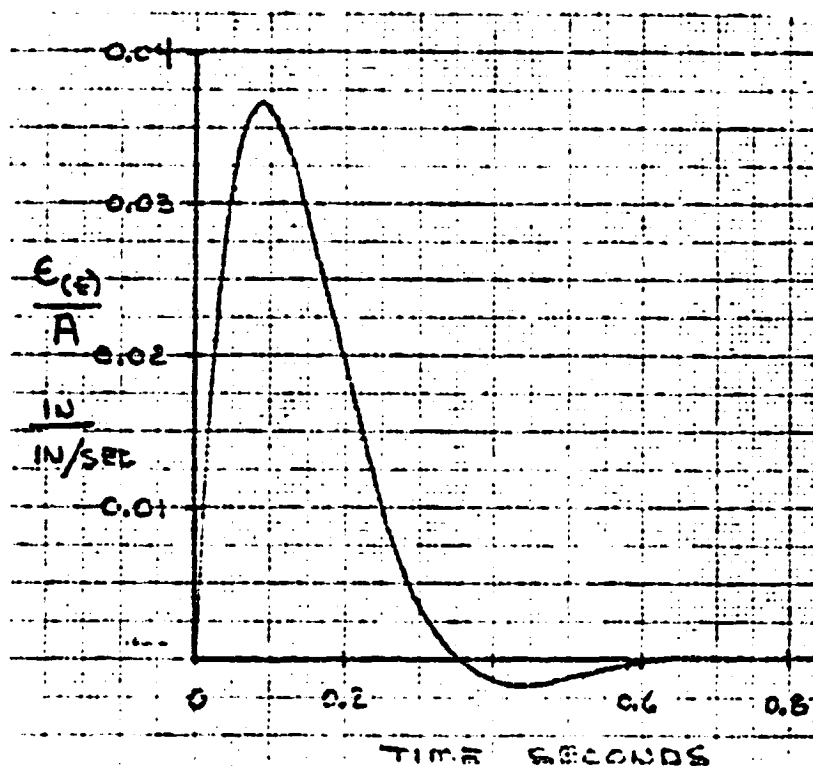
In the time domain

$$e(t) = \frac{A}{\omega_n \sqrt{1-\zeta^2}} e^{-\zeta\omega_n t} \sin \omega_n \sqrt{1-\zeta^2} t$$

Selecting  $\omega_n = 12.5$  rad/sec and  $\zeta = 0.7$

$$e(t) = 0.112 A e^{-8.75t} \sin (8.93t)$$

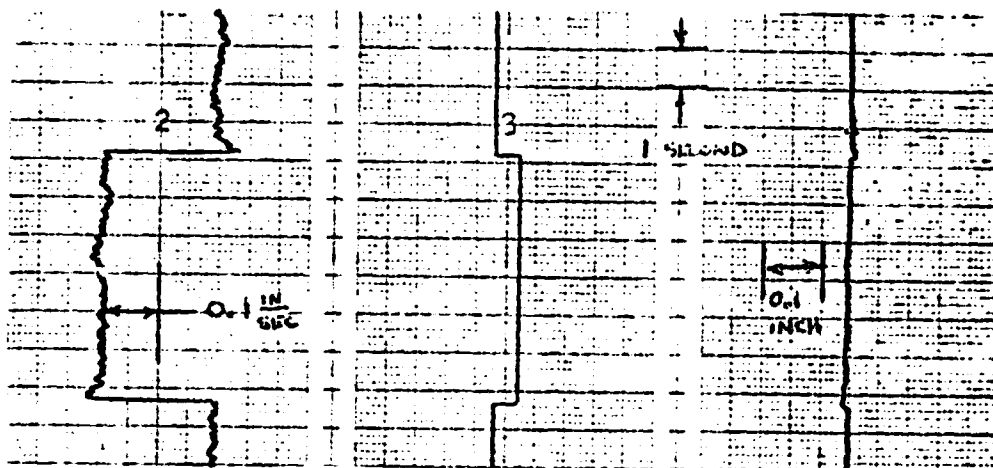
A time history plot of the above yields:



From the plot the maximum position error is 0.036 inches and occurs at 0.08 seconds after the step. The position error is down to 5% of the maximum in 0.32 seconds.

The Northrop terrain model gantry X-axis servo is closed in a similar manner. A strip chart recorder trace is shown below for a  $\pm 0.1$  in/sec step in velocity with the resultant position error.

101-104-104-104



Tachometer  
Output

Velocity Command

Position Error

A good agreement exists between the predicted position error and the error shown on the recorder tape.

### Probe Rotation Requirements

The mechanism within the probe assembly which orients the optical system relative to the terrain model consists of a pitch gimbal supported by a yaw gimbal which is mounted to the housing of the probe. Roll motion is achieved by rotation of an optical element about the optical axis (see Figure 4.2.1-1).

A right hand coordinate system is assumed in this analysis as shown in the figure. Each gimbal has its own coordinate system. When gimbal angles are zero, their coordinate systems coincide with the inertial coordinate system shown.

The following nomenclature defines terms used in this analysis:

$\phi_M, \dot{\phi}_M, \ddot{\phi}_M$	Roll element angular displacement velocity and acceleration relative to the fixed housing
$\theta_M, \dot{\theta}_M, \ddot{\theta}_M$	Pitch gimbal angular displacement, velocity and acceleration relative to the yaw gimbal
$\psi_M, \dot{\psi}_M, \ddot{\psi}_M$	Yaw gimbal angular displacement, velocity and acceleration relative to the fixed housing
$p, q, r$	Simulated aircraft roll, pitch, and yaw velocities
$\dot{p}, \dot{q}, \dot{r}$	Simulated aircraft roll, pitch, and yaw accelerations

For clarity the subscripts p are dropped in the majority of this analysis.

The first optical element encountered by light rays emanating from the terrain model is mounted on the pitch gimbal. To provide the correct image orientation, the coordinate system of this gimbal must coincide with that of the simulated aircraft and have the same velocities and accelerations.

Therefore, through coordinate transformations, the relative velocities  $\dot{\theta}_p$ , and  $\dot{\psi}_p$  are written in the pitch coordinate system. (The roll velocity  $\dot{\phi}$  requires no such transformation since this element could theoretically be placed at any point along the optical axis). These velocities are then set equal to the aircraft rates.

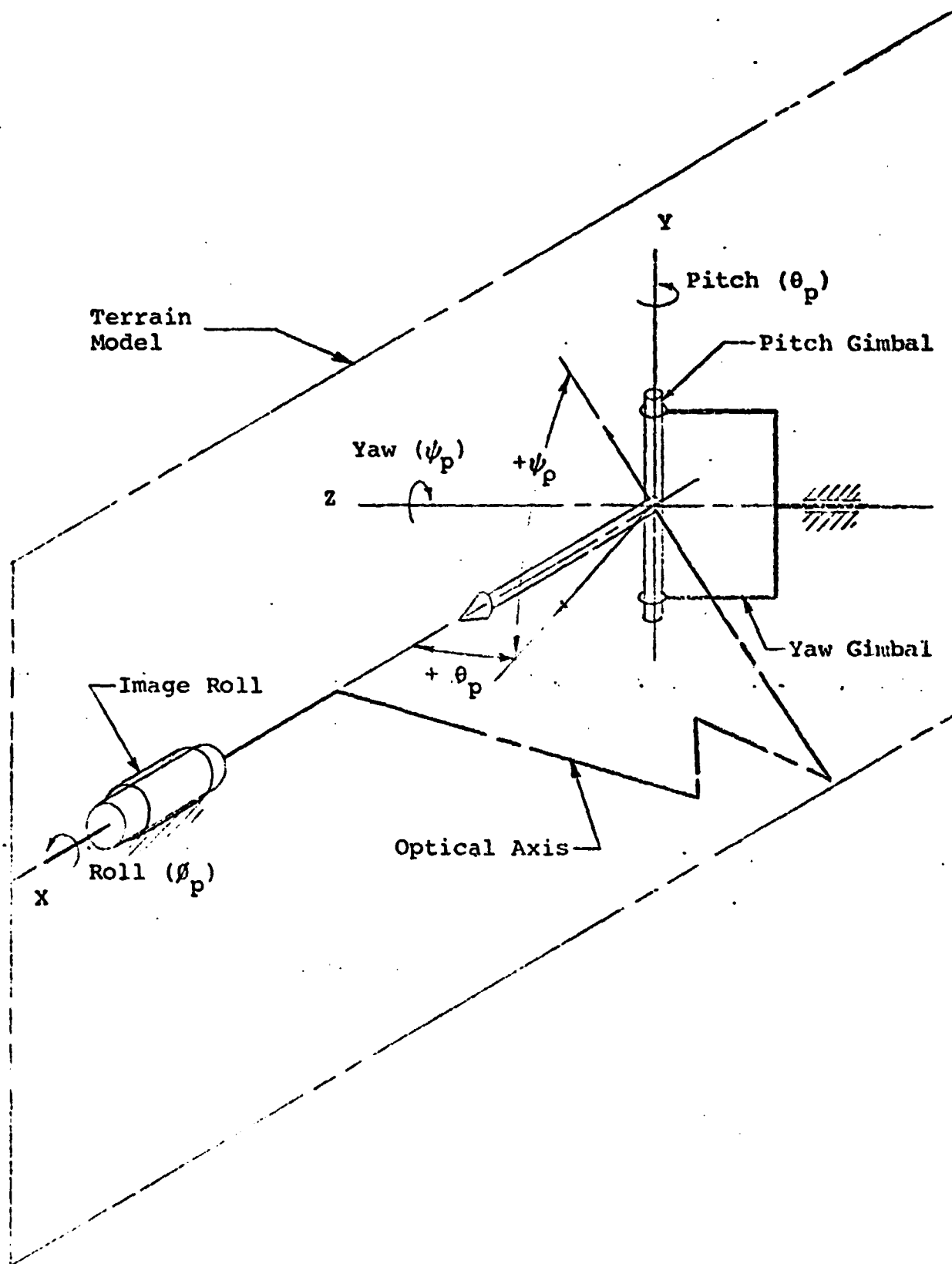


FIGURE 4.2.1-1 PROBE GIMBAL COORDINATES

$$\begin{bmatrix} 1 & 0 & -\sin \theta \\ 0 & 1 & 0 \\ 0 & 0 & \cos \theta \end{bmatrix} \begin{Bmatrix} \dot{\phi} \\ \dot{\theta} \\ \dot{\psi} \end{Bmatrix} = \begin{Bmatrix} p \\ q \\ r \end{Bmatrix} \quad (1)$$

By inverting this matrix we obtain the gimbal relative velocities in terms of p, q and r

$$\begin{Bmatrix} \dot{\phi} \\ \dot{\theta} \\ \dot{\psi} \end{Bmatrix} = \begin{bmatrix} 1 & 0 & \tan \theta \\ 0 & 1 & 0 \\ 0 & 0 & \sec \theta \end{bmatrix} \begin{Bmatrix} p \\ q \\ r \end{Bmatrix} \quad (2)$$

$\dot{\phi}$  as computed in these equations corresponds to aircraft rates. However, rotation of the pitch and yaw gimbals introduces additional roll which must be removed by "de-roll" of the roll mechanism. Since any of the terms above can take on positive or negative signs

$$\dot{\phi}_{p \max} = \dot{\phi} + \dot{\theta} + \dot{\psi} = p + q + r (\tan \theta + \sec \theta) \quad (3)$$

The pitch gimbal is limited in motion

$$-60^\circ \leq \theta \leq 30^\circ$$

The roll and yaw motion are continuous.

Using the maximum (either positive or negative) values of the aircraft rates (p, q, and r) as given in Table 2. the maximum velocities can be computed. The maximum velocity in pitch from equations (2) is:

$$\dot{\theta}_{p \max} = q = 1.05 \text{ ra/sec}$$

To obtain the maximum yaw velocity, the angle  $\theta$  must be at  $-60^\circ$  and the value of r is negative. This velocity is:

$$\dot{\psi}_{p \max} = r \sec \theta = 3.5 \text{ ra/sec}$$

The maximum roll velocity, again assuming  $\theta = -60^\circ$  and that  $r$  is negative, is from equation (3).

$$\dot{\theta}_p \max = p + q + r (\tan \theta + \sec \theta) = 9.3 \text{ ra/sec}$$

These maximum velocities can be taken as the no-load velocities in the design of these probe servos.

In general for gimbal systems the acceleration relative to inertial space governs the maximum acceleration for which servo systems must be designed. However, in this case there are no external accelerations acting on the system so the problem is simplified.

The acceleration of the pitch gimbal must equal the pitch rate of the aircraft.

$$\ddot{\theta} = \dot{q}$$

$$\ddot{\theta}_{\max} = \dot{q}_{\max} = 1.75 \text{ ra/sec}^2$$

The yaw gimbal is directly supported by fixed structure. Therefore, its inertial acceleration about the axis of rotation is simply the derivative of the velocity as given in equation (2).

$$\begin{aligned} \ddot{\psi} &= \frac{d}{dt} r \sec \theta \\ &= \dot{r} \sec \theta + \dot{\theta} r \sec \theta \tan \theta \\ &= \sec \theta (\dot{r} + q r \tan \theta) \end{aligned}$$

This value is maximum when  $\theta = -60^\circ$  and  $r$  is negative

$$\ddot{\psi}_{\max} = 9.9 \text{ ra/sec}^2$$

Similarly the acceleration of the roll mechanism is the derivative of equation (3).

$$\begin{aligned}\ddot{\theta} &= \dot{p} + \dot{q} + \dot{r} (\tan \theta + \sec \theta) + r \dot{\theta} (\sec^2 \theta + \tan \theta \sec \theta) \\ &= \dot{p} + \dot{q} + \dot{r} (\tan \theta + \sec \theta) + r q \sec \theta (\sec \theta + \tan \theta)\end{aligned}$$

This is maximum when  $\theta = -60^\circ$ , and  $r$  and  $\dot{r}$  are negative

$$\ddot{\theta}_{\max} = 24.6 \text{ ra/sec}^2$$

The servo motors must be capable of accelerating the inertia loads while they are at some velocity. Therefore, it is assumed that they must be capable of these maximum accelerations when the velocities are one-half of their maximum values. Assuming a straight line torque-velocity characteristic for the torque motors, the stall acceleration for which the servos must be designed become double these maximum values.

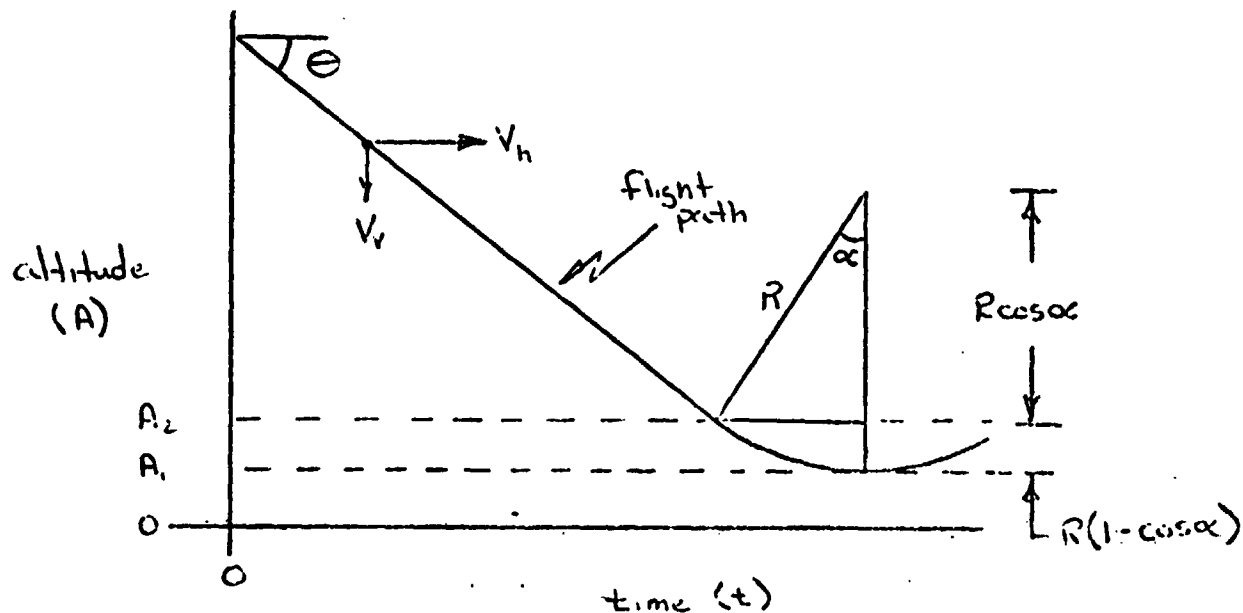
$$\ddot{\theta}_{p \text{ stall}} = 50 \text{ ra/sec}^2$$

$$\ddot{\theta}_{p \text{ stall}} = 20 \text{ ra/sec}^2$$

$$\ddot{\psi}_{p \text{ stall}} = 3.5 \text{ ra/sec}^2$$

### Focus Servo Requirements

The probe focus servo ( $F_M$ ) motions are a function of the combined motions of the probe pitch and yaw along with the vertical ( $Z_M$ ) motions of the gantry when it is near the terrain model. As a worst case change in altitude near the ground it is assumed the helicopter is in a dive and executes a maximum g pull-up at an altitude of  $A_2$  such that the aircraft will clear the terrain by an altitude  $A_1$ .



- $V_h$  = horizontal velocity
- $V_v$  = vertical velocity
- $\theta$  = flight path dive angle

Above the altitude  $A_2$  the vertical velocity is  $V_v$ .  
Below  $A_2$  the vertical velocity is governed by the circle with radius  $R$ .  
The equations for vertical motion below altitude  $A_2$  are:

$$\begin{aligned} A &= R (1 - \cos \alpha) + A_1 \\ \dot{A} &= R \dot{\alpha} \sin \alpha \\ \ddot{A} &= R \dot{\alpha}^2 \cos \alpha + R \ddot{\alpha} \sin \alpha \end{aligned}$$

### Focus Servo

If  $V_h \gg V_v$  the tangential velocity around the circle is approximately  $V_h$ . The radius  $R$  then becomes:

$$R = \frac{V_h}{32.2g} \quad \text{When } g \text{ is the pull-up acceleration}$$

Listed below are the helicopter performance characteristics and terrain clearance specification which are to apply for this analysis.

$$V_h = 200 \text{ ft/sec (120 kts)}$$

$$V_v = 50 \text{ ft/sec}$$

$$g = 2 \text{ (3 g pull-up less one gravity)}$$

$$A_1 = 16 \text{ feet}$$

The equations for vertical motion below altitude  $A_2$  then becomes:

$$\begin{aligned} A &= 621 (1 - \cos \alpha) + 16 && \text{ft} \\ \dot{A} &= 200 \sin \alpha && \text{ft/sec} \\ \ddot{A} &= 64.4 \cos \alpha && \text{ft/sec}^2 \end{aligned}$$

Selecting  $\alpha$  from 0 to 14° in 2° increments and applying the terrain scale factor of 300:1 \* yields the vertical probe motion near the model.

Altitude (mm)	Vertical Velocity (mm/sec)	Vertical Acceleration (mm/sec <sup>2</sup> )
16.0	0	64.4
16.4	7	64.4
17.5	14	64.2
19.4	21	64.1
22.0	28	63.8
25.4	35	63.4
29.6	42	63.0
34.5	48	62.5
40.0	50	0

\*The final scale factor selected which would yield the worst case vertical motion is 250:1. A scale factor of 300:1 was the requirement sent to the probe study subcontractor. The difference is 20% and will not significantly effect the final probe servo power requirements.

#### 4.2.2 PROJECTOR ROLL MECHANISM

The projector roll mechanism, together with the probe roll mechanism in the image generation system, controls the roll motion of the image as projected on the screen. A high degree of smoothness and accuracy is imperative in the display so that the scene as viewed by the pilot will be accurately presented and be free of discernable jitter.

The capability of the projector roll servo to achieve this smoothness and accuracy is highly dependent on the dynamic characteristics of the projector support structure. A dynamic analysis of this structure and an analysis of the servo system are presented in this section.

##### Structural Dynamics

A preliminary design of the roll mechanism support structure is shown in drawing PD 500 (see Section 5.3). It includes the rotating structure, which supports the three detailed display projectors and the two peripheral projectors, and the "back-up" structure which reacts the servo motor torque.

Since no knowledge of the moving base structure is available at this time it is assumed that the mechanical impedance of the structure is high enough that it can be considered infinitely rigid for purposes of this preliminary investigation. Therefore the roll support structure is considered to be terminated at the point where the yaw support member is attached to the moving base.

Drawing PD 500 served as a basis for constructing an analytical model of the structure. This model is shown in Figure 4.2.2-1. Due to the extremely preliminary nature of this design a highly detailed representation of the structure was not warranted and simplifications were made to expedite the analysis.

The roll structure was considered only in the zero angular position. Also the sloping yaw support member and the member supporting the detailed display projectors were assumed to be horizontal. These assumptions effectively decouple the structural dynamics in the roll axis from those in the pitch axis.

With the projectors in the zero roll position the structure was assumed to be infinitely rigid about the vertical axis. This is of course not true but it is quite rigid about this axis and considerably more rigidity than is shown in the present state of the design can be readily incorporated.

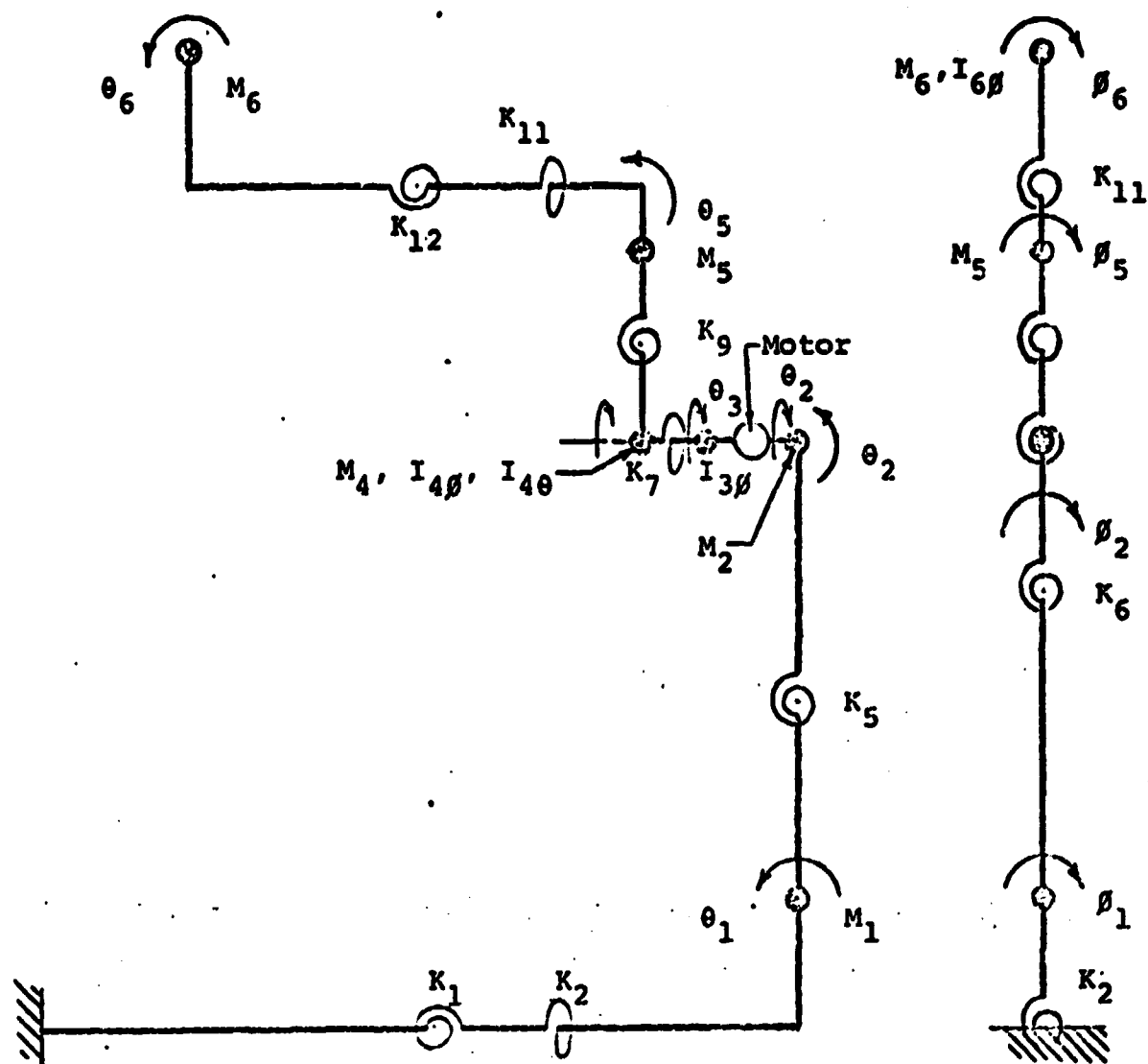
With these basic assumptions the structural analysis divides into two parts:

1. Dynamics of the structure about the roll axis
2. Dynamics in the x - y plane (about the pitch axis)

In constructing the model with lumped springs and masses, the stiffness of all bending members was represented by a single torsional spring with rigid members joining the springs to the lumped masses. Torsional members were of course represented by additional torsional springs. Spring constants were estimated from the structure shown in drawing PD 500 assuming the material to be aluminum.

The three detailed display projectors with their support bracketry were lumped together as one mass. The two peripheral projectors, the counterbalance weight, and surrounding supports were lumped together as another mass. A small rotating inertia was incorporated for analytical convenience to represent the inertia of the motor and gear train. Three other relatively small masses were located to represent support structure mass.

The values assigned to each mass and spring are shown in Figure 4.2.2-1.



$$M_1 = 250 \text{ lb} \left. \vphantom{\begin{matrix} M_1 \\ M_2 \end{matrix}} \right\}$$

$$M_2 = 200 \text{ lb} \left. \vphantom{\begin{matrix} M_1 \\ M_2 \end{matrix}} \right\}$$

$$I_{30} = 2.5 \times 10^4 \text{ lb-in}^2$$

$$M_4 = 2400 \text{ lb}$$

$$I_{40} = 1.1 \times 10^6 \text{ lb-in}^2 \left. \vphantom{\begin{matrix} I_{40} \\ I_{40} \end{matrix}} \right\}$$

$$I_{40} = 7.0 \times 10^5 \text{ lb-in}^2 \left. \vphantom{\begin{matrix} I_{40} \\ I_{40} \end{matrix}} \right\}$$

$$M_5 = 75 \text{ lb}$$

$$M_6 = 800 \text{ lb}$$

$$I_{60} = 2.0 \times 10^5 \text{ lb-in}^2 \left. \vphantom{\begin{matrix} I_{60} \\ I_{60} \end{matrix}} \right\}$$

Structure

Motor Inertia

Peripheral Proj.  
and  
Counterbalance

Structure

Detail Display  
Projectors

$$K_1 = 2.0 \times 10^8 \text{ in-lb/ra}$$

$$K_2 = 7.9 \times 10^8$$

$$K_5 = 1.0 \times 10^8$$

$$K_6 = 4.8 \times 10^8$$

$$K_7 = 2.6 \times 10^7$$

$$K_9 = 1.4 \times 10^7$$

$$K_{10} = 4.0 \times 10^8$$

$$K_{11} = 5.0 \times 10^7$$

$$K_{12} = 6.0 \times 10^7$$

FIGURE 4.2.2-1  
PROJECTOR SUPPORT STRUCTURAL DYNAMICS MODEL

### Roll Axis Structural Dynamics

Six coordinates were required to describe the motion of the projector support structure about the roll axis. These were designated  $\theta_1$ ,  $\theta_2$ ,  $\theta_3$ ,  $\theta_4$ ,  $\theta_5$ , and  $\theta_6$  as shown in Figure 4.2.2-1. In the servo analysis a coordinate describing the differential motion between the torque motor output shaft and the back-up structure was required. This coordinate

$$\Delta \theta = \theta_3 - \theta_2$$

was substituted in the equations of the motion in place of  $\theta_3$ .

Three transfer functions were required for the servo analysis:

1. Driving point mobility (drive point velocity divided by the applied torque).
2. Transmissibility between the drive point and the position to be controlled (the three detailed display projectors)
3. Transmissibility between the drive point and the motion measured by the feedback potentiometer (differential motion between the rotating structure and the back-up structure).

The drive point mobility (in Laplace transforms) obtained from the dynamic analysis is

$$\frac{\Delta \dot{\theta}}{T} = \frac{\left(\frac{s^2+54.2^2}{54.2^2}\right)\left(\frac{s^2+165^2}{165^2}\right)\left(\frac{s^2+297^2}{297^2}\right)\left(\frac{s^2+1450^2}{1450^2}\right)\left(\frac{s^2+3520^2}{3520^2}\right)}{4.395\left(\frac{s^2+152^2}{152^2}\right)\left(\frac{s^2+290^2}{290^2}\right)\left(\frac{s^2+638^2}{638^2}\right)\left(\frac{s^2+1450^2}{1450^2}\right)\left(\frac{s^2+4270^2}{4270^2}\right)}$$

The squared values in the ()'s are the frequencies in radians per second where zeroes and poles appear in the frequency spectrum. The constant 4.39 in the denominator represents the total inertia of the rotating parts (7020 lb-in-sec<sup>2</sup>) divided by the square of the gear ratio (40:1) between the drive motor and the rotating structure. It was not necessary to include this gear train in the structural model except for its rigidity (as modified by the gear ratio) represented by the spring  $K_7$ . However the servo analysis is based on using the motor as the driving point so this modification of the inertia is included here.

The transmissibility from the driving point to the projectors is

$$\frac{\phi_6}{\Delta\theta} = \frac{\left(\frac{s^2+141^2}{141^2}\right)\left(\frac{s^2-389^2}{389^2}\right)\left(\frac{s^2-741^2}{741^2}\right)\left(\frac{\quad}{\quad}\right)\left(\frac{\quad}{\quad}\right)}{40 \left(\frac{s^2+54.2^2}{54.2^2}\right)\left(\frac{s^2+165^2}{165^2}\right)\left(\frac{s^2+297^2}{297^2}\right)\left(\frac{s^2+1450^2}{1450^2}\right)\left(\frac{s^2+3520^2}{3520^2}\right)}$$

Two items in this transfer function warrant further explanation. The negative values in the numerator place zeros for the transfer function in the right half plane of a root locus plot. This means that a 180 degree phase shift referred to the drive point has taken place. This actually occurs at the higher natural frequencies of vibration.

The two blank terms in the numerator indicate that two more roots exist. However their values are unknown due to the not uncommon occurrence where eigenvalue computer programs fail to extract all the roots for ill-conditioned matrices as existed in this case. From other considerations it has been determined that the frequencies of these zeros are higher than the other zeros in this function and will not cause any ill effects in performance.

The transmissibility between the driving point and the differential motion across the feedback potentiometer is

$$\frac{\phi_4 - \phi_z}{\Delta\theta} = \frac{\left(\frac{s^2+100^2}{100^2}\right)\left(\frac{s^2+253^2}{253^2}\right)\left(\frac{s^2+1450^2}{1450^2}\right)\left(\frac{\quad}{\quad}\right)\left(\frac{\quad}{\quad}\right)}{40 \left(\frac{s^2+54.2^2}{54.2^2}\right)\left(\frac{s^2+165^2}{165^2}\right)\left(\frac{s^2+297^2}{297^2}\right)\left(\frac{s^2+1450^2}{1450^2}\right)\left(\frac{s^2+3520^2}{3520^2}\right)}$$

Again the missing zero terms are a result of the failure of the computer program to extract all of the roots.

The greatest contributor to low frequencies in the above transfer functions is the compliance of the spring  $K_7$  which represents the wind-up in the gear train. However this compliance is inside the closed loop of the servo system and, as discussed below in the section on roll analysis, is not detrimental to performance.

### Pitch Axis Structural Dynamics

The equations of motion for the pitch axis structural analysis required four coordinates,  $\theta_1$ ,  $\theta_2$ ,  $\theta_5$ , and  $\theta_6$  as shown in Figure 4.2.2-1 to describe the system. A fifth coordinate  $\theta_0$  is added to define the motion of the base of the structure for computing transmissibility from the base to the detailed display projectors. The resulting transmissibility based on the values shown in Figure 4.2.2-1 is

$$\frac{\theta_6}{\theta_0} = \frac{\left(\frac{s^2 - 55.2^2}{55.2^2}\right)\left(\frac{s^2 + 157^2}{157^2}\right)\left(\frac{s^2 + 578^2}{578^2}\right)}{\left(\frac{s^2 + 38.9^2}{38.9^2}\right)\left(\frac{s^2 + 122^2}{122^2}\right)\left(\frac{s^2 + 171^2}{171^2}\right)\left(\frac{s^2 + 1420^2}{1420^2}\right)}$$

The low frequency of 38.9 rad/sec poses a problem since this is only about twice the band width of the motion base servos. Since the structure is lightly damped an amplification of 20-25 db can be expected at resonance. This would cause unacceptable motion of the projected scene. For the purposes of this analysis an acceptable motion of the projected image is on the order of  $\pm 0.2$  degrees.

Each of the six degrees of freedom of the motion base will have the motion characteristics of a 3 Hz, 0.7 damped second order system. Considering only the pitch motion, for example, with a nominal 1 rad/sec<sup>2</sup> acceleration the lowest natural frequency of the structure should be greater than 70 rad/sec (11.1 Hz) in order to limit objectionable motion to  $\pm 0.2$  degrees. Superimposed additional base motions such as heave (0.31 g) would mean even higher natural frequencies would be required to meet this criterion.

It therefore becomes apparent that a more rigid structure than that shown in drawing PD 500 is required. However there are practical limits to the rigidity which can be achieved since the frequency varies as the square root of the stiffness and space limitations become a problem. A reasonable goal for the lowest natural frequency is 15 Hz (94 rad/sec).

To increase the frequencies to required values, considerable modification of the structure shown in drawing PD 500 will be required. In particular the vertical member

which supports the roll axis will require considerable enlargement to cross section. To obtain the space required for such a structure an opening may be required in the rear portion of the screen. Such an opening may be desirable in any case for ease of access to the cockpit and would not be a problem in design. It would not limit the operation of the simulator in any way.

Additional rigidity in other members of the support structure can be readily achieved by use of thicker plates (1/4-inch plates were assumed for much of the structure in this analysis) and by enlargement of cross sections. Space does not appear to pose a problem except for the vertical support discussed above.

In addition to the problem existing in the pitch axis as shown by this analysis, the effects on the roll servo system must be considered. In this analysis with the projectors at the zero position angle, pitch axis dynamics are not coupled with roll. However when the projectors are rolled to off-zero angles, coupling will exist. Analysis of this condition is beyond the scope of this preliminary investigation, but it must certainly be considered when proceeding with a final design.

As a matter of interest the problems of low frequencies in projector supports has been experienced in Northrop's Large Amplitude Simulator. A successful solution which has in no way degraded the simulation has been to limit all motion base commands to frequencies below 10 Hz.

A source of higher frequency vibration which could excite natural frequencies of the projector support system is the possible inclusion of a buffet seat in the cockpit. It is imperative that the design of such a seat be such that the buffet forces would be inherently self-cancelling so minimum vibration would be transmitted to the base and projectors.

## Roll Servo Analysis

Power Requirements - The roll of the image is the sum of the projector roll and the optical scanning probe roll. The power required for the projection roll servo is a function of how these two rolls are mixed.

One approach consists of mixing the roll motions such that most of the roll between  $\pm 45$  degrees is performed by the projector and the remaining roll (up to  $\pm 90^\circ$ )\* by the probe. This approach requires large roll accelerations in the transition between the servos. This can be illustrated by assuming the image rolled  $90^\circ$  and then commanded to level. If the image is rolling at  $100^\circ/\text{sec}$  as it enters the transition region and it is desired to accelerate the projector roll servo up to the image roll velocity in  $10^\circ$  the roll acceleration becomes:

$$\ddot{\theta}_p = \frac{\dot{\theta}_p^2}{2\theta_p} = \frac{100^2}{2(10)} = 500 \text{ deg/sec}$$

This acceleration is not practical for the large projector roll servo. In addition, the scene will show some deterioration during the transition from one servo to the other.

A more acceptable mixing function would require one half the image roll from the projector and the other half from the probe for roll angles up to  $\pm 90^\circ$ . This has the effect of eliminating the transition region and reducing the required motions of the projector roll servo to one half the aircraft roll performance parameters of Table 2.2-2.

---

\*If image roll angles of greater than  $\pm 90^\circ$  are required for a particular task the projector roll will be locked and the total roll performed by the probe. This is required since the projector window will be rolled the wrong way as the scene rolls past  $90^\circ$ .

For tasks which require roll angles limited to  $\pm 45^\circ$  the total roll could be performed by the projector roll. In this case the projector roll must have the capability of reproducing the motions of the aircraft.

The peak motion envelope for this servo will, therefore, be established by sizing the drive components with the capability of reproducing the aircraft maximum roll motion requirements during disturbance inputs from the motion base. The projector roll is mass balanced and will not be effected by the motion base rectilinear accelerations. The worst case disturbance will occur when the projector system has its maximum yaw angle of  $40^\circ$ . In this position a component of both pitch and roll acceleration will be seen by the projector roll servo. From Table 2.2-3 the motion base pitch and roll accelerations are both  $\pm 1 \text{ rad/sec}^2$ . The projector roll servo will then experience a disturbance acceleration of

$$\ddot{\theta}_p (\text{disturbance}) = 1 \cos 40^\circ + 1 \cos (90^\circ - 40^\circ) = 1.41 \text{ r/s}^2$$

The required aircraft roll motion (Table 2.2-2) are:

$$\dot{\theta} (\text{aircraft}) = \pm 100^\circ/\text{sec} = 1.75 \text{ r/s}$$

$$\ddot{\theta} (\text{aircraft}) = \pm 150^\circ/\text{sec}^2 = 2.62 \text{ r/s}^2$$

These motions are not peak requirements and are, therefore, increased by 2/3 such that simultaneous aircraft motions may be performed.

The projector roll stall acceleration and no-load velocity requirement then become

$$\dot{\theta}_p (\text{no-load}) = (1 \frac{2}{3})(1.75) = 2.92 \text{ r/s}$$

$$\ddot{\theta}_p (\text{stall}) = (1 \frac{2}{3})(2.62) + 1.41 = 5.78 \text{ r/s}^2$$

From the mobility determined in the beginning of this section the total load inertia referenced about the roll pivot point is  $7019 \text{ in-lb-sec}^2$ . The torque about the roll pivot point then becomes:

$$T = I \ddot{\theta}_p (\text{stall}) = 7019(5.78) = 40,570 \text{ in-lb.}$$

The size of this torque along with the velocity requirements overwhelmingly favors a hydraulic drive. Stiffness of the hydraulic system is of particular importance. For this reason

a WSI Model 35 axial rolling vane hydraulic motor has been selected. This motor has a large torque with a small volume of trapped fluid within the motor. The amount of trapped fluid determines the effective spring rate due to fluid compliance. The motor with a 10:1 integral gear head package has the capability of producing 11,080 in-lb of torque with a differential pressure of 2000 psi. The maximum motor output speed is  $15.7 \text{ rad/sec}$ . With an additional 4:1 spur gear reduction added the motor will produce

$$T_{\text{motor}} = 11,020 (4) = 44,320 \text{ in-lb}$$

$$\dot{\theta}_{\text{motor}} = \frac{15.7}{4} = 3.93 \text{ rad/sec}$$

These are well within the requirements and allow for items which have been ignored such as friction, tolerance on calculated inertia, etc.

Analytical Development Of The  $\theta_p$  - Servo - The projector roll hydraulic control system is analyzed utilizing the following symbol definitions:

$C_i$	Valve flow coefficient with respect to the input current to the valve coil
$C_p$	Valve flow coefficient with respect to load differential pressure
$e$	System drive voltage at main summing junction
$e_1$	Difference between $e$ and the sum of position and velocity feedback voltages
$e_2$	Valve coil input voltage
$i$	Valve coil current
$k_o$	Effective spring rate due to fluid compliance
$K$	DC forward loop gain
$K_p$	Feedback position sensor electrical gain
$K_v$	Feedback rate sensor electrical gain
$L$	Leakage coefficient of hydraulic motor
$N$	Adiabatic bulk modulus of hydraulic fluid
$P_L$	Differential pressure across hydraulic motor

$P_s$	System supply pressure
$Q$	Total flow rate from the servo valve
$q_c$	Flow rate which results in fluid compression
$q_o$	Flow rate which results in motor motion
$q_p$	Flow rate which leaks past motor
$S$	Laplace operator
$\Delta \dot{\theta}_{pm}$	Differential velocity between the hydraulic motor rotor and the motor frame
$\Delta \dot{\theta}_{pl}$	Differential velocity between yaw support structure and the roll support structure
$\dot{\theta}_p$	Velocity of the projector platform
$T_m$	Output torque of the hydraulic motor referenced to the motor shaft
$TR_1$	Transmissibility of the structure relating the motor differential motion to the motion of the projector platform
$TR_2$	Transmissibility of the structure relating the motor motion to the motion of the feedback elements
$\tau_c$	Driving point mobility of the total load referenced to the motor shaft
$V_d$	Volumetric displacement of the hydraulic motor
$V_t$	Trapped fluid volume within hydraulic motor
$\omega_n$	Generalized undamped natural frequency of the hydraulic servo valve
$\zeta$	Damping ratio of the servo valve

Using the aforementioned notations the following relationships may be formed. Equation (2) represents the operation of a 4-way flow control valve with constant (linearized) flow coefficients. Equation 6 is computed for a rotary motor including trapped fluid in hydraulic lines and valve.

$$Q = q_o + q_c + q_p \quad (1)$$

$$Q = \frac{C_i i}{\frac{s^2 + 2\zeta\omega_n s + \omega_n^2}{\omega_n^2}} - C_p P_L \quad (2)$$

$$q_o = v_d \text{ (motor differential velocity)} \quad (3)$$

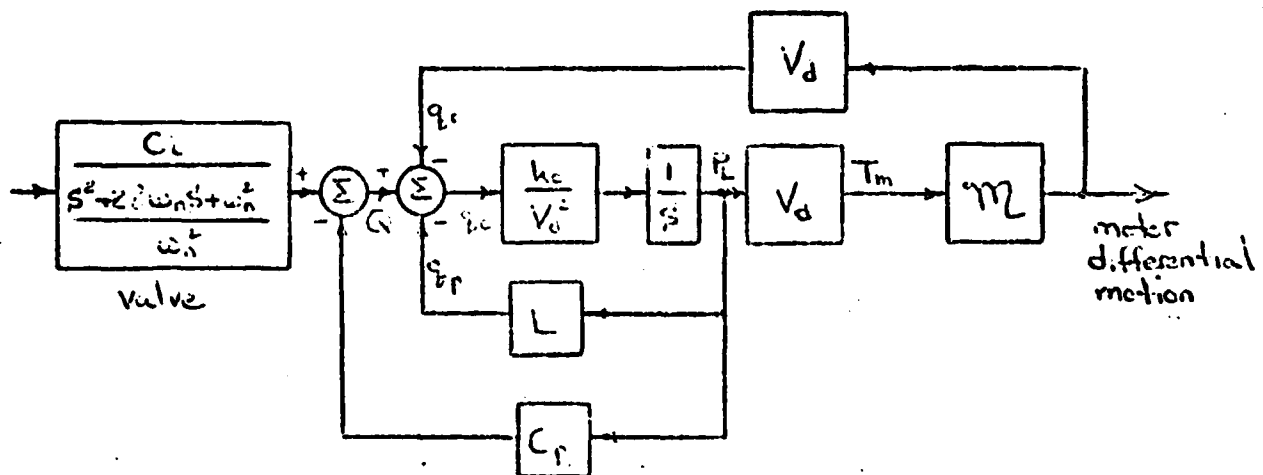
$$q_c = \frac{v_d^2 s P_L}{k_o} \quad (4)$$

$$q_p = I P_L \quad (5)$$

$$k_o = \frac{4v_d^2 N}{v_t} \quad (6)$$

$$T_m = v_d P_L \quad (7)$$

The above equations form the block diagram below:



The equation for the flow through a 4-way valve is:

$$Q = K i \sqrt{P_s - P_L} \quad (8)$$

$K$  = orifice coefficient

The values of  $C_i$  and  $C_p$  are defined as follows:

$$C_i = \left( \frac{\partial Q}{\partial i} \right) \quad P_L = \text{constant} \quad (9)$$

$$C_p = \left( \frac{\partial Q}{\partial P_L} \right) \quad i = \text{constant} \quad (10)$$

Combining equations 8, 9, and 10

$$C_i = K \sqrt{P_s - P_L}$$

$$C_p = -\frac{K}{2} \cdot \frac{i}{\sqrt{P_s - P_L}}$$

A Moog series 73-104 valve has been selected. This valve has the following characteristics:

Valve coil inductance (series coils) ( $L_c$ ) = 3 henry

Valve coil resistance (series coils) ( $R_c$ ) = 400  $\Omega$

Rated current for full flow (series coils) = 7.5 ma

Rated flow @ 1000 psi valve drop = 81.62 in<sup>3</sup>/sec.

The valve flow coefficient is found utilizing the above parameters and equation 8

$$K = \frac{Q}{i \sqrt{P_s - P_L}} = \frac{81.62 \text{ in}^3/\text{sec}}{7.5 \text{ ma} \sqrt{1000}} = 0.34$$

Selecting an operating point where the valve opening is 5% of maximum and  $P_L$  is 1/3 of the 2000 psi supply pressure the valve linearized flow coefficients become:

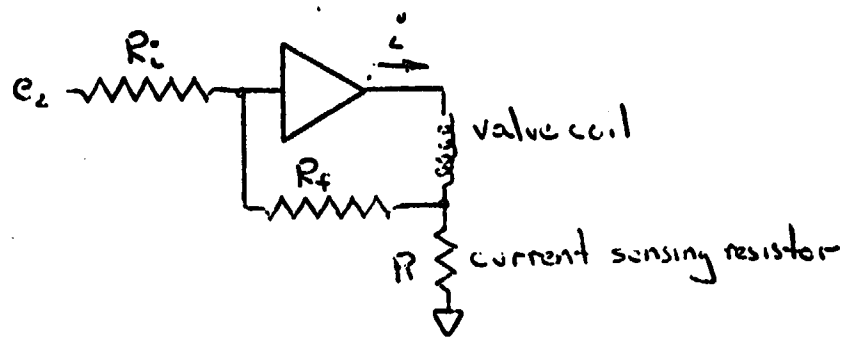
$$C_p = - \frac{0.34 \times 7.5 \times 0.05}{2 \sqrt{1333}} = -1.75 \times 10^{-3} \frac{\text{in}^3/\text{sec}}{\text{lb/in}^2}$$

$$C_i = 0.34 \sqrt{1333} = 12.4 \frac{\text{in}^3/\text{sec}}{\text{ma}}$$

The relationship between valve coil voltage to valve coil current is:

$$\frac{i}{e_2} = \frac{1/R_c}{s + \frac{R_c/L_c}{R_c/L_c}} = \frac{2.5}{\left( \frac{s + 133}{133} \right)} \frac{\text{ma}}{\text{volt}}$$

The lag produced by the  $\frac{L_c}{R_c}$  time constant may be removed by utilizing current feedback around the driving amplifier.



Selecting  $R = R_c$  and  $R_i = R_f$  the transfer function for the above becomes:

$$\frac{i}{e_2} = -2.5 \frac{\text{ma}}{\text{volt}}$$

The dynamic value characteristics relating load flow with zero load pressure drop to input current (see equation 2) is shown by a frequency response plot in the valve specifications. The amplitude and phase characteristics of this frequency response are adequately represented by a 0.9 damped second order system with a natural frequency of 880 rad/sec.

The Washington Scientific Industries hydraulic motor model 35 has a volumetric displacement ( $V_d$ ) of  $0.554 \text{ in}^3/\text{rad}$ . The volume of fluid under compression within the motor is  $1.75 \text{ in}^3$ . An additional  $3 \text{ in}^3$  volume of fluid is trapped in the valve and manifold block. The total trapped fluid volume ( $V_t$ ) then becomes  $4.75 \text{ in}^3$ . From equation 6 the spring rate due to fluid compliance then becomes:

$$k_o = \frac{4 V_d^2 N}{V_t} = \frac{4 \times 0.554 \times 0.554 \times 2 \times 10^5}{4.75}$$

$$k_o = 5.17 \times 10^4 \frac{\text{in-lb}}{\text{radian}}$$

The maximum port to port leakage ( $L$ ) for a  $2.5 \text{ in}^3$  per revolution hydraulic motor is  $0.065 \text{ in}^3/\text{min}/\text{psi}$  obtained from an evaluation conducted by Pagasus Laboratories in February 1968. It is assumed the maximum port to port leakage for the larger  $3.48 \text{ in}^3$  per revolution hydraulic motor is

$$\begin{aligned} L &= \frac{3.48}{2.5} \times 0.065 = 0.091 \text{ in}^3/\text{min}/\text{psi} \\ &= 1.52 \times 10^{-3} \text{ in}^3/\text{sec}/\text{psi} \end{aligned}$$

The basic block diagram of the  $\theta_p$  - servo is shown in Figure 4.2.2-2. The mobility and transmissibilities were derived previously and is listed below

$$\eta = \frac{\left( \frac{s^2 + 54.2^2}{54.2^2} \right) \left( \frac{s^2 + 165^2}{165^2} \right)}{4.39 s \left( \frac{s^2 + 152^2}{152^2} \right)}$$

Dynamics above 40 Hz have been neglected

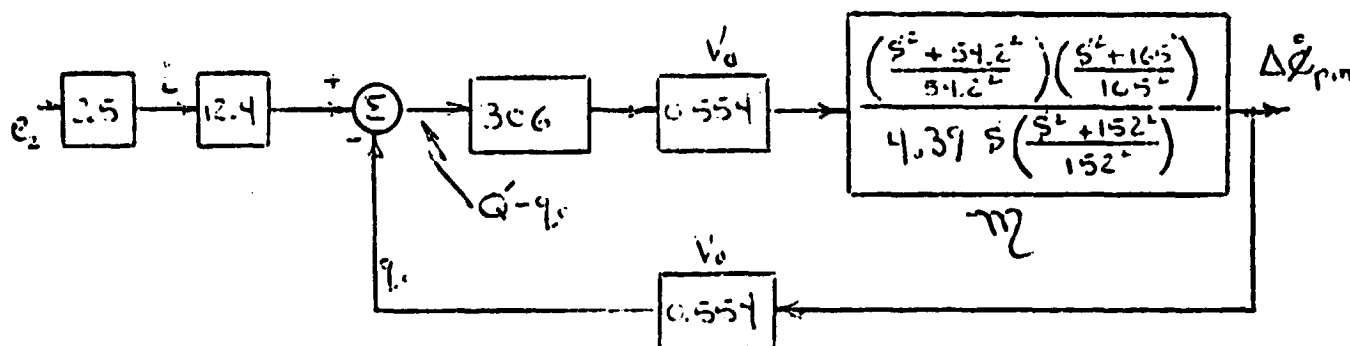
$$TR_1 = \frac{\left( \frac{s^2 + 141^2}{141^2} \right)}{40 \left( \frac{s^2 + 54.2^2}{54.2^2} \right) \left( \frac{s^2 + 165^2}{165^2} \right)}$$

$$TR_2 = \frac{\left( \frac{s^2 + 100^2}{100^2} \right)}{40 \left( \frac{s^2 + 54.2^2}{54.4^2} \right) \left( \frac{s^2 + 165^2}{165^2} \right)}$$

The inner  $C_p + L$  loop closure of Figure 4.2.2-2 yields:

$$\frac{P_L}{Q - q_o} = \frac{306}{\left( \frac{s + 551}{551} \right)}$$

The combined load, valve and motor loop is next solved by the solution of the following block diagram. Dynamics above 40 Hz have been neglected.



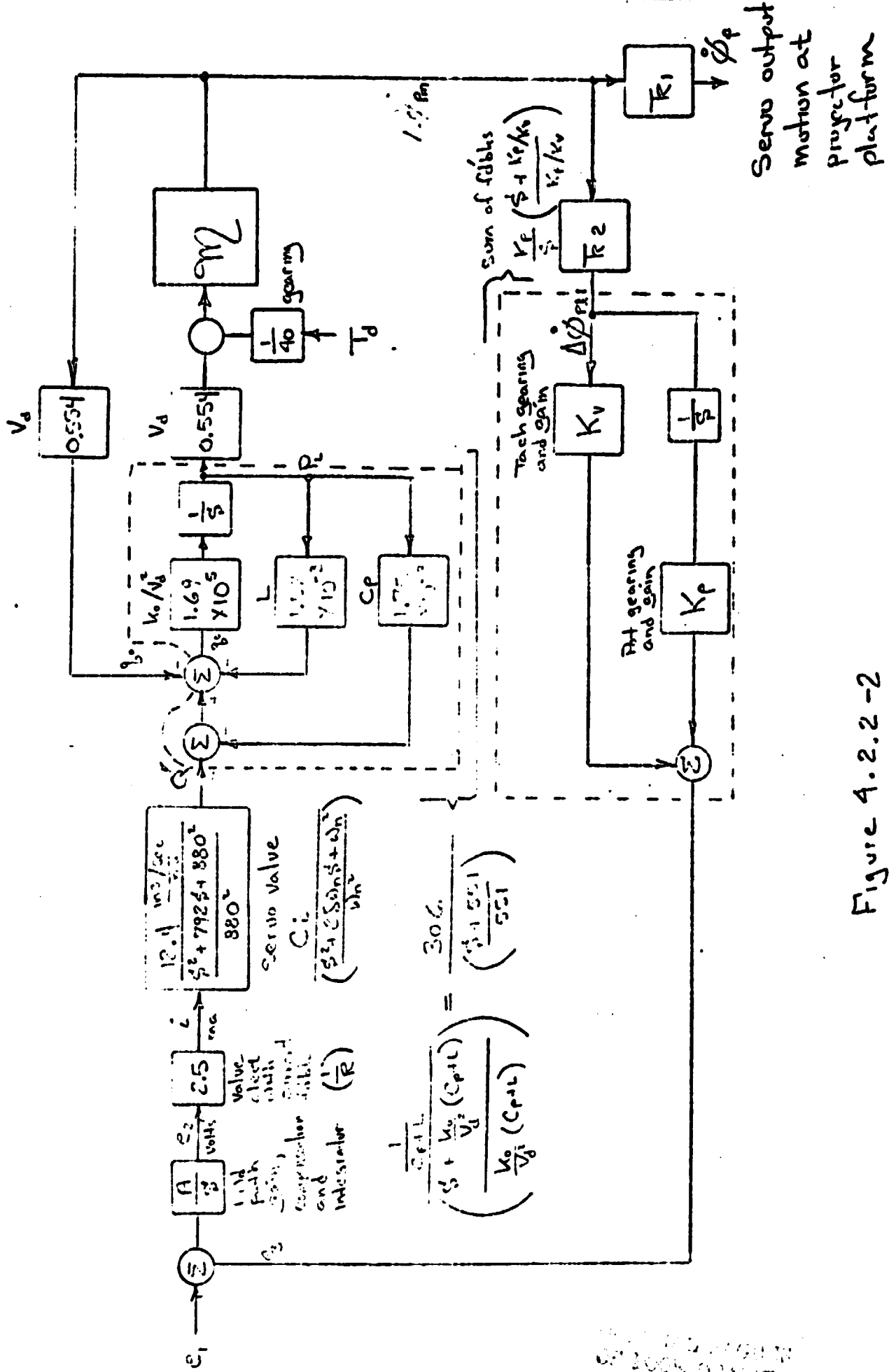


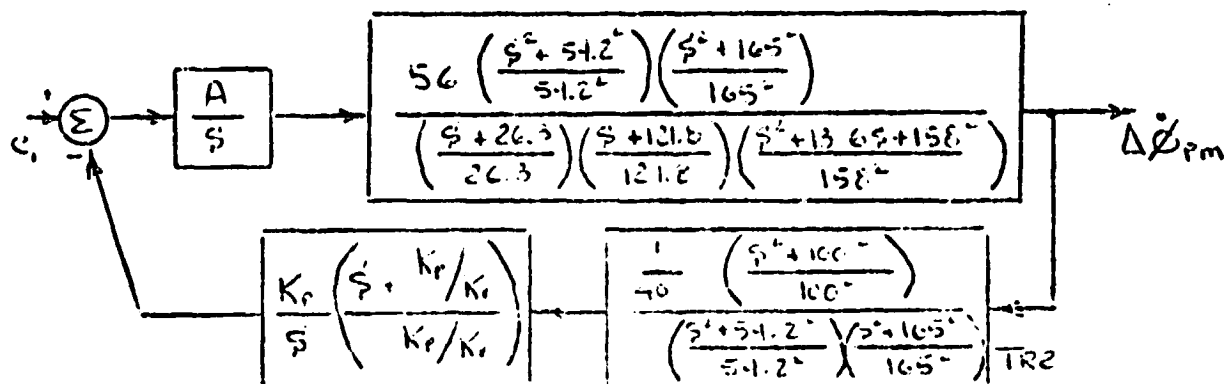
Figure 4.2.2-2

$\phi_o$  = Servo Block Diagram

$$\frac{\Delta \dot{\theta}_{PM}}{e_2} = 31 \left[ \frac{(306) (.554) \left( \frac{1}{4.39} \right) \left( \frac{s^2 + 54.2^2}{54.2^2} \right) \left( \frac{s^2 + 165^2}{165^2} \right)}{(306) (.554)^2 \left( \frac{1}{4.39} \right) \left( \frac{s^2 + 54.2^2}{54.2^2} \right) \left( \frac{s^2 + 165^2}{165^2} \right) + s \left( \frac{s^2 + 152^2}{152^2} \right)} \right]$$

$$= 56 \frac{\left( \frac{s^2 + 54.2^2}{54.2^2} \right) \left( \frac{s^2 + 165^2}{165^2} \right)}{\left( \frac{s + 26.3}{26.3} \right) \left( \frac{s + 121.8}{121.8} \right) \left( \frac{s^2 + 13.6s + 158^2}{158^2} \right)}$$

The final form of the  $\theta_p$  - Servo block diagram then becomes:



Judiciously selecting  $A = K \left( \frac{s + 26.3}{26.3} \right)$  and  $K_p/K_v = 5$  leads to the root locus plot of Figure 4.2.2-3. Closing the loop with a gain of  $\frac{56KK_p}{40} = 220$  yields closed loop poles with desirable locations.

The final closed loop transfer function between voltage command to motor differential motion is:

$$\frac{\Delta \dot{\theta}_{PM}}{e_1} = \frac{\frac{40}{K_p} \left( \frac{s^2 + 54.2^2}{54.2^2} \right) \left( \frac{s^2 + 165^2}{165^2} \right) s}{\left( \frac{s + 5.7}{5.7} \right) \left( \frac{s^2 + 85.7s + 60.8^2}{60.8^2} \right) \left( \frac{s^2 + 44.2s + 177^2}{177^2} \right)}$$

To obtain a servo which is characterized by a 0.7 damped, 25 rad/sec second order system the above transfer function is modified by open loop input compensation constructed in part by the sum of

X = OPEN LOOP POLE

O = OPEN LOOP ZERO

X = CLOSED LOOP POLE

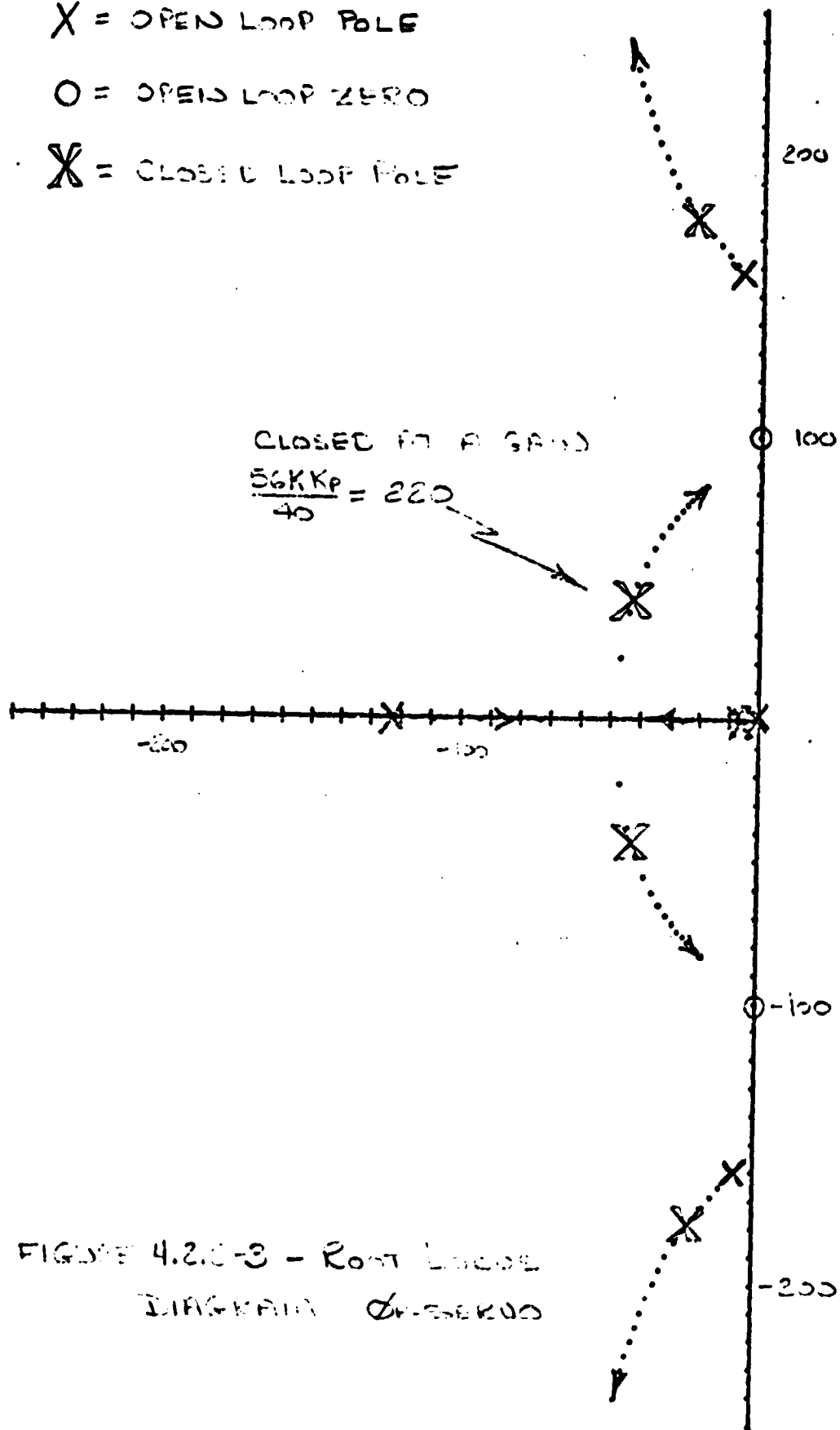


FIGURE 4.2.0-3 - Root Locus  
Diagram of a system

the rate and position command signals. The desired compensation with respect to rate command will have the following transfer function:

$$\frac{e_c \text{ (command velocity)}}{e_1} = \underbrace{\frac{K_c \left( \frac{s + 5.7}{5.7} \right)}{s}}_{\text{rate plus position command signal}} \underbrace{\left( \frac{s^2 + 85.7s + 60.8^2}{60.8^2} \right) \left( \frac{s^2 + 35s + 25^2}{25^2} \right)}_{\text{electrical input compensation}}$$

Combining the input compensation and the transmissibility relating motor differential motion to the motion of the projector platform yields the final closed loop results.

$$\frac{\ddot{\theta}_p}{e_c} = \frac{\frac{K_c}{K_p} \left( \frac{s^2 + 141^2}{141^2} \right)}{\left( \frac{s^2 + 35s + 25^2}{25^2} \right) \left( \frac{s^2 + 44.2s + 177^2}{177^2} \right)}$$

This transfer function is a match within 2 degrees of an ideal 0.7 damped 25 rad/sec second-order system out to 25 rad/sec. . This is well within the frequency phase angle requirements.

The system closed-loop complex compliance may now be calculated using the block diagram of Figure 4.2.2-2. The relationship between inputs at the torque summing point and inputs at the primary voltage summing point is given by:

$$\begin{aligned} \frac{T_d}{e_1} &= \frac{(40) (0.554) (306) (12.4) (2.5) K \left( \frac{s + 26.3}{26.3} \right)}{s} \\ &= \frac{2.1 \times 10^5 K}{s} \left( \frac{s + 26.3}{26.3} \right) \end{aligned}$$

Combining  $\frac{T_{md}}{e_1}$  with the expression for the closed loop transfer function relating  $\frac{\Delta \theta_{PM}}{e_1}$  and the transmissibility relating

$\frac{\ddot{\theta}_p}{\ddot{\theta}_{PM}}$  yields the closed loop compliance.

$$\frac{\theta_p}{T_d} = \frac{e_1}{T_d} = \frac{\ddot{\theta}_{PM}}{e_1} \cdot \frac{\ddot{\theta}_p}{\ddot{\theta}_{PM}} \cdot \frac{1}{s}$$

$$= \frac{s \left( \frac{s^2 + 141^2}{141^2} \right)}{2.1 \times 10^5 K K_p \left( \frac{s + 5.7}{5.7} \right) \left( \frac{s + 26.3}{26.3} \right) \left( \frac{s^2 + 85.7s + 60.8^2}{60.8^2} \right) \left( \frac{s^2 + 44.2s + 177^2}{177^2} \right)}$$

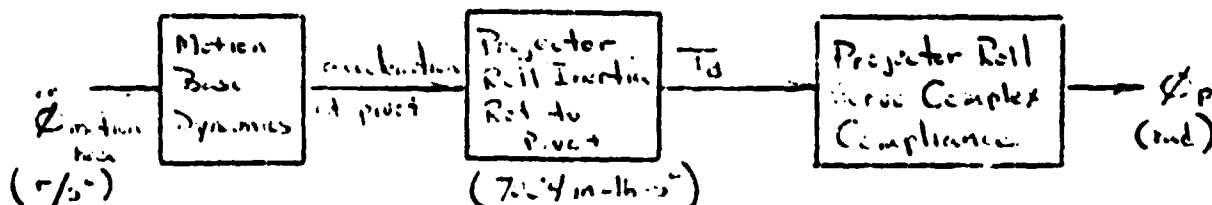
However,  $\frac{56 K K_p}{40} = 220$  (the position/velocity open loop gain)

The constant for the  $\frac{\theta_p}{T_d}$  transfer function then becomes

$$\frac{56}{2.1 \times 10^5 \times 220 \times 40} = 3.03 \times 10^{-8}$$

The maximum complex compliance amplitude of  $1.42 \times 10^{-7} \frac{\text{rad}}{\text{in-lb}}$  occurs at a frequency of 12 rad/sec (1.9 Hz).

It is assumed that the accelerations from the motion base are applied to the roll projector total inertia referenced to the pivot point of the roll projector. In addition the motion base accelerations will be filtered by the dynamics of the motion base. From section 2.2 the motion base dynamics are characterized by a 0.7 damped 18.8 rad/sec second order system. The motion base acceleration to projector motion (with respect to the motion base) then becomes:



Then

$$\frac{\ddot{\theta}_p}{\ddot{\theta}_{\text{motion base}}} = \frac{2.13 \times 10^{-4} s \left( \frac{s^2 + 141^2}{141^2} \right)}{\left[ \left( \frac{s^2 + 26.3s + 18.8^2}{18.8^2} \right) \left( \frac{s + 5.7}{5.7} \right) \left( \frac{s + 26.3}{26.3} \right) \cdot \right. \\ \left. \left( \frac{s^2 + 85.7s + 60.8^2}{60.8^2} \right) \left( \frac{s^2 + 44.2s + 177^2}{177^2} \right) \right]}$$

This transfer function has a maximum amplitude of  $9.54 \times 10^{-4}$  rad/rad/sec<sup>2</sup> occurring at a frequency of 10 rad/sec. (1.6 Hz).

The worst case motion base acceleration coupling to the projector roll servo will occur with the projector assembly at its maximum yaw angle of 40 degrees. In this position a component of acceleration from both the motion base pitch and yaw are disturbance inputs to the roll projector servo. From Table 2.2-3 the maximum value of motion base pitch and yaw accelerations are both  $\pm 1$  rad/sec<sup>2</sup>. The maximum yielding of the roll projector servo is then:

$$\begin{aligned} \theta_p \text{ (servo yield)} &= \pm (9.54 \times 10^{-4}) (\cos 40^\circ + \cos (90^\circ - 40^\circ)) \\ &= \pm 1.34 \times 10^{-3} \text{ radian } (\pm 0.08^\circ) \end{aligned}$$

#### 4.2.3 Sky-Horizon Projector Kinematics

The Sky-Horizon projector must be designed to provide angular accelerations and velocities of the projected image which will correspond with the maneuvering performance in roll, pitch, and yaw of the simulated helicopter. In addition to providing these operating characteristics, it must withstand the accelerations imposed by the moving base of the simulator.

The direct effect of the velocities and accelerations on the Sky-Horizon projector design is in the selection of drive motors and gear ratios (if any) which can provide required torques and velocities. In addition, the angular accelerations plus those of gravity and translational accelerations determine the loads on the gimbal bearings.

In this analysis it is assumed that all gimbals are statically balanced. Therefore the translational motion of the moving base of the simulator will have no effect on the gimbal motion and need only be considered in computing bearing loads.

The helicopter performance criteria to be considered in designing the Sky-Horizon gimbals are the roll, pitch, and yaw velocities ( $p$ ,  $q$ , and  $r$  respectively) and the roll, pitch, and yaw accelerations ( $\dot{p}$ ,  $\dot{q}$ , and  $\dot{r}$  respectively). In addition, the motion base characteristics of roll, pitch, and yaw velocities ( $\dot{\theta}_C$ ,  $\dot{\theta}_C$ ,  $\dot{\psi}_C$ , respectively) and roll, pitch, and yaw accelerations ( $\ddot{\theta}_C$ ,  $\ddot{\theta}_C$ ,  $\ddot{\psi}_C$ , respectively) are presented to achieve desired simulator performance.

An assumption has been made in the analysis that the maximum angular velocities and accelerations of the moving base will occur when it is near the center of its travel, i.e., the angular displacement is small enough that its effects can be ignored.

A right hand coordinate system as shown in Figure 4.2.3-1 was selected for defining the Sky-Horizon projector geometry. Each gimbal contains its own coordinate system and when all gimbals are at an angle of zero as shown in the figure,

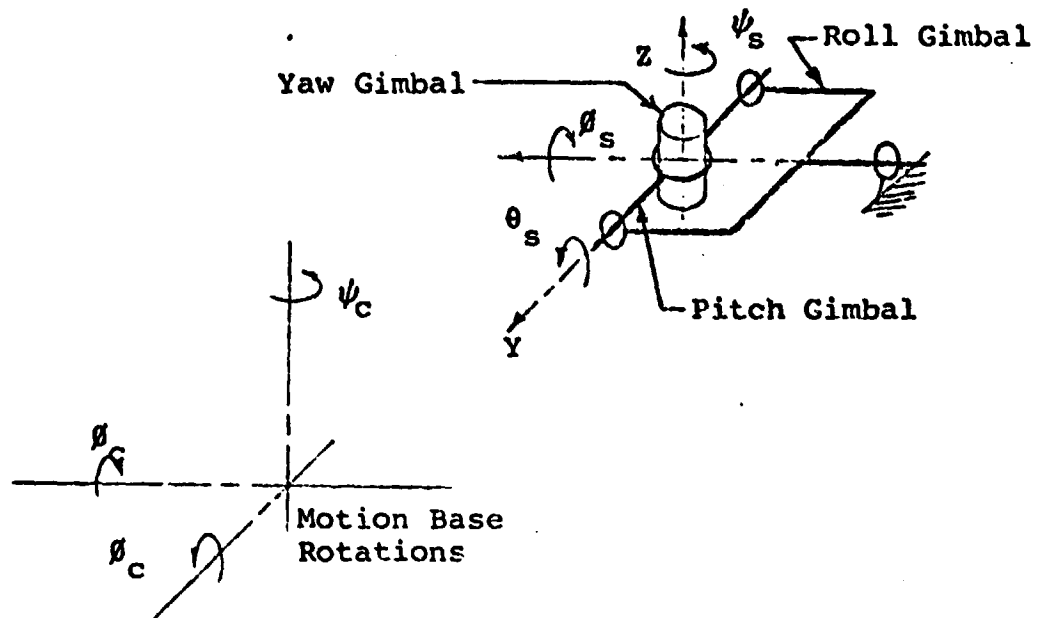


FIGURE 4.2.3-1 SKY-HORIZON PROJECTOR COORDINATES

the three gimbal coordinate systems coincide.

To provide the proper image on the screen the outermost gimbal (yaw gimbal) must have motion relative to the cockpit of the simulator which is exactly opposite to that of the helicopter maneuvers. Since the aircraft motion parameters  $p, q, r, \dot{p}, \dot{q}, \dot{r}$  can take either positive or negative signs, it was convenient in this analysis to attribute these motions to the yaw gimbal with positive signs as for a right hand system. (The aircraft would of necessity then be in a left hand system, but this is of no consequence here.)

The first step in the analysis is to define the motions of each gimbal relative to its supporting gimbal.

- $\dot{\psi}_s$  = velocity of the yaw gimbal relative to the pitch gimbal
- $\dot{\theta}_s$  = velocity of the pitch gimbal relative to the roll gimbal
- $\dot{\phi}_s$  = velocity of the roll gimbal relative to the cockpit
- $\ddot{\psi}_s$  = acceleration of the yaw gimbal relative to the pitch gimbal
- $\ddot{\theta}_s$  = acceleration of the pitch gimbal relative to the roll gimbal
- $\ddot{\phi}_s$  = acceleration of the roll gimbal relative to the cockpit

For clarity these subscripts will be dropped in the following equations.

The relative gimbal velocities have been derived in terms of the helicopter maneuvering velocity:

$$\begin{Bmatrix} \dot{\phi} \\ \dot{\theta} \\ \dot{\psi} \end{Bmatrix} = \begin{bmatrix} 1 & \sin \phi & \tan \theta & -\cos \phi & \tan \theta \\ 0 & \cos \phi & & \sin \phi & \\ 0 & -\sin \phi & \sec \theta & \cos \phi & \sec \theta \end{bmatrix} \begin{Bmatrix} p \\ q \\ r \end{Bmatrix} \quad (1)$$

where  $\phi$  = roll gimbal angle  
 $\theta$  = pitch gimbal angle

The relative gimbal accelerations are determined in terms of the helicopter accelerations and the gimbal velocities

$$\begin{Bmatrix} \ddot{\phi} \\ \ddot{\theta} \\ \ddot{\psi} \end{Bmatrix} = \begin{bmatrix} 1 & \sin \phi & \tan \theta & -\cos \phi & \tan \theta \\ 0 & \cos \phi & & \sin \phi & \\ 0 & -\sin \phi & \sec \theta & \cos \phi & \sec \theta \end{bmatrix} \begin{Bmatrix} \dot{p} \\ \dot{q} \\ \dot{r} \end{Bmatrix} + \begin{bmatrix} \tan \theta & 0 & -\sec \theta \\ 0 & \cos \theta & 0 \\ -\sec \theta & 0 & \tan \theta \end{bmatrix} \begin{Bmatrix} \dot{\phi} \dot{\theta} \\ \dot{\phi} \dot{\psi} \\ \dot{\theta} \dot{\psi} \end{Bmatrix} \quad (2)$$

Note in the above equations  $\dot{\phi}$ ,  $\dot{\theta}$ ,  $\dot{\psi}$  and  $\ddot{\phi}$ ,  $\ddot{\theta}$ , and  $\ddot{\psi}$  are scalar values and are not to be considered as vector quantities as might be indicated by the form of the equations.

The velocity requirements for the gimbals depend only on those velocities required to meet helicopter performance criteria. This follows from the fact that all gimbals are supported on the cockpit base and are not influenced by the motion of the base. Therefore equations (1) suffice for determining gimbal velocity requirements.

The acceleration requirements, however, which are required for sizing torque motors and for computing bearing loads depend on motion in inertial space. Therefore, the moving

base velocities ( $\dot{\theta}_C$ ,  $\dot{\phi}_C$ , and  $\dot{\psi}_C$ ) and accelerations ( $\ddot{\theta}_C$ ,  $\ddot{\phi}_C$ , and  $\ddot{\psi}_C$ ) must be taken into account.

These accelerations are designated as inertial accelerations to distinguish their difference from the gimbal-to-gimbal relative accelerations given in equations (2). The following matrix equations for the inertial accelerations are written in terms of the moving base motion characteristics and the values given in equations (1) and (2).

The inertial acceleration vector for the roll gimbal relative to the cockpit is:

$$\begin{Bmatrix} \ddot{\theta}_{cp} \end{Bmatrix} = \begin{bmatrix} 1 & 0 & 0 \\ 0 & \cos \theta & \sin \theta \\ 0 & -\sin \theta & \cos \theta \end{bmatrix} \begin{Bmatrix} \ddot{\theta}_C + \ddot{\theta} \\ \ddot{\phi}_C + \dot{\theta} \dot{\psi}_C \\ \dot{\psi}_C - \dot{\theta} \dot{\phi}_C \end{Bmatrix} \quad (3)$$

The first component of this vector is the acceleration about the roll axis. The second and third components are the accelerations about the y and z axes of the roll gimbal and contribute to bearing loads.

The inertial acceleration vector for the pitch gimbal relative to the roll gimbal is:

$$\begin{Bmatrix} \ddot{\theta}_p \end{Bmatrix} = \begin{bmatrix} \cos \theta & \sin \theta \sin \theta & -\cos \theta \sin \theta \\ 0 & \cos \theta & \sin \theta \\ \sin \theta & -\sin \theta \cos \theta & \cos \theta \cos \theta \end{bmatrix} \begin{Bmatrix} \ddot{\theta}_C + \dot{\theta}_C \dot{\theta} \sin \theta \\ + \ddot{\theta} - \dot{\psi}_C \dot{\theta} \cos \theta \\ \ddot{\phi}_C + \ddot{\theta} \cos \theta - \dot{\psi}_C \dot{\theta} \\ - \dot{\theta} \sin \theta (\dot{\theta} + \dot{\phi}_C) \\ \ddot{\psi}_C + \ddot{\theta} \sin \theta - \dot{\theta}_C \dot{\theta} \\ + \dot{\theta} \cos \theta (\dot{\theta} + \dot{\phi}_C) \end{Bmatrix} \quad (4)$$

The second component provides the acceleration about the pitch axis. The first and third components are accelerations about the x and z axis of the pitch gimbal for computing bearing loads.

The inertial acceleration vector for the yaw gimbal relative to the pitch gimbal is:

$$\left\{ \ddot{\psi}_{\theta} \right\} = \begin{bmatrix} \cos \psi \cos \theta & \cos \psi \sin \theta \sin \theta & -\cos \psi \cos \theta \sin \theta \\ & + \sin \psi \cos \theta & + \sin \psi \sin \theta \\ -\sin \psi \cos \theta & -\sin \psi \sin \theta \sin \theta & \sin \psi \cos \theta \sin \theta \\ & + \cos \psi \cos \theta & + \cos \psi \sin \theta \\ \sin \theta & -\sin \theta \cos \theta & \cos \theta \cos \theta \end{bmatrix} \begin{bmatrix} \ddot{\psi}_c + \dot{\theta}_c r \\ + \dot{p} - \dot{\psi}_c q \\ \ddot{\theta}_c + \dot{\psi}_c p \\ + \dot{q} - \dot{\theta}_c r \\ \ddot{\psi}_c + \dot{\theta}_c q \\ + \dot{r} - \dot{\theta}_c r \end{bmatrix} \quad (5)$$

The third component is the acceleration about the yaw axis. The first and second components are about the x and y axis of the yaw gimbal.

#### Maximum Gimbal Velocities

The maximum gimbal velocities are obtained by maximizing equation (1) and substituting the maximum aircraft velocities as given in Table 2.2-1:

$$p = 100 \text{ deg/sec} = 1.75 \text{ ra/sec}$$

$$q = 60 \text{ deg/sec} = 1.05 \text{ ra/sec}$$

$$r = 100 \text{ deg/sec} = 1.75 \text{ ra/sec}$$

The pitch angle

$$\theta = \theta_{\max} = 70^\circ$$

results in maximum velocities.

The maximum roll gimbal velocity relative to the cockpit is:

$$\dot{\theta}_{\max} = p + \tan \theta \sqrt{q^2 + r^2} = 7.36 \text{ ra/sec}$$

The maximum pitch gimbal velocity relative to the roll gimbal is:

$$\dot{\theta}_{\max} = \sqrt{q^2 + r^2} = 2.04 \text{ ra/sec}$$

The maximum yaw gimbal velocity relative to the pitch gimbal is:

$$\dot{\psi}_{\max} = \sec \theta \sqrt{q^2 + r^2} = 5.97 \text{ ra/sec}$$

These maximum velocities are the no-load velocities which the gimbal torque motors must achieve.

### Maximum Gimbal Inertial Accelerations

The maximum gimbal inertial accelerations about the rotating axes of the gimbals are obtained by maximizing the appropriate component from equations (3), (4) and (5). Expressions for the velocity and acceleration terms are substituted from equations (1) and (2). Subsequently, values for aircraft velocities and accelerations and moving base velocities and accelerations are substituted before maximizing the equations.

#### Roll Gimbal Acceleration

$$\ddot{\theta}_{cp} = \ddot{\theta}_c + \dot{p} + \tan \theta [(\dot{q} + pr) \sin \theta (\dot{r} + pq) \cos \theta] \\ + \sec^2 \theta (1 + \sin^2 \theta) [(q^2 - r^2) \sin \theta \cos \theta + qr (\sin^2 \theta - \cos^2 \theta)]$$

the terms containing  $\theta$  reach their maximum positive value when

$$\theta = \theta_{\max} = 70^\circ$$

Assuming maximum values of velocity ( $p$ ,  $q$ , and  $r$  as given above)

$$q_{\max} < r_{\max}$$

Therefore the term  $(q^2 - r^2)$  is negative.

With the roll gimbal angle in the second quadrant so that  $\cos \theta$  is negative, all terms (with the possible exception of  $\sin^2 \theta - \cos^2 \theta$ ) are positive. By substituting maximum positive values of velocities and accelerations from Tables 2.2-2 and 2.2-3 an equation which can be maximized in respect to  $\theta$  is obtained.

$$\begin{aligned} \dot{p} &= 150 \text{ ra/sec}^2 = 2.62 \text{ ra/sec}^2 \\ \dot{q} &= 100 \text{ ra/sec}^2 = 1.75 \text{ ra/sec}^2 \\ \dot{r} &= 100 \text{ ra/sec}^2 = 1.75 \text{ ra/sec}^2 \end{aligned}$$

$$\begin{aligned} \dot{\theta}_c &= 0.5 \text{ ra/sec} & \ddot{\theta}_c &= 1 \text{ ra/sec}^2 \\ \dot{\theta}_c &= 0.5 \text{ ra/sec} & \ddot{\theta}_c &= 1 \text{ ra/sec}^2 \\ \dot{\psi}_c &= 0.6 \text{ ra/sec} & \ddot{\psi}_c &= 1 \text{ ra/sec}^2 \end{aligned}$$

$$\ddot{\theta}_{cp \max} = 3.62 + 13.22 \sin \theta - 9.857 \cos \theta \\ - 31.556 \sin \theta \cos \theta + 29.584 (\sin^2 \theta + \cos^2 \theta)$$

Maximizing this equation in respect to  $\theta$

$$\ddot{\theta}_{cp \max} = 52.5 \text{ ra/sec}^2 \text{ at an angle of } \theta = 106^\circ$$

It is unreasonable to expect all velocities and accelerations to reach their maximum positive values simultaneously. In fact, if the velocity is at its maximum positive value, the corresponding acceleration could only be less than or equal to zero.

A reasonable assumption is to compute a maximum acceleration when all aircraft velocities and accelerations are at one-half their maximum values. The resulting value of roll acceleration is:

$$\ddot{\theta}_{cp \max} = 14.1 \text{ ra/sec}^2 \text{ at an angle of } \theta = 105^\circ$$

Since under these assumed conditions the gimbal is moving at some velocity, the required stall acceleration must be considerably higher. Based on the torquer having a straight line torque-velocity characteristic a reasonable assumption is to double this value for the stall acceleration.

$$\ddot{\theta}_{cp \text{ stall}} = 28.2 \text{ ra/sec}^2$$

Pitch Gimbal Acceleration:

$$\ddot{\theta}_\theta = (\ddot{\theta}_c + \dot{q} - p \dot{\psi}_c + pr) \cos \theta + (\ddot{\psi}_c + \dot{r} - p \dot{\theta}_c - pq) \sin \theta \\ - \tan \theta (q \sin \theta - r \cos \theta) [(\dot{\theta}_c + q) \sin \theta + (\dot{\psi}_c - r) \cos \theta]$$

Again assume  $\theta = \theta_{\max} = 70^\circ$

If  $\ddot{\theta}_c$ ,  $\ddot{\psi}_c$ ,  $\dot{r}$ ,  $\dot{q}$ , and  $r$  assume their maximum negative values, the remaining terms are at their maximum positive values and  $\theta$  is in the first quadrant,  $\ddot{\theta}_\theta$  will reach its maximum value (negative in this case).

$$\ddot{\theta}_{\theta} = -6.863 \cos \theta - 5.463 \sin \theta \\ - \tan 70^{\circ} (1.05 \sin \theta + 1.75 \cos \theta) (1.55 \sin \theta + 2.35 \cos \theta)$$

By maximizing this expression in respect to  $\theta$

$$\ddot{\theta}_{\theta \text{ max}} = -24.51 \text{ ra/sec}^2 \text{ at } \theta = 34^{\circ}$$

As above we will consider velocities and accelerations at one-half of their maximum values.

$$\ddot{\theta}_{\theta \text{ max}} = -9.21 \text{ ra/sec}^2 \text{ at } \theta = 35^{\circ}$$

Again we double this value to obtain a stall acceleration:

$$\ddot{\theta}_{\theta \text{ stall}} = 18.4 \text{ ra/sec}^2$$

#### Yaw Gimbal Acceleration

$$\ddot{\psi}_{\theta} = \sin \theta (\ddot{\theta}_c + \dot{p} + \dot{\theta}_c r - \dot{\psi}_c q) \\ - \cos \theta [(\ddot{\theta}_c + \dot{q} + \dot{\psi}_c p - \dot{\theta}_c r) \sin \theta - (\ddot{\psi}_c + \dot{r} + \dot{\theta}_c q \\ - \dot{\theta}_c p) \cos \theta]$$

Maximizing this expression in respect to  $\theta$  and  $\theta$

$$\ddot{\psi}_{\theta \text{ max}} = \left[ (\ddot{\theta}_c + \dot{p} + \dot{\theta}_c r - \dot{\psi}_c q)^2 + (\ddot{\theta}_c + \dot{q} + \dot{\psi}_c p - \dot{\theta}_c r)^2 \right. \\ \left. + (\ddot{\psi}_c + \dot{r} + \dot{\theta}_c q - \dot{\theta}_c p)^2 \right]^{1/2}$$

It is apparent that each of the expression in ( )'s will be maximum if all signs are positive or all signs are negative. The signs of  $\ddot{\theta}_c$ ,  $\ddot{\psi}_c$ ,  $\dot{p}$ ,  $\dot{q}$ , and  $\dot{r}$  can be changed as desired to meet this maximum condition. However, a sign change in any one of the terms  $\dot{\theta}_c$ ,  $\dot{\psi}_c$ ,  $p$ ,  $q$ , or  $r$  will change signs in two and only two of the three expressions.

Therefore it is necessary to substitute actual values in these expressions to determine which changes will result in a maximum acceleration. Again one-half of the maximum values of aircraft velocities and accelerations were assumed.

The maximum acceleration resulted when  $\dot{\psi}$ ,  $\delta_c$ ,  $\dot{\psi}_c$ ,  $\dot{q}$  and  $\dot{r}$  were taken to be negative with all other values positive. A similar result was obtained with  $r$ ,  $\ddot{\psi}_c$ ,  $\ddot{\psi}_c$ ,  $\dot{p}$  and  $\dot{r}$  negative with the other values positive. This acceleration is:

$$\ddot{\psi}_{\theta \text{ max}} = 4.65 \text{ ra/sec}^2$$

On doubling this value we obtain a stall acceleration of

$$\ddot{\psi}_{\theta \text{ stall}} = 9.3 \text{ ra/sec}^2$$

#### 4.3 PROBE PROTECTION DESIGN ANALYSIS

Why is a probe protection system necessary? The optical probe is a critical element of any modelboard terrain image generator. High quality wide angle probes are state-of-the-art devices. As such they are very expensive, and have long lead times for both purchase and factory rebuild. As if this were not enough, their delicacy, necessarily exposed position, and usage with the terrain board combine to make the probe a highly likely candidate for damage. Clearly adequate protective measures of some sort are required, if the modelboard terrain image generation subsystem is to be of practical use.

Some specialized techniques are in use at various existing facilities. One approach is to limit gantry travel such that the probe is not permitted to approach the modelboard any closer than the highest terrain feature. This technique may be extended slightly by partitioning the modelboard into a few rectangles and using hardwired logic to select minimum allowable probe altitude depending on probe location. In addition, some positive way to stop the gantry or retract the probe above all terrain must be added. Obviously neither of the approaches is suitable for a useful terrain following simulation. Another approach is to integrate a laser rangefinder with the probe optics to determine slant range to obstacles within the field-of-view. That is a big step forward for airplane simulation. However, the ability of a helicopter to fly backwards and sideways also introduces ways of crashing the probe, unprotected by the rangefinder. Even for conventional airplanes, the laser rangefinder would not protect against hardover lateral gantry drive failures or more likely manual gantry mis-operation. A physical height sensor could be located behind the probe. Unfortunately for real probe geometrics and useful terrain scales the maximum terrain gradients would be limited to a few degrees and/or the minimum terrain clearance height would exceed a hundred feet. Many other protection schemes from seemingly simple to complex have been considered and rejected for reasons of technical risk or lack of ability to protect against foreseeable consequences of normal operation,

abnormal operation or equipment failures. In apparent desperation, some probes (not wide angle) intended for terrain following use have been designed with the optical mirror mounted on a long slender replaceable extension. While this makes the unit field repairable, given a stock of spares at a few hundred dollars each, the simulator would still be down for several hours in the event of a crash, which can severely disrupt some tight test schedules. Worse yet, the approach simply sidesteps the basic problem of preventing crashes. Since these probes can be easily crashed in seconds by unskilled labor and require hours of skilled technician time to repair, the potential exists for rather low system availability.

#### 4.3.1 Design Analysis (Dynamic Clearance)

Assume that the gantry drives fail hardover at the initial time of this analysis from an arbitrary flight condition.

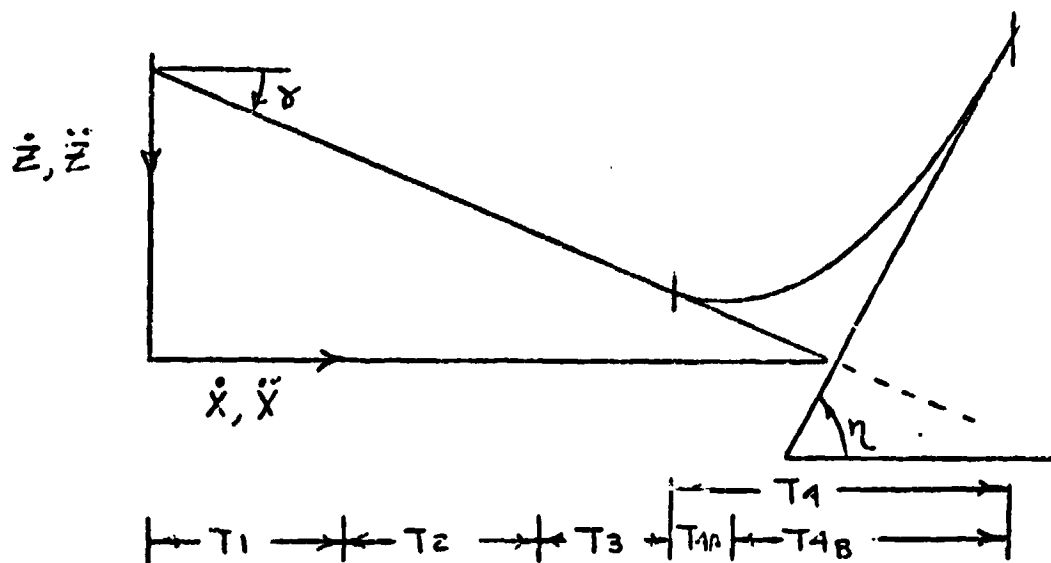


Figure 4.3-1

T1	Time from failure to input of sensor data
T2	Time for computer to recognize unsafe condition
T3	Time for trigger mechanism to respons
T4	Time from trigger release to tangential terrain clearance
T4A	Time for retract mechanism to achieve upward motion
T4B	Time from zero vertical velocity to tangential terrain clearance

$X_n$  Horizontal distance traveled from point of failure through time interval  $n$   
 $Z_n$  Vertical equivalent of  $X_n$   
 $A_R$  Probe retract acceleration  
 $\eta$  Terrain angle  
 $\gamma$  Initial flight path angle  
 $t_n$  Time at the end of interval  $n$   
 $n$  As a subscript implies value of variable at  $t_n$   
 $T_D$   $T_1 + T_2 + T_3$  Total reaction delay  
 $a_x$  Maximum gantry horizontal acceleration (frictionless)  
 $a_z$  Maximum gantry vertical acceleration (frictionless)  
 $\hat{z}_4$  Vertical position of probe at  $t_4$  w/o retraction

This analysis assume circular velocity limiting:  
 $(x^2 + y^2)^{1/2}$  HVL (horizontal velocity limit). This makes the dynamic clearance requirement analysis independent of heading.

Since data from the gantry sensors are sampled at time intervals of  $T_2$ , the worst case time from failure to sensing,  $T_1$ , is equal to the sampling interval.

$$T_1 = T_2$$

Worst case time for computing recognition of the last condition input as being unsafe,  $T_2$ , is a system design parameter. Likewise, the time for trigger release,  $T_3$ , is a system design parameter. The retract times  $T_4$  and  $T_5$  are functions of gantry rates, terrain gradient and retract acceleration.

This analysis determines the total horizontal and vertical dynamic clearance requirements  $X_4$  and  $Z_4$  respectively. The following section of analysis would then add static clearances and solve for  $T_D$  as a function of the clearances and other system parameters.

$$X_4 = \int_{T_1} \dot{X}(t) dt + \int_{T_2} \dot{X}(t) dt + \int_{T_3} \dot{X}(t) dt + \int_{T_4} \dot{X}(t) dt \quad (1)$$

For a hardover servo  $\ddot{X}$  can be assumed constant such that  $\ddot{X} = \ddot{X}_0$ . Then (2)

$$\begin{aligned} X_4 &= \int_{T_1, T_2, T_3, T_4} \dot{X}(t) dt \\ &= \int_0^{t_4} (\dot{X}_0 + \ddot{X}_0 t) dt \\ &= \dot{X}_0 t_4 + \frac{1}{2} \ddot{X}_0 t_4^2 \\ &= \dot{X}_0 (T_0 + T_4) + \frac{1}{2} \ddot{X}_0 (T_0 + T_4)^2 \end{aligned} \quad (3)$$

$$Z_4 = \int_{T_1} \dot{Z}(t) dt + \int_{T_2} \dot{Z}(t) dt + \int_{T_3} \dot{Z}(t) dt + \int_{T_4} \dot{Z}(t) dt \quad (4)$$

The assumed vertical acceleration profile is  $\ddot{Z}_3 = \ddot{Z}_2 = \ddot{Z}_1 = \ddot{Z}_0$ . For the time interval from  $t_3$  to  $t_4$   $\ddot{Z} = \ddot{Z}_0 - A_R$ . Then

$$\begin{aligned} Z_4 &= \int_{T_1, T_2, T_3} \dot{Z}(t) dt + \int_{T_4} \dot{Z}(t) dt \\ &= \int_0^{t_3} (\dot{Z}_0 + \ddot{Z}_0 t) dt + \int_{t_3}^{t_4} [\dot{Z}_3 + (\ddot{Z}_0 - A_R)t] dt \quad (5) \end{aligned}$$

However  $\dot{Z}_3 = \dot{Z}_0 - \int_0^{t_3} \ddot{Z}_0 dt$

$$\dot{Z}_3 = \dot{Z}_0 + \ddot{Z}_0 T_0 \quad (6)$$

Substituting equation 6 into equation 5 yields

$$\begin{aligned} Z_4 &= \int_0^{t_3} (\dot{Z}_0 + \ddot{Z}_0 t) dt + \int_{t_3}^{t_4} [\dot{Z}_0 + \ddot{Z}_0 T_0 + (\ddot{Z}_0 - A_R)t] dt \\ &= \dot{Z}_0 t_3 + \frac{1}{2} \ddot{Z}_0 t_3^2 + \dot{Z}_0 T_4 + \ddot{Z}_0 T_0 T_4 + \frac{1}{2} (\ddot{Z}_0 - A_R) t_4^2 - \frac{1}{2} (\ddot{Z}_0 - A_R) t_3^2 \\ &= \dot{Z}_0 T_0 + \frac{1}{2} \ddot{Z}_0 T_0^2 + \dot{Z}_0 T_4 + \ddot{Z}_0 T_0 T_4 + \frac{1}{2} (\ddot{Z}_0 - A_R) (T_0 + T_4)^2 \\ &\quad - \frac{1}{2} (\ddot{Z}_0 - A_R) T_0^2 \\ &= \dot{Z}_0 T_0 + \dot{Z}_0 T_4 + \frac{1}{2} \ddot{Z}_0 T_0^2 + (2\ddot{Z}_0 - A_R) T_0 T_4 + \frac{1}{2} (\ddot{Z}_0 - A_R) T_4^2 \quad (7) \end{aligned}$$

Now  $T_4$  must be found as a function of system design parameters. From figure 4.3-1 it can be seen that at  $t_4$

$$-\frac{\partial Z}{\partial X} = \tan \eta \quad (8)$$

Since  $\frac{\partial Z}{\partial X} = \frac{\dot{Z}}{\dot{X}}$  equation 8 becomes

$$-\frac{\dot{Z}_4}{\dot{X}_4} = \tan \eta \quad (9)$$

ORIGINAL PAGE IS  
OF POOR QUALITY

$\dot{X}_4$  and  $\dot{Z}_4$  as functions of  $T_4$  then become

$$\dot{X}_4 = \dot{X}_0 + \ddot{X}_0 (T_D + T_4) \quad (10)$$

$$\dot{Z}_4 = \dot{Z}_3 + (\ddot{Z}_0 - A_R) T_4$$

However  $\dot{Z}_3 = \dot{Z}_0 + \ddot{Z}_0 T_D$  and  $\dot{Z}_4$  becomes

$$\dot{Z}_4 = \dot{Z}_0 + \ddot{Z}_0 T_D + (\ddot{Z}_0 - A_R) T_4 \quad (11)$$

Substituting equations 10 and 11 into equation 9 yields

$$\tan \eta = \frac{-[\dot{Z}_0 + \ddot{Z}_0 T_D + \ddot{Z}_0 T_4 - A_R T_4]}{\dot{X}_0 + \ddot{X}_0 T_D + \ddot{X}_0 T_4}$$

Solving for  $T_4$  yields

$$T_4 = \frac{(\dot{X}_0 + \ddot{X}_0 T_D) \tan \eta + \dot{Z}_0 + \ddot{Z}_0 T_D}{A_R - \ddot{Z}_0 - \ddot{X}_0 \tan \eta} \quad (12)$$

The  $Z_4$  found in equation 7 represents probe position at  $T_4$  during retraction. The computer must look ahead to  $t_4$  to determine if a crash would occur without retraction. Call the vertical position for that condition  $Z_4$ . This is easy to compute as a function of  $t_4$  since the conditions duplicate the X-axis calculations of equations 2 and 3. By similarity

$$\hat{Z}_4 = \dot{Z}_0 (T_D + T_4) + 1/2 \ddot{Z}_0 (T_D + T_4)^2$$

#### 4.3.1 Design Analysis (Dynamic Clearance) (continued)

The easiest way to evaluate these required dynamic clearances  $X_4$  and  $\hat{Z}_4$  is by means of a simple computer program which can tabulate these values for values of design parameters of interest. The data used in this computer evaluation are shown in Table 4.3-1. The program and results are found in Section 5. Significant results for terrain slope of  $45^\circ$  and a time delay of 70ms are listed in Table 4.3-2.

TABLE 4.3-1

#### PROBE PROTECT SUBSYSTEM PARAMETERS

Data Storage:  $690 \text{ ft}^2 @ 1 \text{ in}^2 \text{ grid}(500:1) = 99360 \text{ bytes}$   
 $690 \text{ ft}^2 @ 1/2 \text{ in grid}(250:1) = \underline{397440 \text{ bytes}}$   
 496800 bytes

Accelerations:	Model	Diag.	250:1 Equiv.	500:1 Equiv.
X, Y Gantry	0.017G*	0.024G	6.0G (Diag)	12.0G (Diag)
Z Gantry	0.014G*		3.5G	7.0G
Retract	5G		1250G	2500G

Static Clearances:	Diag.	250:1	500:1
Probe (circular)	1.12in	23.3 ft	46.7 ft
Quantization X 0.5 in	0.707in	14.7 ft	NA
Quantization X 1.0 in	1.414in	NA	58.9 ft
Pot. Repeatability X 0.024 in	0.034in	<u>0.7 ft</u> 38.7 ft	<u>1.4 ft</u> 107.0 ft
Probe Z 0.236 in		4.92 ft	9.83 ft
Quantization Z 0.056 in		1.17 ft	2.33 ft
Stability Z 0.039 in		<u>0.81 ft</u> 6.9 ft	<u>1.63 ft</u> 13.8 ft

#### Delay Time:

Computer frametime	30 msec X 2 = 60 msec
Trigger releasetime	<u>10 msec</u>
Maximum Delay	70 msec

\* Worst case, friction on gantry drives assumed zero.

Table 4.3-2

Significant Results From Computer Evaluation

Aircraft Velocity		Scale Factor of Model	Minimum Approach Distance*	
Horz. (knots)	Vert. Down (ft/sec)		Horz. (ft)	Vertical (ft)
0	0	250	39.3	7.2
120	0	250	54.7	7.2
120	50	250	54.9	11.1
0	0	500	108.0	14.4
120	0	500	122.8	14.4
120	50	500	123.0	18.1

\* This is the minimum approach distance to an obstruction along the horizontal and vertical component of the aircraft velocity vector before probe retract.

4.4.1 Requirements For A Color Display

Investigations and studies to determine the requirement for color in Simulator displays is limited. In the real world when performing low altitude flight maneuvers, colors are very discernible where at high altitude they tend to become monochromatic. Since the altitude requirement for the Helicopter Simulator is in the range of 10 feet to 1000 feet, color is required to generate an accurate analog of the real world. It is generally accepted that color provides additional cues that can aid in target detection and search tasks. Therefore, it would appear that color is a requirement for the Detailed Display. In as much as the eye is relatively insensitive to color in the peripheral vision, a monochromatic peripheral display with a green tint is probably acceptable. However, the requirement for a blue sky in all displays indicates that all displays should be color.

4.4.2 TV Camera System Selection

Since the Image Generation System is comprised of multiple color TV cameras sharing a common optical system, raster shaping in the camera is required to correct for optical distortions. This precludes the use of single tube camera systems for the following reasons.

Single tube field sequential cameras use a rotating color filter wheel to obtain the color information. Raster shaping results in image degradation due to the cam shaped wheel not being parallel to the scan lines at all points in the image. Optically encoded cameras (stripe filter) require linear scan lines to obtain the color information.

A logical choice appears to be a conventional RGB System which provides simultaneous color using beamsplitting dichroics to split the input image to the three camera tubes.

### Camera Tube

The camera tubes considered for use in the RGB color camera system are listed below:

- (1)  $\text{Sb}_2\text{S}_3$  Vidicon (standard)
- (2)  $\text{PbO}$  Vidicon (Plumbicon)
- (3) Silicon Target Vidicon
- (4)  $\text{CdSe}$  Vidicon (chalnicon)
- (5) Silicon Intensifier Target (SIT) tube
- (6) Image Isocon

At the present time, very few silicon-target tubes can be made with the quality required for high resolution or broadcast color cameras. These tubes lack dynamic range which results in blooming of image highlights and also exhibit lower resolution and higher blemish defect level than other vidicons. For these reasons, the silicon-target vidicon and SIT tube were not given further consideration.

Camera tubes that were considered suitable for use in high resolution cameras were the vidicon ( $\text{Sb}_2\text{S}_3$ ,  $\text{PbO}$ ,  $\text{CdSe}$ ) and the image isocon. Performance characteristics considered to be of primary importance for cameras used in simulator applications are Resolution, Lag, and Sensitivity. A comparison of these parameters for the candidate tubes, is made in Table 4.4.2-1. Other performance characteristics required to produce a high quality image are signal-to-noise ratio (S/N ratio) and blemish defect level. The S/N ratio for the candidate vidicons is 46DB to 49DB. The S/N ratio of the image isocon is unique as it has a higher S/N ratio for the picture blacks than whites, with S/N ratio being 49DB and 30DB respectively. S/N ratio and blemish defect level for all of the candidate tubes are such that a high quality image can be produced.

Performance of the image isocon and large format plumbicon is superior to the other tubes listed in Table 4.4.2-1 in many categories, however, they were not considered practical for use in a multi-tube color camera for the following reasons:

TABLE 4.4.2-1 CAMERA TUBE COMPARISON

	8541A Vidicon	E5063 Chalnicon	XQ1020 Plumbicon	45X0 Plumbicon	4807 Isocon
Faceplate Illumination (lm/ft <sup>2</sup> ) (NOTE 1)	3.0	0.1	0.4	0.24	0.001
Lag-Decay (% @ 50 ms)	20	0	< 5	7	6
Resolution • MTF @ 400 TV lines • Limiting TV lines	60 1000	55 850	55 ≥ 750	80 1400	75 1000
Format Diagonal - 4:3 Aspect ratio (mm)	16	16	21	28	40
Probe f/no required for the specified format	12	12	16	21	30
Probe input brightness required for f/no listed (ft. lamberts) (NOTE 2)	1728	58	410	423	3.6

NOTES:

- (1) Actual illumination required to obtain best resolution and lowest lag.
- (2) Does not include transmission of the probe or color separation optics.

- (1) Development of a multi-tube color camera would be required for either tube. Cost and technical risk would probably prohibit this development.
- (2) The image isocon is very large and the drive requirements more complex than the vidicon.
- (3) The large format plumbicon is still in the development stage and tubes suitable for use in the color cameras have not been demonstrated.

The  $\text{Sb}_2\text{S}_3$  8541 vidicon was eliminated because of its lack of sensitivity and marginal lag characteristics. The low sensitivity requires extremely high model illumination and the higher lag results in the lowest dynamic resolution.

Choosing between the E5063 fast response Chalnicon and the XQ1020 plumbicon is primarily a tradeoff between sensitivity and lag (dynamic resolution). Both tubes have a gamma of at least 0.9 and have approximately the same S/N ratio, and both are capable of producing high quality color images. The plumbicon provides the highest dynamic resolution, but requires (7) seven times more model illumination than the chalnicon. Selection of the chalnicon is recommended because the lag response (10% at 50 ms) is fairly good and the sensitivity is very good.

The Chalnicon offers other advantages such as uniform lag in each color channel, low dark current with good temperature stability, and good spectral response over the visible wavelengths. The spectral response for the Chalnicon camera tube can be found in Appendix 2. Figure 4.4.2-1 compares the Chalnicon spectral response with that of the probe optics.

Table 4.4.2-1 compares the performance of the camera tubes under normal simulator operating conditions. The faceplate illumination listed is the value required to simultaneously provide the highest resolution and lowest lag. The ratio of model illumination required for a given tube requires that the tube format and probe f/no be considered. The probe relay optics must be selected to be compatible with the camera tube format.

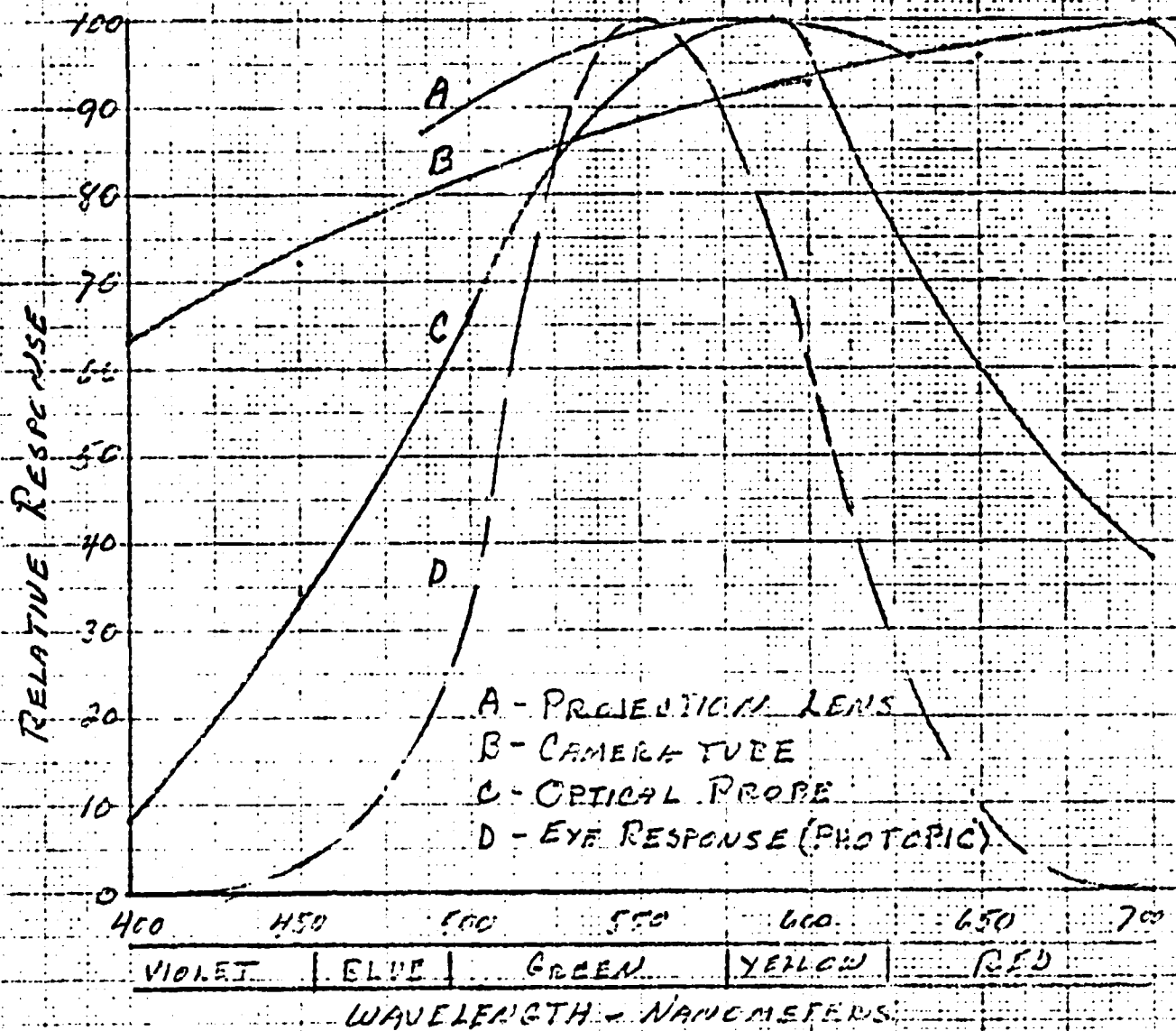


FIGURE 4.4.2-1 SPECTRAL RESPONSE CURVES

ORIGINAL PAGE IS  
OF POOR QUALITY

The probe has a fixed aperture of 1.0 mm, therefore, if the focal length is in milli-meters the f/no is numerically the same as the focal length, and increases as the size of the camera tube format increases. The focal length for a probe with F $\theta$  mapping and a field angle of 76 degrees can be determined as follows:

$$F \text{ (focal length)} = \frac{h \text{ (camera tube diagonal)}}{\theta \text{ (field angle in radians)}}$$

Inorder to determine the relative model illumination required the basic camera tube sensitivity must be modified by the probe f/no. established by the size of the format. The source brightness required to produced the required faceplate illumination (neglecting transmission losses) is determined by:

$$B_s = 4f^2 E_p$$

Where:

$B_s$  = Source brightness - ft. lamberts

$f$  = f/number @ infinity

$E_p$  = faceplate illumination - lm/ft<sup>2</sup>

To determine the actual model illumination required, the transmission of the optics and reflectance of the model must be considered. With an optical transmission of .084 (0.21 probe and 0.4 color separation optics), the model brightness required to produce the 0.1 lm/ft<sup>2</sup> faceplate illumination required for the chalnicon is 690 ft. lamberts. Assuming 0.5 reflectivity of the model highlights, the model illumination required is 1380 lm/ft<sup>2</sup>.

#### Camera Signal-to-Noise Ratio

The visual equivalent signal-to-noise ratio is normally defined as the ratio of highlight video-signal current to RMS noise current multiplied by a factor of 3, and is measured with a high gain, low noise, video preamplifier with a bandwidth of 5MHz. Therefore, a well disgned camera with a 5MHz bandwidth will have a S/N ratio comparable with the camera tube. However, high resolution cameras with wide band video amplifiers will have lower S/N ratio. S/N ratio of a high quality camera with a bandwidth of 27 MHz will be reduced to approximately 40 - 42DB.

### Raster Shaping

Shaping of the individual rasters is required to accurately match the contiguous segments of the single wide angle image generated by the optical probe. Shaping is also required to minimize the distortions caused by the  $h' - f\theta$  mapping of the probe. For this mapping function the image height is a linear function of the semi-field angle ( $\theta$ ), given a focal length  $f$ . The type of distortion introduced by this mapping function is shown in figure 4.4.2-2. To insure that distortions are adequately corrected the raster corrections shown in figure 4.4.2-3 should be provided.

### Stability and Registration

Sophisticated geometric correction electronics are required to correct for optical distortions. Performance in an RGB color camera can be impaired if this circuitry is not highly stable. Systems Research Laboratories has demonstrated in a 24 hour test of a similar system, stability better than 0.1%. This included the combined degradations of the analog geometry correction and linear scanning circuits. The goal for the helicopter simulator TV camera system will be 0.5%.

PART OF PROBE  
FIELD-OF-VIEW  
USED TO PROVIDE  
A 120° X 60° DISPLAY

OPTICAL PROBE  
TOTAL CIRCULAR  
FIELD-OF-VIEW 140°

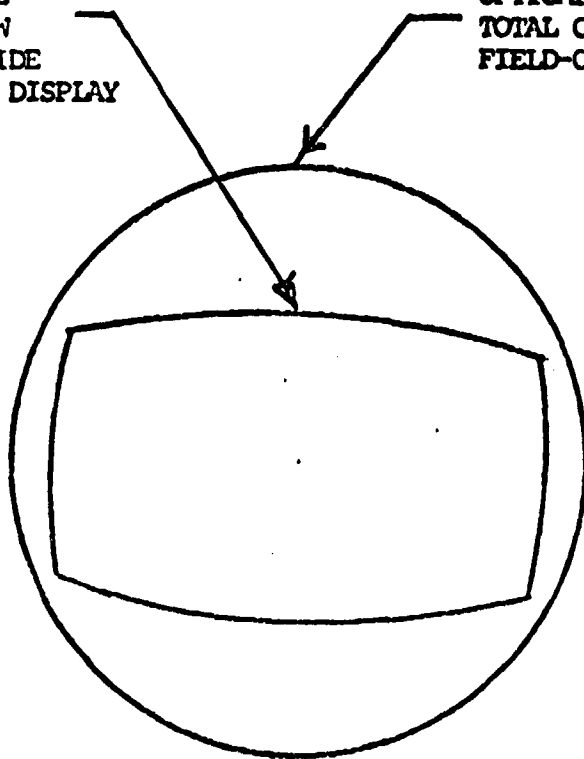


FIGURE 4.4.2-2

TYPICAL PROBE DISTORTION FOR  $h' = f \theta$  MAPPING

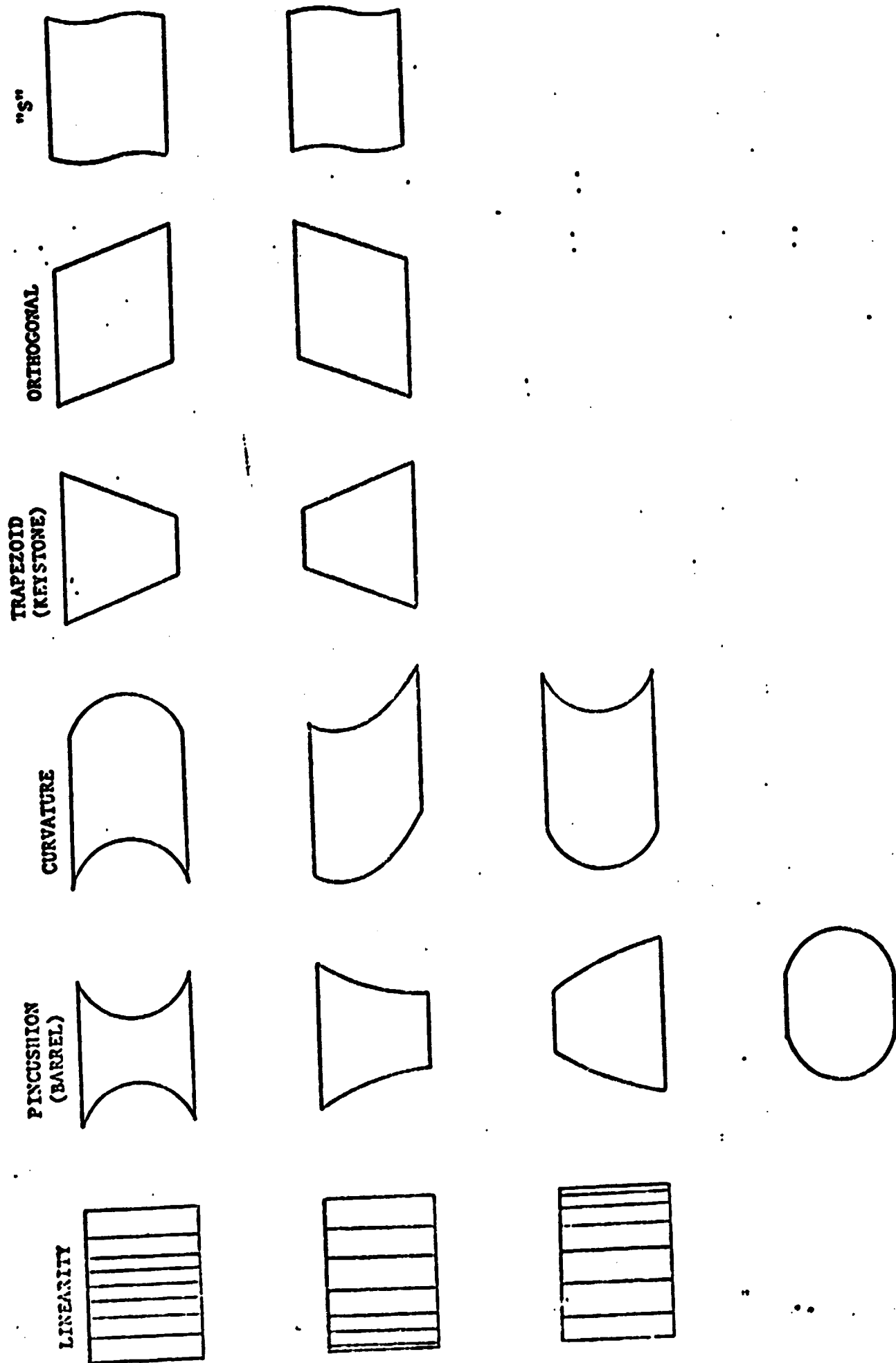


FIGURE 4.4.2-3

PASTER CORRECTIONS

#### 4.4.3 TV Projection System

Practical methods of producing a real image display of video information are presently limited to light valve projectors and CRT projectors, with both types capable of projecting color. Another method reported as feasible is the laser scanning system. Since this system requires further development, it will not be considered here.

The technique recommended to provide a wide angle, high resolution projection display requires accurate mosaicking of multiple displays. For the helicopter simulator the projectors are required to project onto a spherical screen from locations offset from the screen center. This requires shaping of each display to minimize distortions, and to edge match the images of contiguous displays.

Light valve projectors, such as the Eidophor and G.E. Systems, use a light source and deformable oil film in conjunction with schlieren optics. These systems do not provide a raster shaping capability. Techniques that do provide this capability are the CRT projector and the liquid crystal light valve (LCLV) projector. Current CRT projector designs can satisfy most of the simulator display requirements. The LCLV projector requires some further development before it can be considered to have demonstrated feasibility. For this reason the CRT projection technique is the recommended approach at this time. However, because of the similarity of the basic video and deflection electronics for the CRT and LCLV projectors, a brief discussion of the LCLV projector will be included.

##### LCLV Projector

The LCLV projector uses a CRT as a light modulating source. This writing light tilts the molecules of the liquid crystal and results in modulation of reflected light. An external xenon light source and polarizing beamsplitter is used to produce a high brightness image. Feasibility of the system has been adequately demonstrated. However, there are at least two areas of development remaining. The first is development

of production techniques to consistently produce uniform cells to specifications. The second is to reduce the response time of the cell to be consistent with CRT's.

The CRT and electronics technology required to drive the LCLV is the same as for the CRT projector. The video amplifiers, deflection amplifiers, and raster shaping circuitry required for the LCLV CRT and projection CRT are the same. However, lower deflection and high voltage power is required for the LCLV CRT as it operates at lower anode voltage. Although LCLV uses a single optical system, three CRT's are used to produce color.

From the above, it appears that in the future when the LCLV deficiencies are corrected, a transition to the LCLV, using existing electronics, would be feasible. Additional information for the LCLV projector is included in Appendix 3.

#### CRT Projector

The quality of the projected image produced by a CRT projector is determined by the resolution brightness, contrast, color fidelity, and image stability. This is the same as in any other display system. Resolution is dependent on the scanning parameters, video bandwidth, and registration accuracy and stability, in the same manner as the TV camera. In the projector, resolution is highly dependent on the CRT line width (or spot size), CRT and projection lens compatibility, and display brightness requirements.

Projection CRT - Resolution is primarily dependent on the CRT size and line width. Factors determining CRT size and line width are listed below:

- (1) Anode voltage and beam current
- (2) Phosphor luminous efficiency
- (3) Focusing method (electromagnetic or electrostatic)
- (4) CRT size compatible with practicable optics

Higher anode voltages are used to obtain higher CRT beam energy and display brightness. This results in lowering the beam current and reducing the beam diameter which in turn results in increased resolution.

Selecting phosphors with high luminous efficiency and providing faceplate cooling also results in resolution improvement. For a given CRT luminance beam current can be reduced and therefore the spot diameter becomes smaller.

Utilizing electromagnetic focus will provide a finer focus of the spot than electrostatic focus. This also improves resolution.

Finally, the usable CRT format and spot diameter determine the maximum limiting resolution that is attainable. The maximum CRT usable format is constrained by projection lens  $f$ /number and projection angle. Designing a practicable  $f/1.0$ , 60 degree lens requires a smaller format than  $f/1.0$ , narrow angle lens. Current low  $f$ /no. 60 degree projectors provide optimum performance with a 5 inch circular format (6 inch CRT). Some narrow angle low  $f$ /no. projectors use a 6 inch format (7 inch CRT). CRT's designed for wide angle projection are in use and have demonstrated performance. Table 4.4.3-1 lists the measured performance of a typical 6M124 tube set.

Projection Electronics - The same general requirements apply to the projector electronics as to the camera electronics. The projector electronics must have the same video bandwidth, registration and stability accuracy, and raster shaping capability. However, because of the high power requirements of the video amplifiers, deflection amplifiers, and high voltage power supplies, these must be given special consideration. All of these components must be provided with adequate cooling. Lead length of the deflection coils must be short and the operating voltages of the linear deflection amplifiers should be high to insure short ( $< 8\mu s$ ) retrace time. The high voltage power supply must be common to the CRT trio and must be highly regulated. This is required to preclude any possibility of the display size changing due to variation in voltage caused by changes in brightness or video content.

CRT Cooling - Efficient CRT cooling must be provided to provide maximum luminous efficiency and tube life. An effective cooling method compatible with refractive optics is to use a ported ring manifold supplied with high pressure air.

Raster Shaping - Shaping of the raster is required to correct for distortion due to the projection geometry. Figure 4.4.3-1 shows the correction magnitude and shaping required to produce a distortionless display format.

#### Display Compatability With CGI

Generation of imagery with sufficient detail to perform NOE flight tasks requires a probe-camera-model system at the present time. However, the digital computer image generation systems are showing the capability of generating greater detail, and in the future could replace the modelboard system. For this reason it is important that the TV projectors be capable of interfacing with high resolution CGI systems.

CGI systems currently being produced operate at line rates of 525 lines/frame to 1023 lines/frame and at field rates of 50 fields/second to 60 fields/second. These systems require fast video rise and fall times to produce a sharp CGI presentation. Typically the rise and fall time is less than 25 nano-seconds. Systems being developed to produce high detail (8000 to 10000 edges) operate at 1023 lines/frame and 30 frames/second, interlaced 2:1, and generate an RGB video output with synchronization in accordance with RS343.

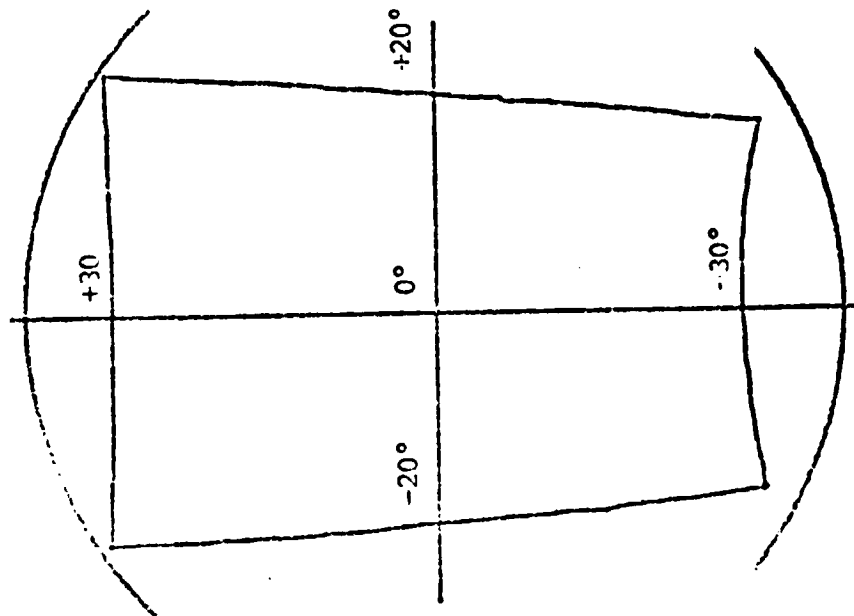
There are no unique requirements for a display system to interface with CGI as long as the scanning, video bandwidth, and color requirements are the same. Therefore, to insure that display TV projectors will interface with various current and future CGI designs, the following performance parameters have been established for all display TV projectors.

Line Rate	- 525 to 1225 lines/frame
Frame Rate	- 15 to 30 frames/second
Video Bandwidth	- $27 \pm 1$ DB MHz
Rise Time	- <20 ns
Color	- RGB
Sync	- RS343

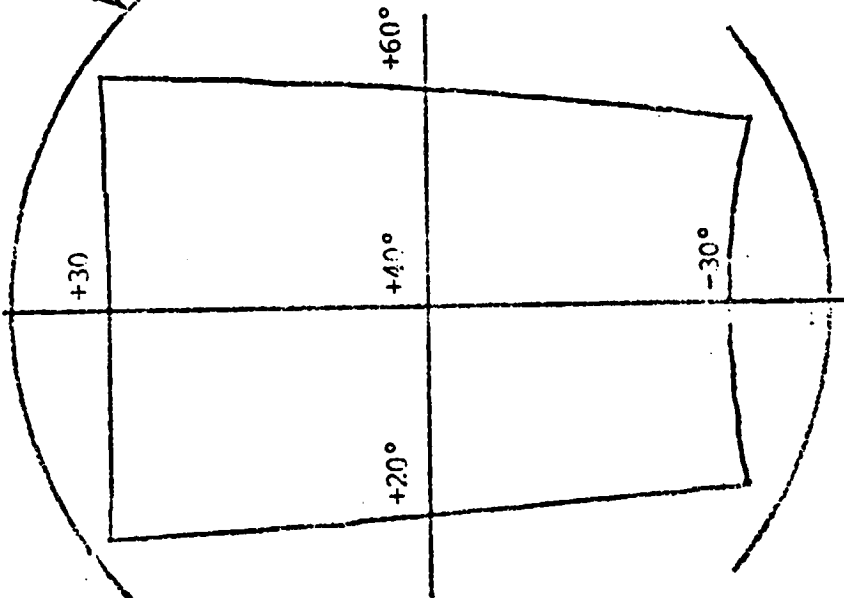
TABLE 4.4.3-1 CRT PERFORMANCE PARAMETER

PARAMETER	VALUE			UNITS
	GREEN	RED	BLUE	
Tube Type	6M124P1M	6M124P22M	6M124P501M	
Anode Voltage	45,000	45,000	45,000	VDC
Grid 1 Voltage	125	120	124	VDC
Grid 2 Voltage	995	1,062	1,023	VDC
Heater Voltage	6.3	6.3	6.3	VDC
Heater Current	600	600	600	MA
Beam Current	2.0	2.0	2.0	MA
Raster Size	1 x 4	1 x 4	1 x 4	Inches
Raster Lines	262	262	262	Lines
Light Output	23,400	14,615	2,320	Ft. Lamb.
Line Width	.0041	.0043	.0046	Inches

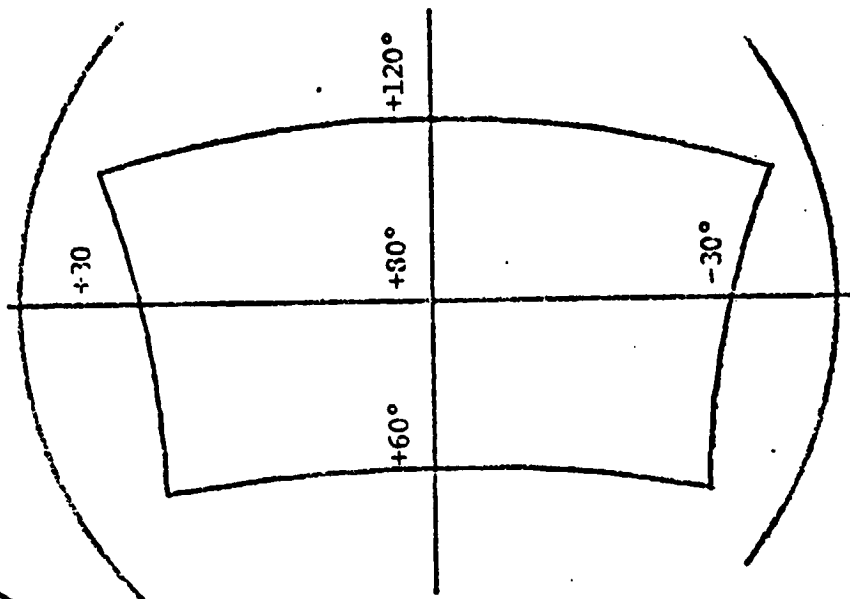
CENTER-DETAILED CRT



RIGHT DETAILED CRT



RIGHT PERIPHERAL CRT



5.3" MAXIMUM PERMISSIBLE CRT FOREFAT (TYPICALS)

NOTE: These are computer plots of corrections required for the center lens/CRT of each projector

FIGURE 4.4.3-1

CRT RASTER CORRECTION

#### 4.5 Field-Of-View, Resolution, and Display Brightness

A basic requirement of this study is to provide a preliminary design for a display system optimized to provide a wide field-of-view with high resolution and high brightness capability. The following discussion will consider achieving this goal using mosaicked, real image, CRT television projectors. Stimulus for the projectors can be from a wide angle multi-sensor probe/camera system or a CGI system.

The desirable performance parameters for the Detailed Display are as follows:

- |                   |                 |
|-------------------|-----------------|
| (1) Field-of-View | 180° H x 60° V  |
| (2) Resolution    | 4 ARC MIN/OLP   |
| (3) Luminance     | 8 Foot Lamberts |
| (4) Contrast      | 20:1            |
| (5) Color         | Yes             |

##### 4.5.1 Field-of-View

Performing NOE and low altitude helicopter flight research appears to require an accurate analog of the real world. Currently the camera-probe-model image generation system best fulfills this requirement. Current wide angle optical probes have a circular field-of-view (FOV) of 120° to 140°. Increasing the FOV beyond 140°, although feasible, would require considerable development and some technical risk. Therefore, the 140° optical probe has been selected for the detailed display pickup.

A single channel video pickup and display system cannot provide adequate resolution for a wide angle display, Therefore, a three channel system is being considered. The optical output of the probe is split into three cameras and displayed on three mosaicked projectors. The three channel system was chosen because the resolution and brightness approached the desired target values, and the number of projector heads required was compatible with the screen and cockpit configuration.

Providing an optimized FOV for each display channel is dependent on the following:

- (1) Compatibility of the combined display FOV with the probe FOV
- (2) Determining the horizontal and vertical FOV that provides best utilization of the camera tube and projection CRT resolution capabilities
- (3) Selecting the video performance parameters compatible with the display FOV

The reason for selecting the Chalnicon E5063 camera tube and Thomas 6M124 CRT are discussed in paragraph 4.4. The projector lens design must provide a total projection angle of  $63^{\circ}$  to provide a total FOV diagonal of the combined displays that is greater than the  $140^{\circ}$  probe diagonal. Because the viewer distance is 120 inches and the projector distance is 150 inches the maximum FOV diagonal for each display is approximately  $82^{\circ}$ . The focal length of the projection lens must be chosen such that the  $82^{\circ}$  FOV is achieved with a 5.3 inch diameter CRT format. Because CRT raster manipulation is required to correct for off axis projection, the non-corrected raster diagonal must be reduced to  $4.9 \pm 0.1$  inches or approximately 75 degrees/display to allow for correction overscan.

Figure 4.5-1 shows the FOV for two display configurations. Configuration (A) is compatible with all of the selected video and optical components of the conceptual system. Configuration (B) shows the display FOV optimized to achieve greater width and resolution. This configuration is not compatible with the candidate probe and camera tube, however, it could be used with high resolution CGI.

Figure 4.5-2 can be used to select the optimum FOV width and height for a given angular resolution. Video system parameters can then be established by converting angular resolution to TV resolution.

#### 4.5.2 Resolution

##### Limiting Resolution

The following analysis assumes that the optics and camera tube are not factors in determining the limiting resolution.

ORIGINAL PAGE IS  
OF POOR QUALITY

FIELD-OF-VIEW	CONFIGURATION A	CONFIGURATION B
EACH SEGMENT	40°X61°	45°X57°
TOTAL	200°X61°	225°X57°
RESOLUTION	6 MIN/LP	5 MIN/LP
SCAN RATE	1023	1225
BANDWIDTH	25 MHz	33 MHz

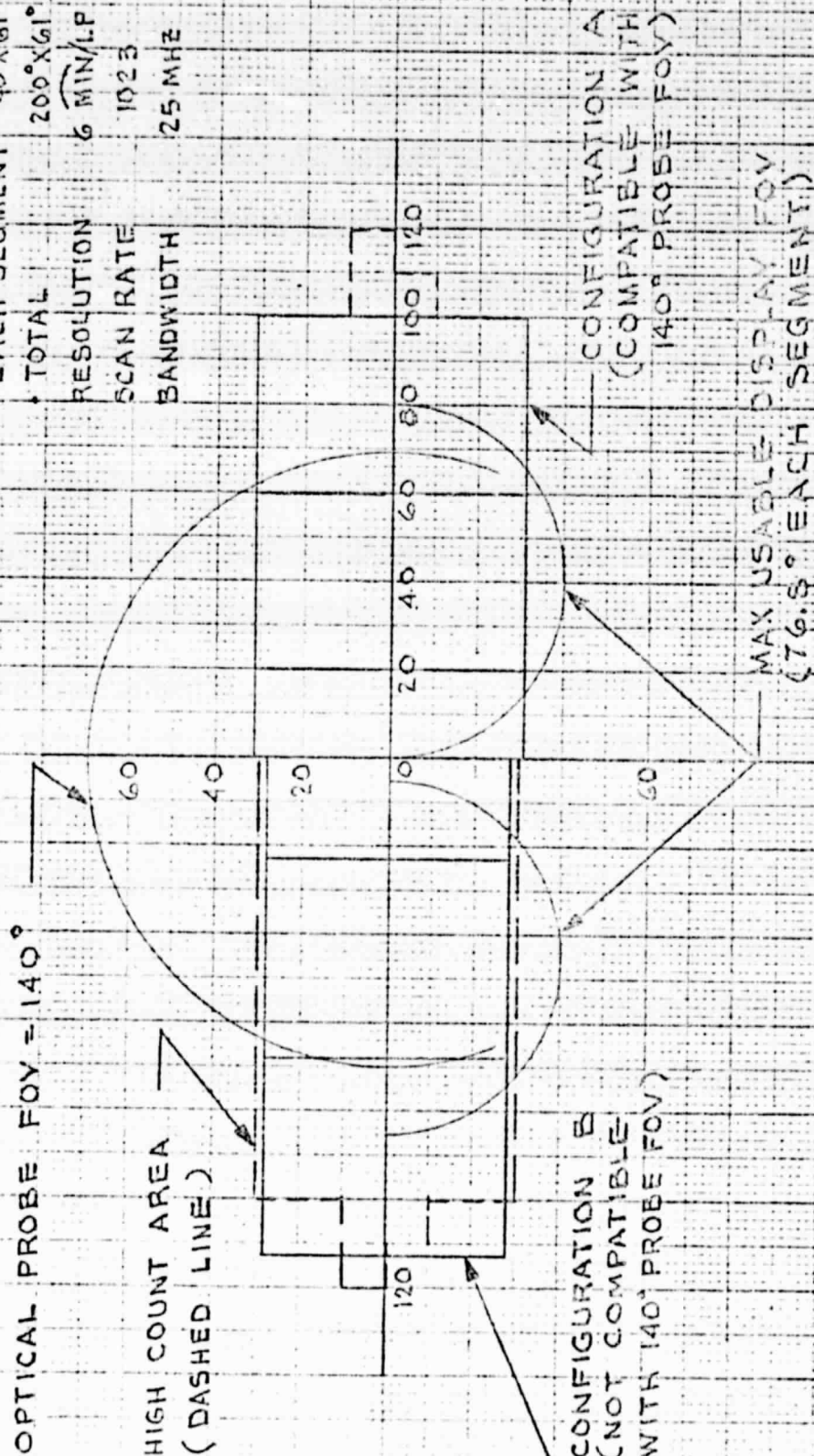


FIGURE 4.5-1 OPTICAL PROBE/ DISPLAY FIELD-OF-VIEW PLOT

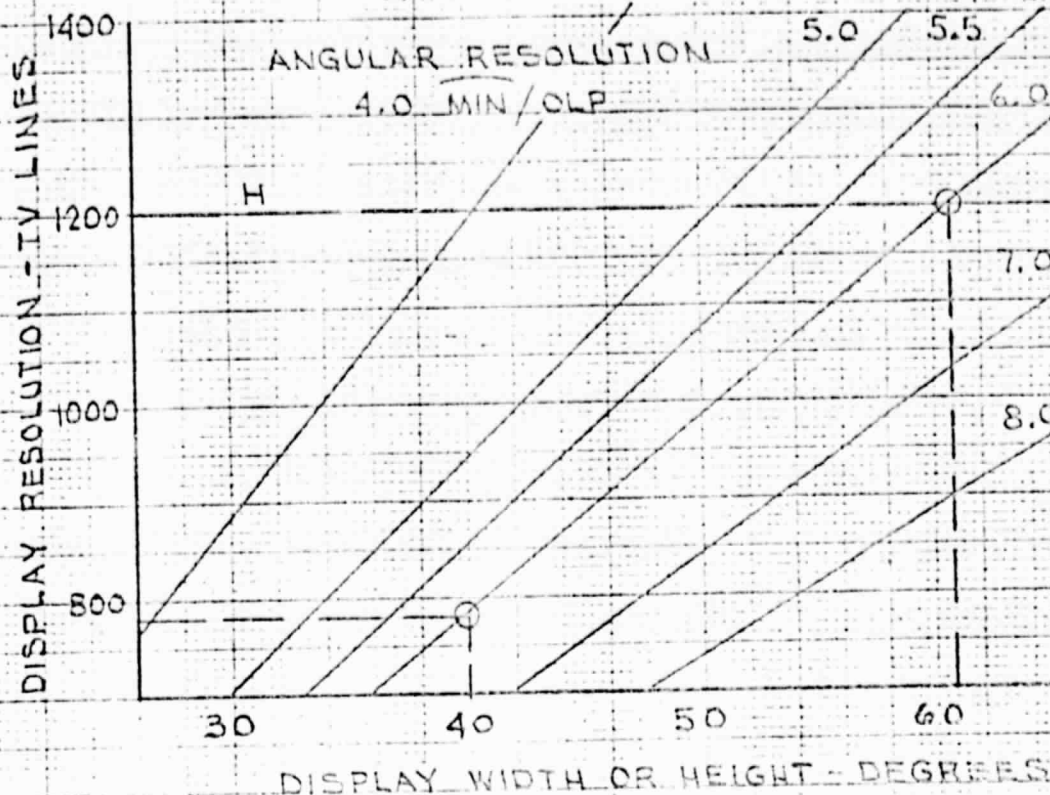


FIG 4.5-2A DISPLAY RESOLUTION VS. FOV

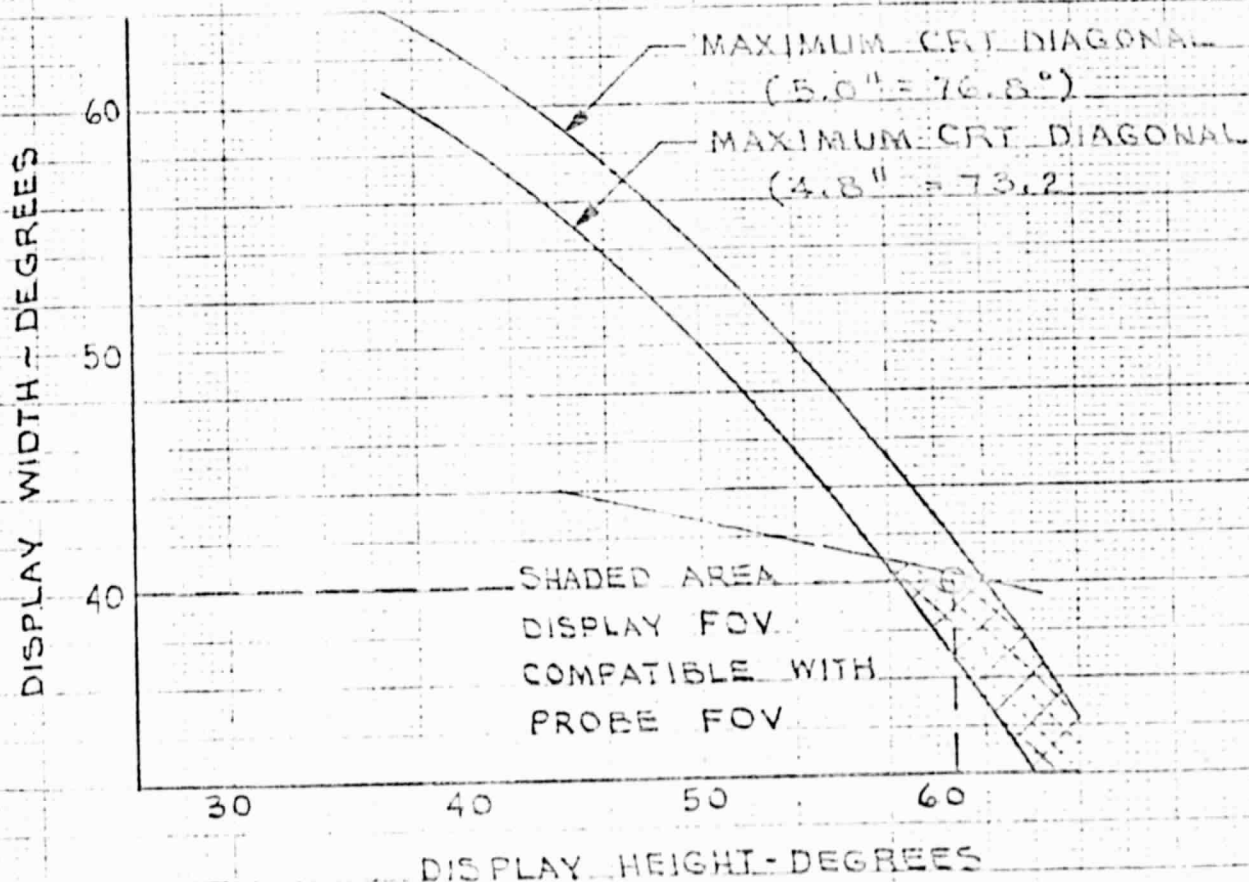


FIG 4.5-2B FOV WIDTH VS. DEGREES

From Figure 4.5-2A we see that in order to obtain a  $40^\circ \times 61^\circ$  FOV with an angular resolution of 6.0 Arc Min/OLP requires a display resolution of 1200 TV lines/display height and 780 TV lines/display width for each display. From Figure 4.5-3 we can determine the raster size required to produce a  $40^\circ \times 61^\circ$  FOV and also determine the CRT line width necessary to obtain CRT resolution compatible with the required display resolution. A 3.3 mil line width is required to satisfy the above. This is within the capability of the selected CRT, which is discussed in more detail in paragraph 4.5.3.

Television system scanning and video response parameters that will satisfy the display resolution requirements can be obtained from Figure 4.5.4. Consideration of the FOV, resolution, and image matching requirements, revealed that the optimum display is obtained if the scan lines are orientated vertically with respect to the viewer. The display resolution requirements previously established are listed below.

- (1) 780 TV Lines or 390 line pairs/display width

$$\text{angular resolution} = \frac{40^\circ \times 60 \text{ MIN/DEG}}{390 \text{ LP}} = 6.1 \text{ Arc Min/LP}$$

- (2) 1200 TV Lines or 600 line paris/display height

$$\text{angular resolution} = \frac{61^\circ \times 60 \text{ MIN/DEG}}{600 \text{ LP}} = 6.1 \text{ Arc Min/LP}$$

From Figure 4.5-4 780 TV lines/display width can be obtained with a scan rate of 1023 scan lines/frame using a kell factor of 0.8 ( $K = 0.8$  is attainable at the higher line rates). For a 1023 line/30 frame system, the horizontal scan period is 32.6 us. Allowing 25% for retrace and blanking the active scan period is 24.45 us. The video bandwidth required to provide 1200 TV lines/display height is as follows:

$$\text{Bandwidth} = \frac{600 \text{ line pairs}}{24.45 \text{ us}} = 24.54 \text{ MHz}$$

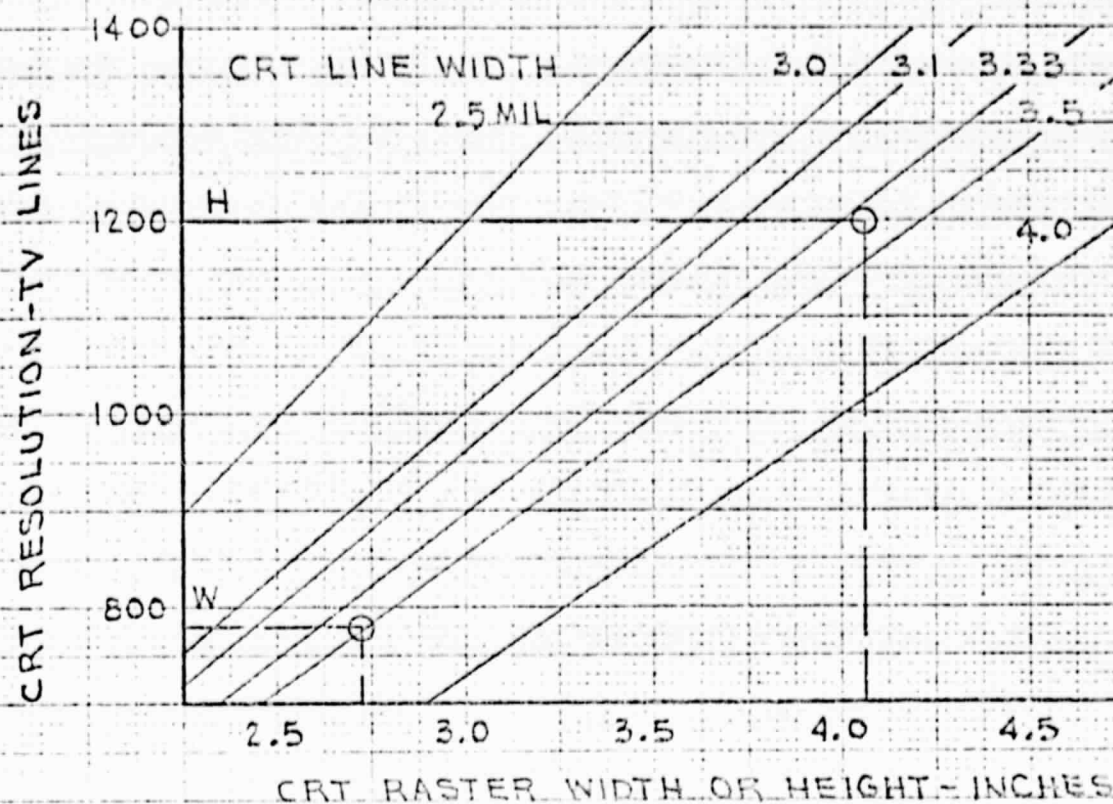


FIG 4.5-3A CRT RESOLUTION VS RASTER SIZE

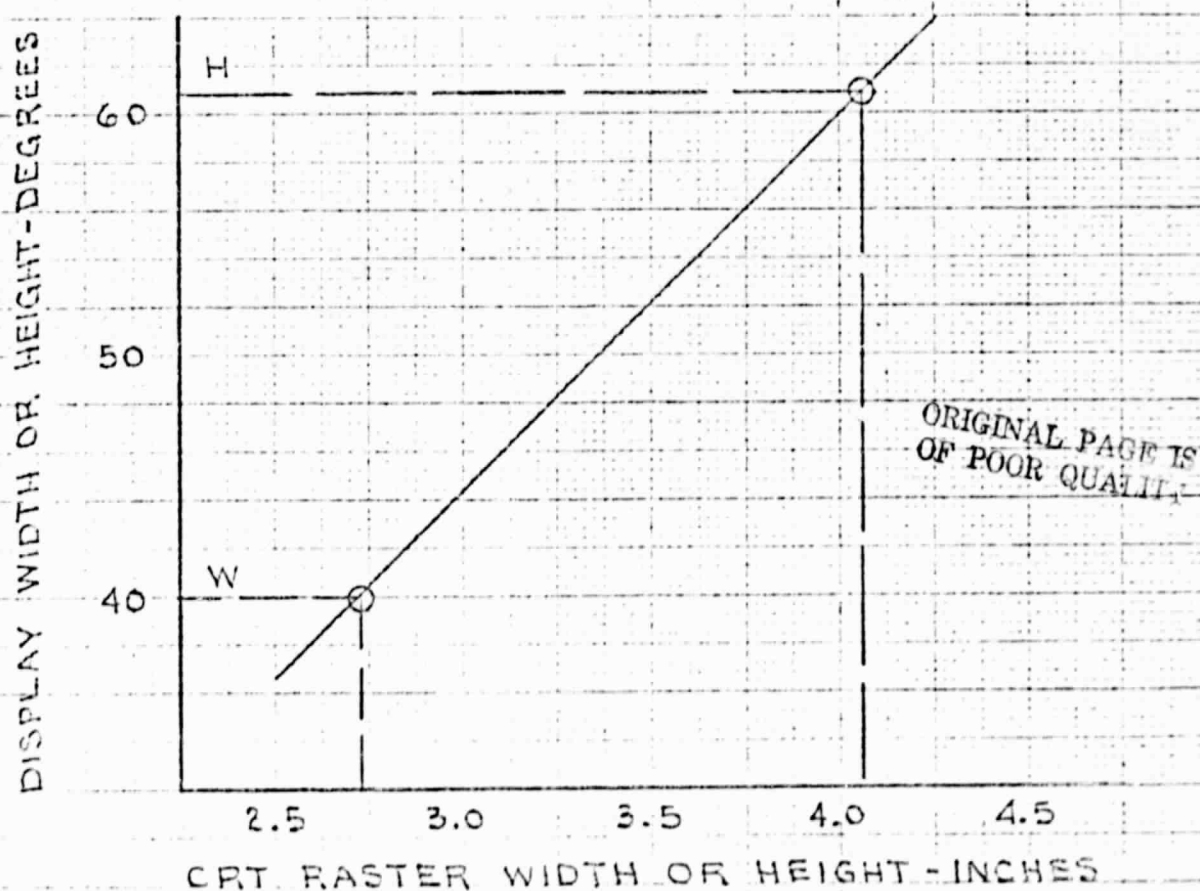
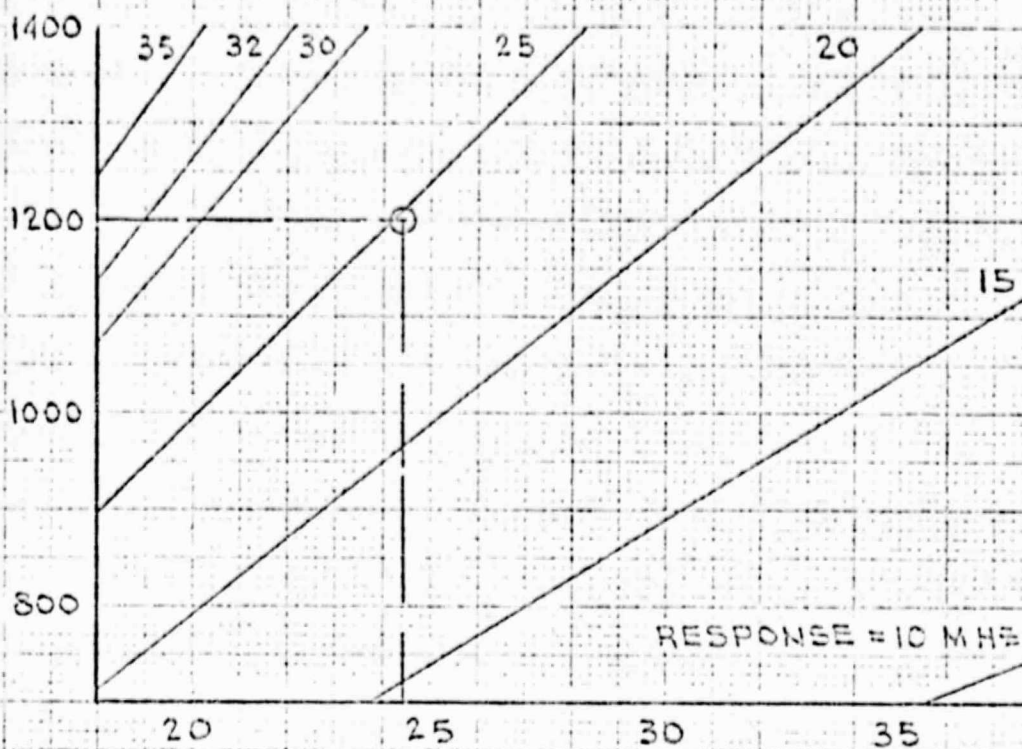


FIG 4.5-3B DISPLAY FOV VS. RASTER SIZE

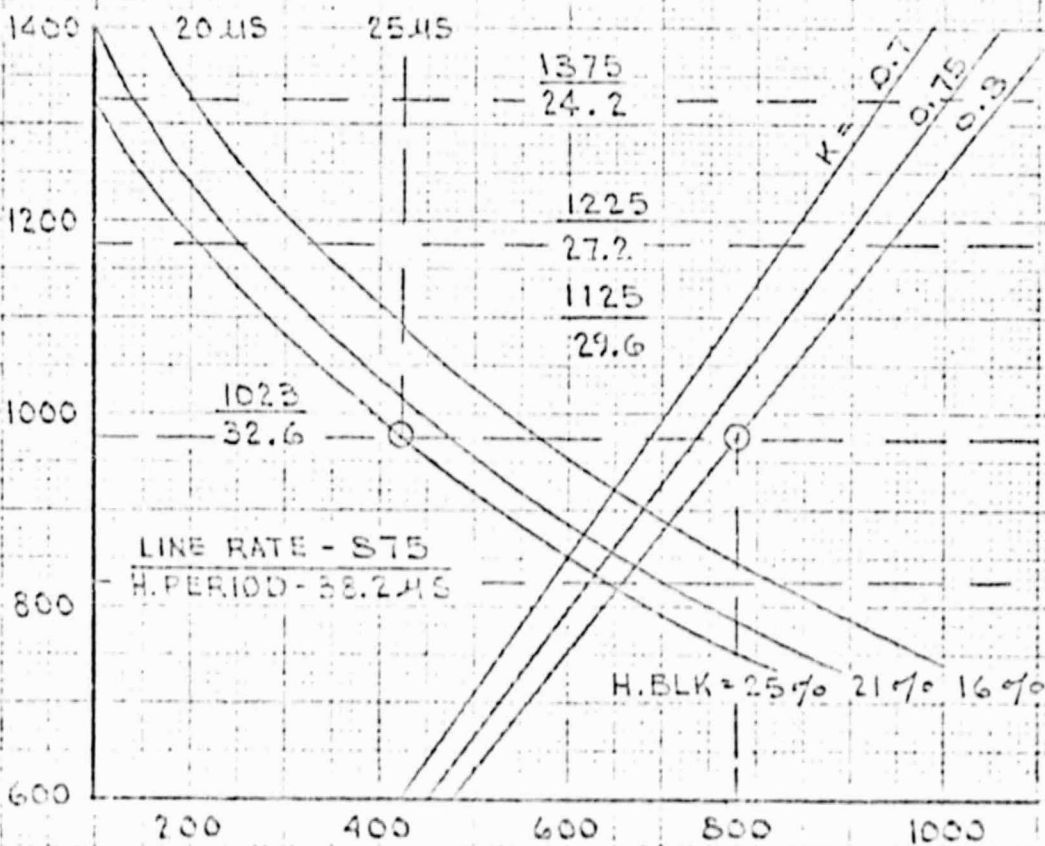
RESOLUTION-TV LINES/DISPL HEIGHT



ACTIVE LINE PERIOD -  $\mu$ S

FIG 4.5.4.A VIDEO RESOLUTION VS ACTIVE SCAN

ACTIVE SCAN LINES / FRAME



RESOLUTION-TV LINES / DISPLAY WIDTH

FIG 4.5-4B ACTIVE SCAN VS RESOLUTION

### System Resolution

The previous discussion established the limiting display resolution within the FOV constraints of the optical probe. We must now consider the combined effects of the following:

- (1) Resolution of the optical probe and projection optics
- (2) Resolution of the camera tube
- (3) Defocusing of the optical probe

Figure 4.5-5 plots the MTF for the probe, projection lens, and camera tube. By comparing the MTF of these components it became apparent that the camera tube is the most significant factor limiting the on-axis resolution to 6.0 Arc Min/OLP.

Figure 4.5-6 compares the resolution of the probe, projection lens and video system as a function of semi-field angle. Probe resolution is based on measured data for the first developmental 140 degree probe produced by Farrand. Projection lens data is from the Pacific Optical Report 5601, and TV system resolution was established in the previous discussion. The curves of 4.5-6 show that the TV system is the primary element limiting the resolution over the full display field-of-view. However, probe resolution is near that of the TV system at full field. This will contribute to some additional loss of resolution in the extreme corners.

Figure 4.5-5 also includes defocusing MTF curves for a probe with a 1.0 MM entrance pupil. Curve E shows the MTF for 4 diopter defocusing. Limiting resolution at 15% relative amplitude is approximately 11 arc min/OLP which is comparable to current 36° X 48° displays operating at 625 lines. Additional curves and a discussion of diopteral defocusing is included in the Farrand Probe Report ER 580 which is included in Section V. Defocusing in diopters is defined as follows:

When the basic in-focus object distance is infinity,  
the defocusing in diopters is  $\text{Def.} = \frac{1,000}{\text{Object Distance In mm}}$

When the basic object distance is finite the defocusing  
in diopters is  $\text{Def.} = \frac{1,000}{\text{Focused Obj. Dist.}} - \frac{1,000}{\text{Defocused Obj. Dist.}}$

18-3  
Double 1/2 dit

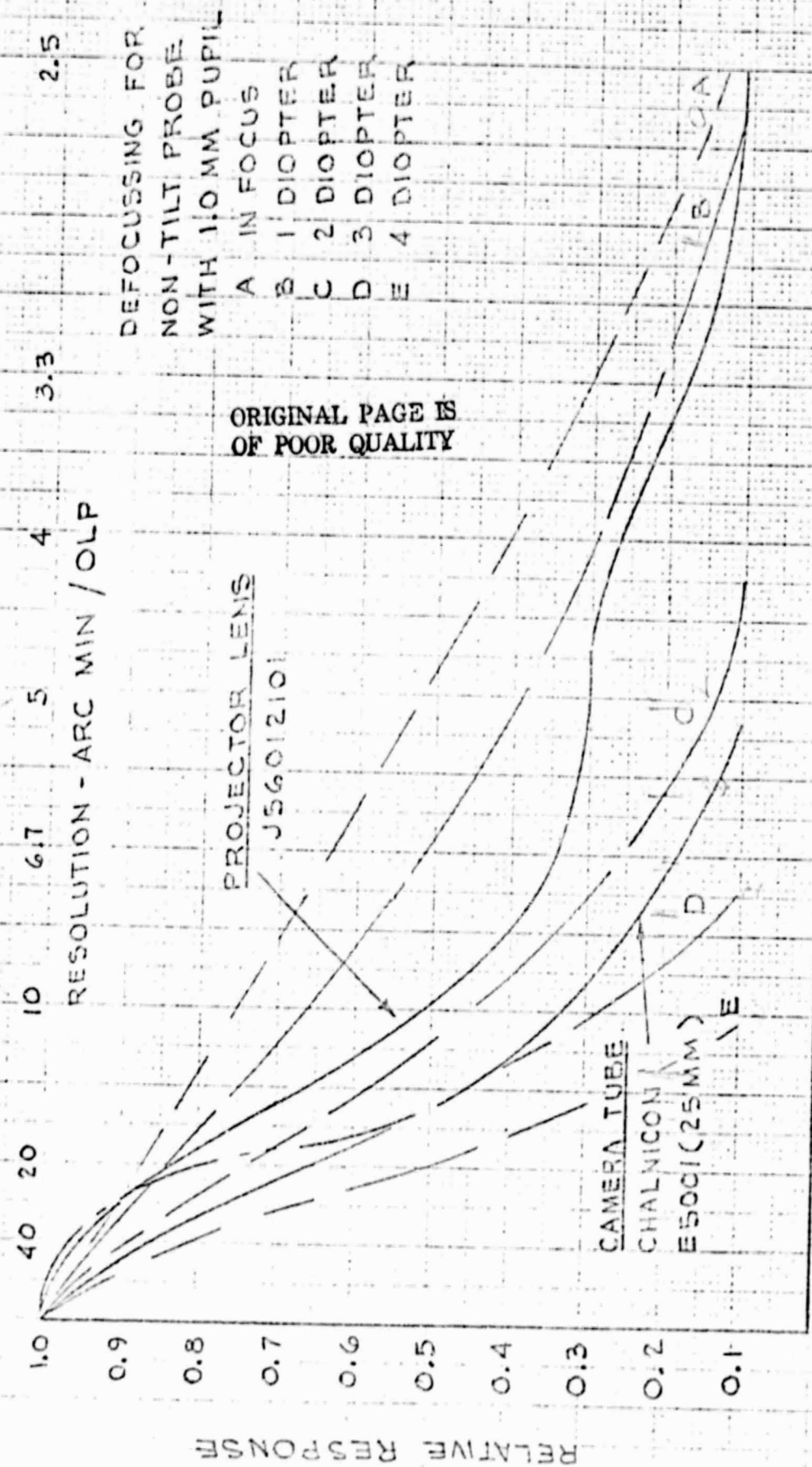


FIG 4.5-5 VARIATION OF MTF WITH FOCUSING

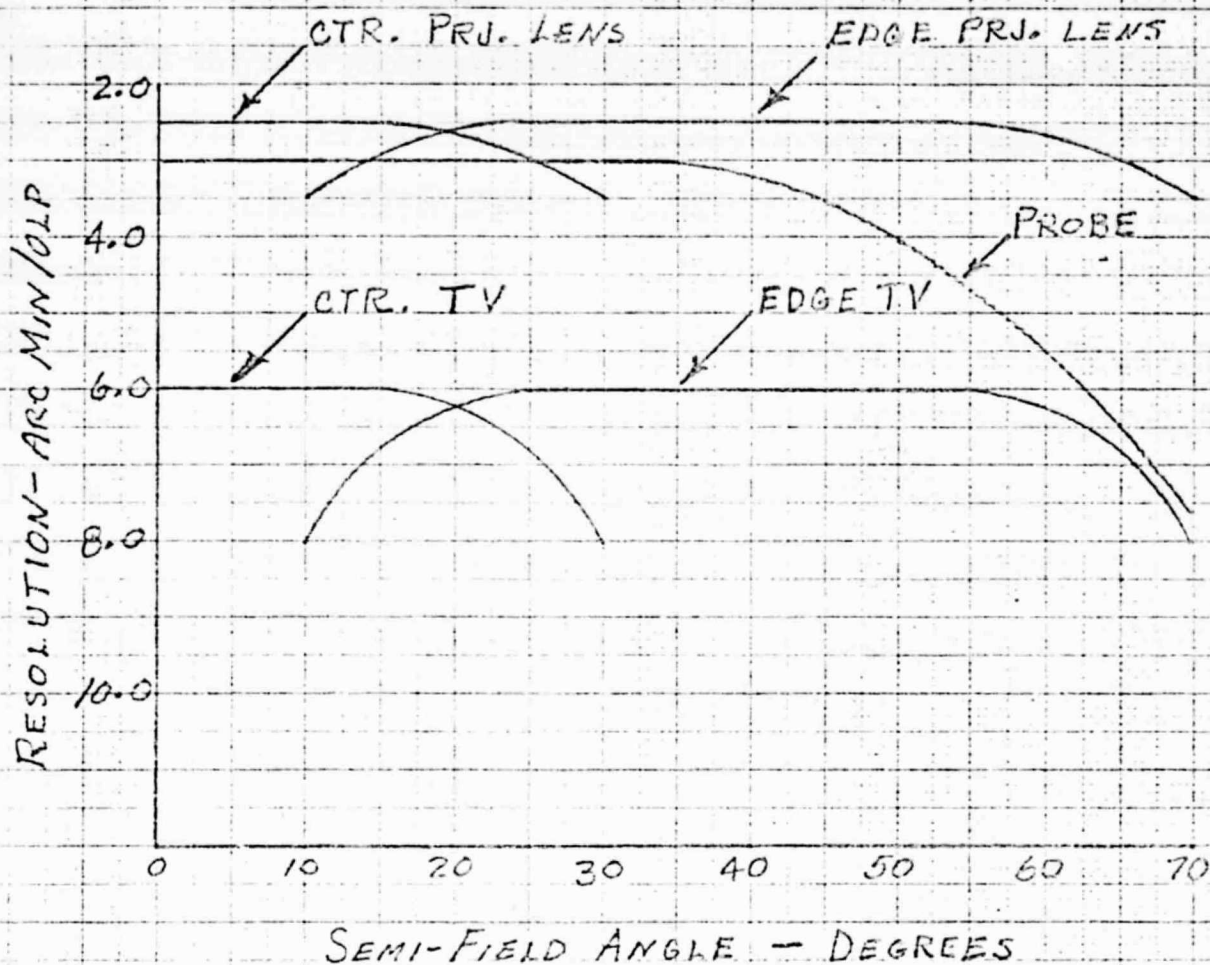


FIG. 4.5-6 RESOLUTION VS. FIELD-OF-VIEW

If the probe is focused at infinity, and an object is located 250 MM from the entrance pupil, defocusing will be 4 diopters. At model scale of 250:1, 250 MM corresponds to a scaled distance of 205 feet. Therefore, defocusing will vary from a maximum of 4 diopters at 205 feet to in focus at infinity. Resolution will vary from 11 Arc Min/OLP at 205 feet to 6 Arc Min/OLP (limited by the camera tube) at infinity. If the probe is focused at 205 feet defocusing will be 4 diopters or less from 100 feet to infinity, and would be 8 diopters at 68 feet. Resolution would then be 22 Arc Min/OLP at 68 feet. This would indicate that there would be no apparent defocusing over the entire operating range using a non-tilt corrected probe with focus fixed at 205 feet. This was subjectively verified on a CH-47 simulator system which was using a non-tilt probe with focus fixed at 200 feet, with a model scale of 250:1.

*for 20'6 PTF*

*7 cmw ... 28*

ORIGINAL PAGE IS  
OF POOR QUALITY

#### 4.5.3 Brightness

Display system brightness for a real image CRT projection system is primarily determined by the following:

- (1) Projection CRT luminance
- (2) Projection lens clear aperature
- (3) Lens-to-screen distance
- (4) Lens transmission and screen gain
- (5) Display resolution requirements

The projection CRT triad described in paragraph 4.4 has the following measured performance:

- (1) Combined luminance of 40,300 foot lamberts on a 1 x 4 inch 262 line full white raster, with a nominal line width of 4.1 mil for the green CRT. Manuractures Measured Data.
- (2) Combined luminance of 51,000 foot lambert highlight on an average terrain scene with a full raster and with cooling applied. Line width was 3.5 mil - in house measured data.

The projection lens described in the Pacific Optical Report 5601 in Section V has the following characteristics:

- (1) Focal length of 5.16 inches with a relative aperature of f/1.0.
- (2) The clear aperature diameter is the focal length/ f number of 5.16 inches
- (3) Transmission 80%

The projection screen has a reflectance of 90% and is located 150 inches from lens.

The on axis screen luminance in foot lamberts can be determined by the following:

$$B_L = B_S tR \sin^2 \theta$$

Where:

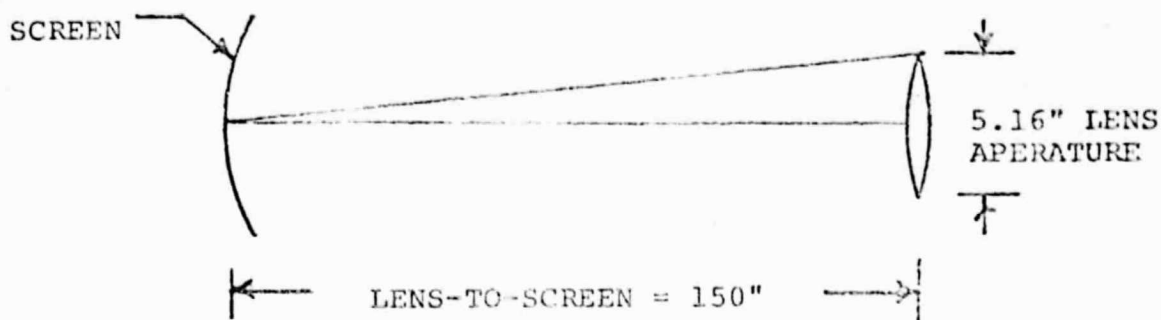
$B_L$  = Screen lumiance in foot lamberts

$B_S$  = CRT lumiance in foot lamberts

$t$  = Lens transmission

$R$  = Screen reflectance

$\theta$  = Semi-angle subtinded by the clear  
aperature at the screen



For an average scene CRT highlight lumiance of  $51 \times 10^3$  foot lambert.

$$B_L = 51 \times 10^3 \times .8 \times .9 \times \left( \frac{2.58}{150} \right)^2$$
$$= 10.86 \text{ foot lamberts}$$

From the above it is apparent that a screen lumiance (average scene highlight) of 10 foot lamberts is attainable with at least one set of CRT's. Figure 4.5.7 shows the relationship of screen lumiance to CRT lumiance for various lens aperatures. With an  $f/1.0$ , 5.16 inch lens and a standard 1 X 4 inch full white raster, 7.2 foot lambert screen lumiance is attainable with the required 3.3 mil line width. Descresasing the aperature to 4.3 inches ( $f/1.2$ ) reduces the screen brightness to 5 foot lamberts under the same operating conditions. Wide angle,  $f/1.2$ , projection lenses currently in use have essentially the same optical characteristics as the afore mentioned  $f/1.0$  lens. However, the  $f/1.2$  lens is smaller and approximately 37 lbs. lighter than the  $f/1.0$  lens.

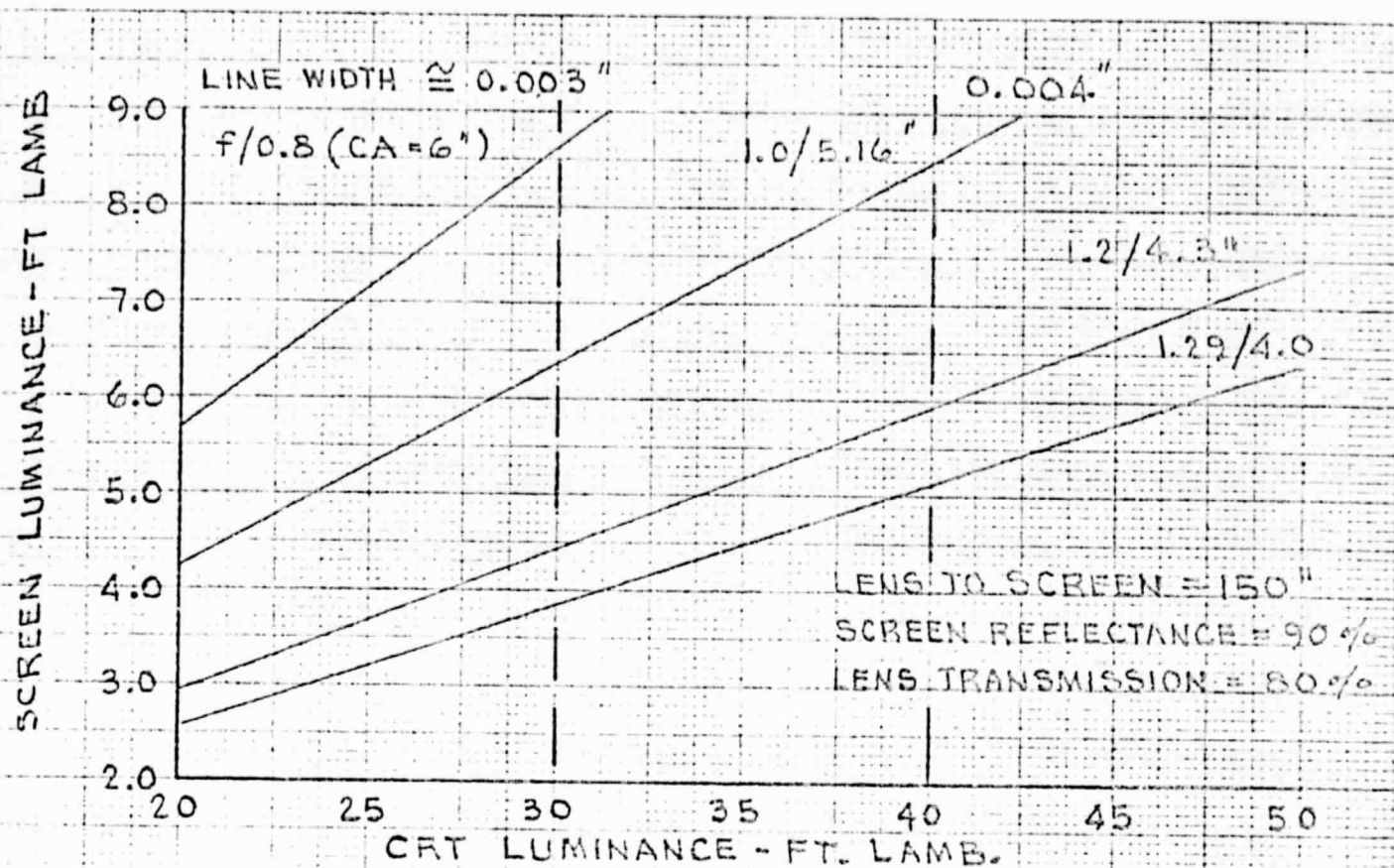


FIG 4.5.7 A SCREEN LUMINANCE VS CRT LUMINANCE

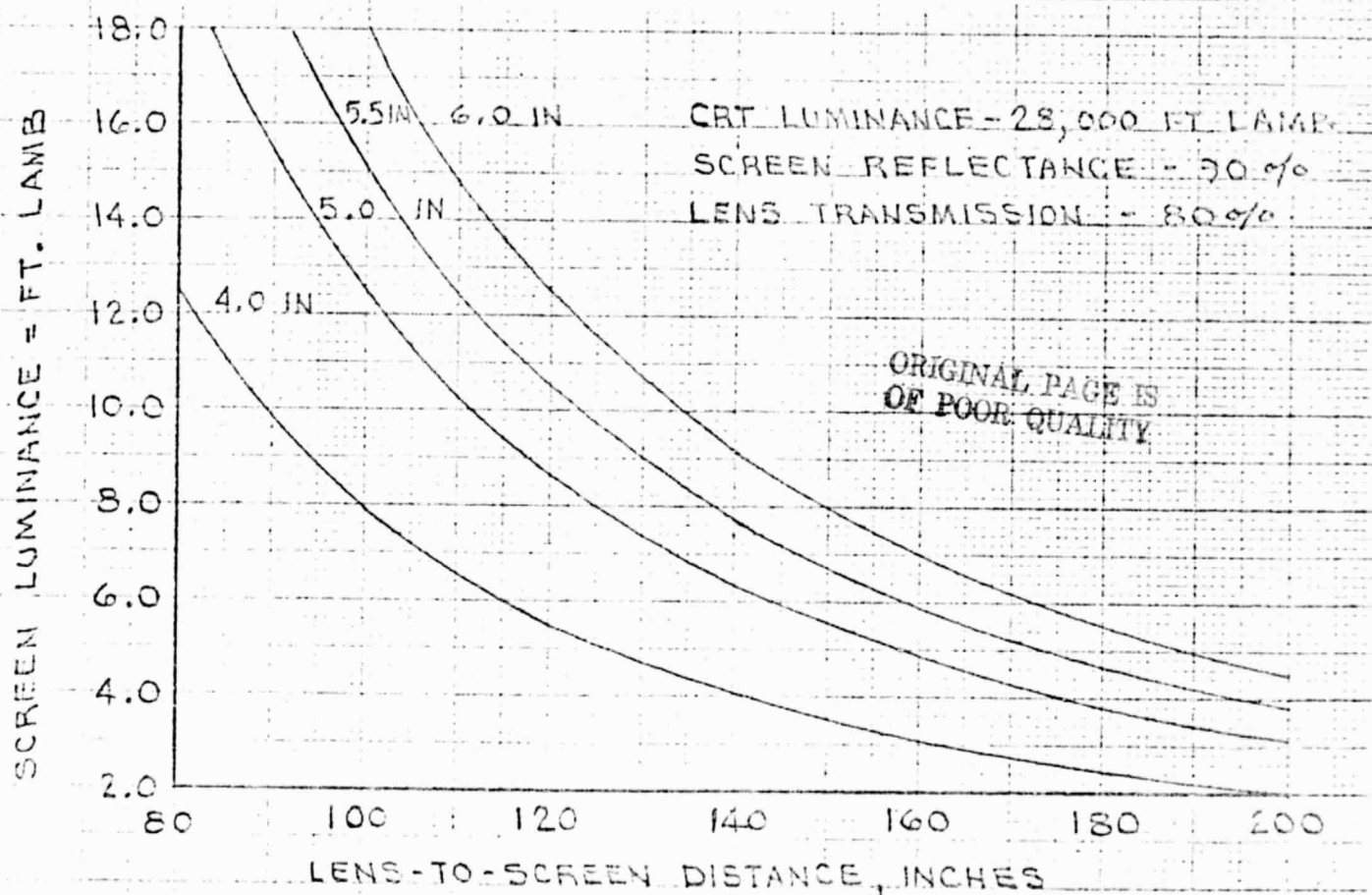
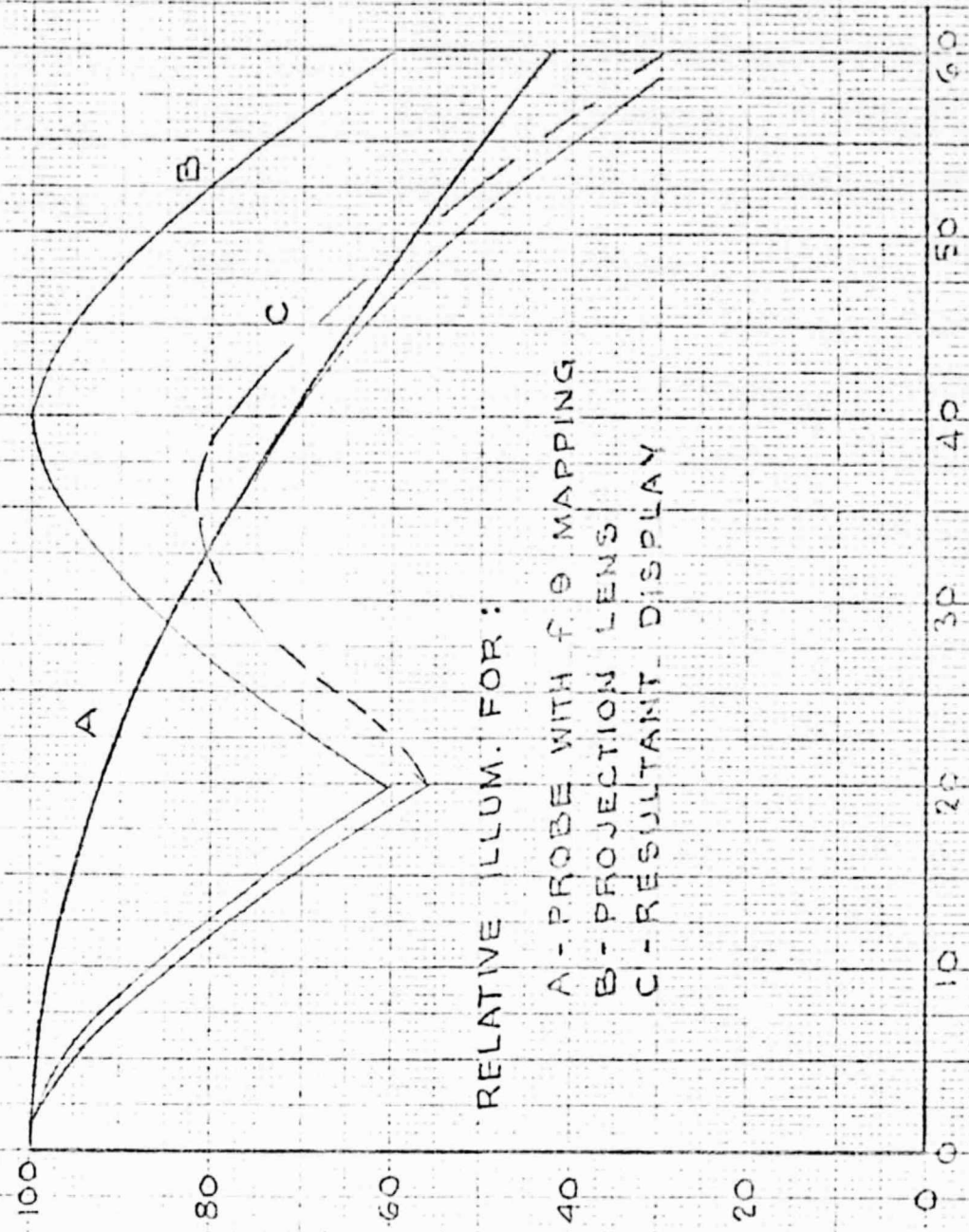


FIG 4.5.7 B SCREEN LUMINANCE VS. LENS-TO-SCREEN DISTANCE

#### 4.5.4 Relative Illumination

The relative illumination over the total display FOV is determined primarily by the relative illumination of the probe and projection optics. The mapping function chosen for the probe is  $h' = f \theta$  where the image height ( $h'$ ) is a linear function of the semi-field angle ( $\theta$ ), given a focal length  $f$ . The relative illumination for this mapping is much better than the distortionless  $h' = f \tan \theta$  mapping. Figure 4.5-8 curve A shows relative illumination for the probe ( $f \theta$  mapping), curve B relative illumination for the projection optics, and curve C is the resultant display relative illumination as seen by the viewer. Curve C shows that illumination is within 100% to 55% for a semi-field of 50 degrees, and has a maximum fall off to 30% at 60 degrees. This appears quite acceptable when compared with 60 degrees systems have 50% illumination at a semi-field of 30 degrees, and with distortionless probes that fall off to less than 10% at a semi-field of 60 degrees.



RELATIVE ILLUM. FOR:

- A - PROBE WITH f. θ MAPPING
- B - PROJECTION LENS
- C - RESULTANT DISPLAY

SEMI-FIELD ANGLE - DEG.  
ILLUMINATION VS. FIELD ANGLE

FIGURE 4.5-2

RELATIVE ILLUMINATION

ORIGINAL PAGE IS  
OF POOR QUALITY

#### 4.6 COCKPIT RELATED VISIBILITY STUDIES

Although the cockpit per se was not considered part of the visual display system - layouts and plots were made to establish the overall cockpit envelope and to analyze cockpit frame occlusions to the projected terrain imagery as seen by the pilot(s).

##### 4.6.1 Cockpit Configuration

The cockpit general arrangement, shown on drawing PD300, was developed from information provided by AMRDL - (dated 11-2-76) Cockpit Envelope/Crew Station Anthropometry. The purpose of the general arrangement drawing was to define a cockpit envelope in terms of visibility and occlusion to the projectors. The cockpit frame layout, shown on drawing PD102 and figure 2.2-4 was developed from information provided by AMRDL - (dated November 1973) USAAVSCOM Technical Report 73-1, pages 3-135, Theoretical OH/UH Configuration. The cockpit frame layout was developed to support the visibility and occlusion analysis described in the following paragraphs.

##### 4.6.2 Visibility and Occlusion Plots

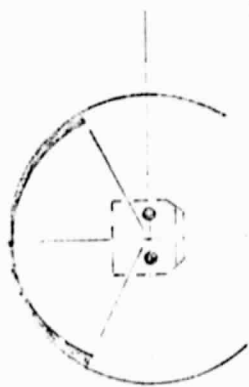
Layouts were developed on drawing PD102 for the purpose of analysing and optimizing the effects of cockpit frame occlusions to the projected terrain imagery. The frame occlusions were plotted on visibility diagrams, shown in Figures 4.6.2-1, 4.6.2-2, 4.6.2-3, 4.6.2-4, 4.6.2-5, and 4.6.2-6. The visibility plots were developed from information provided by AMRDL - (dated November 1973) USAAVSCOM Technical Report 73-1, figure 3.3.5-7A, page 3-112, UH-1H Pilot Visibility Plot. The display field-of-view and occlusions were superimposed on the visibility diagrams as seen by the pilot(s) from various cockpit lateral positions with and without projector roll. Occluded areas are identified on the plots by cross hatching with respect to the projector lens(es) occluded.

The visibility plots show that the canopy does not cause severe occlusions within the area of the field-of-view visible to the pilot(s). The only significant occlusion caused by the canopy is to the beam emanating from the lower lens. In an RGB color system this does not represent total occlusion of the display, however, it does vignette one color channel. Considering the contribution of luminous flux

#### 4.6.2 Visibility and Occlusion Plots (continued)

from each color channel; it is apparent from Table 4.4.3-1 that the luminous flux from the blue channel is a very small percentage of the total. Therefore, by producing the blue image with the lower lens results in very little change in the final image due to vignetting. At the most it will result in a slight change in tint of the image in the area where the blue channel is occluded.

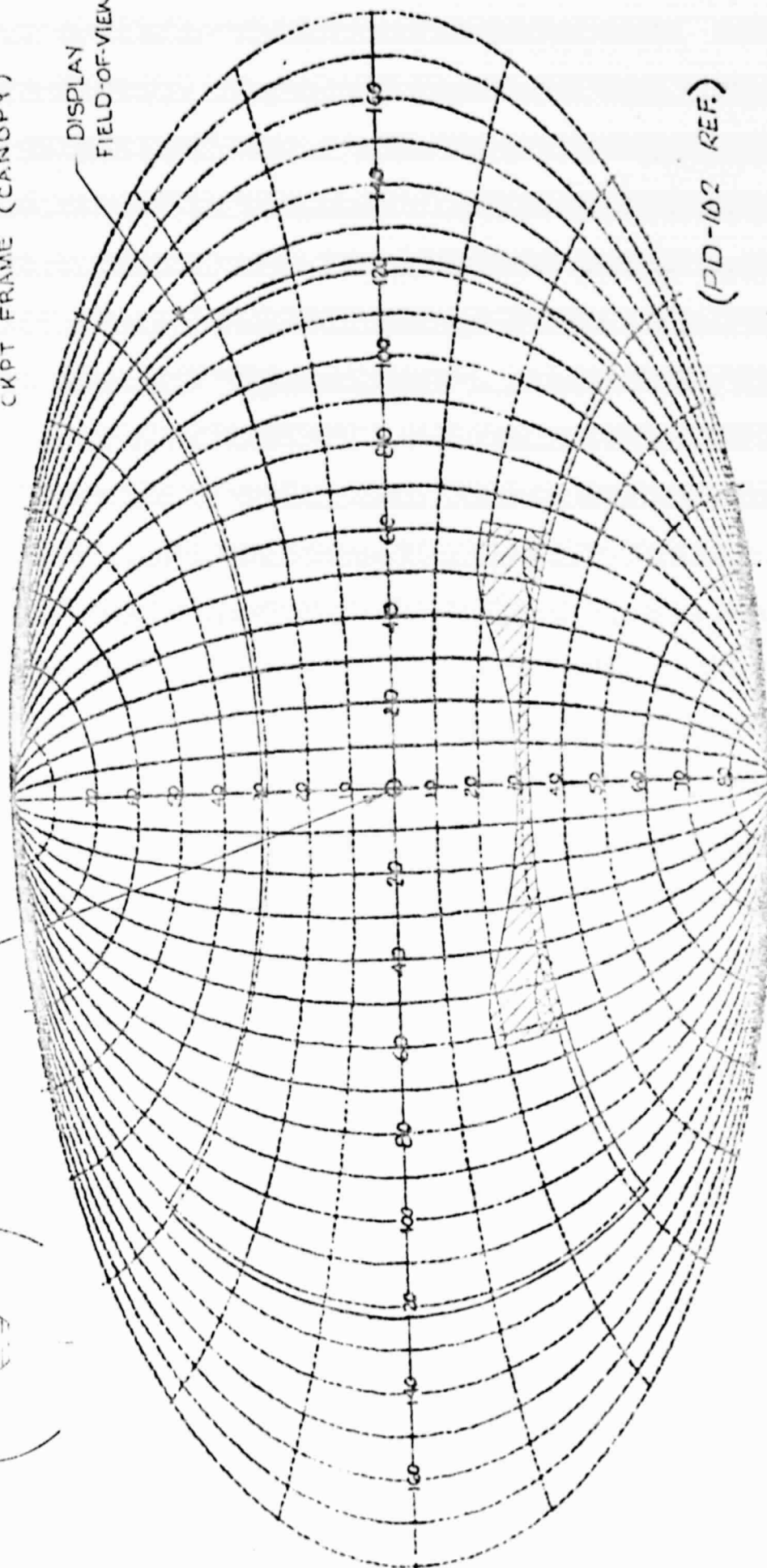
Q OF SCREEN



- NO-OCCLUSION
- LOWER LENS ONLY
- LOWER & CENTER LENS
- PROJ. LENSES OCCLUDED BY CKPT FRAME (CANOPY)

THEO. CENTER OF SCREEN

DISPLAY FIELD-OF-VIEW



(PD-102 REF.)

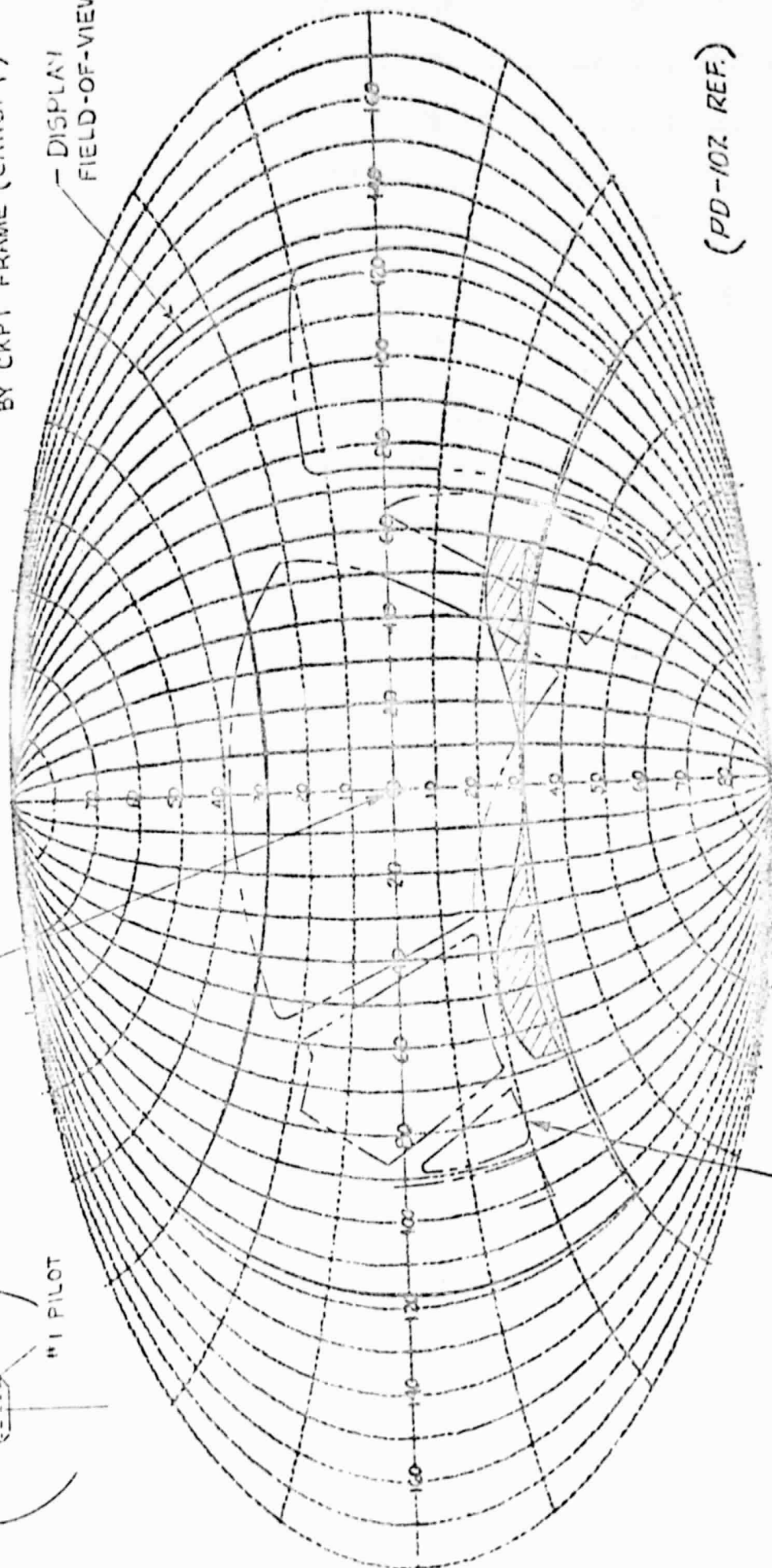
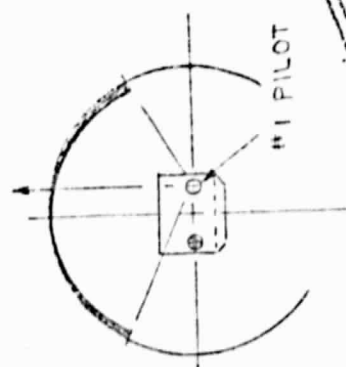
VISIBILITY AND OCCLUSION PLOT  
(COCKPIT FRAME OCCLUSION TO PROJECTORS —  
AS SEEN FROM THE CENTER OF THE COCKPIT)  
CANOPY VISIBILITY PLOT OMITTED FOR CLARITY

FIGURE 4.6.2-1

- NO OCCLUSION
- LOWER LENS ONLY
- LOWER & CENTER LENS
- PROJECTOR LENSES OCCLUDED BY CKPT FRAME (CANOPY)

— DISPLAY  
FIELD-OF-VIEW

#1 PILOT'S EYE POSITION  
(LOCATED 16" TO THE RIGHT  
OF SCREEN CENTER)



(PD-10Z REF.)

+ #1 (RIGHT) PILOT'S  
VISIBILITY PLOT  
(UH-1H REF)

VISIBILITY AND OCCLUSION PLOT

(COCKPIT FRAME OCCLUSION TO PROJECTORS -  
AS SEEN BY #1 PILOT LOCATED 16" RIGHT OF SCREEN CENTER)

FIGURE 4.6.2-2

— 1000000 —

- NO OCCLUSION
- LOWER LENS ONLY
- LOWER & CENTER LENS
- PROJ. LENSES OCCLUDED BY CKPT FRAME (CANOPY) +

HORIZON LINE  
#1 PILOT'S EYE POSITION  
(AT SCREEN CENTER)

#1 PILOT

(PD-102 REF.)

UH-1H HELICOPTER

#1 PILOT VISIBILITY PLOT

(REF FIG 3.3.5-7A)

(TECH REPORT 73-1)

VISIBILITY AND OCCLUSION PLOT

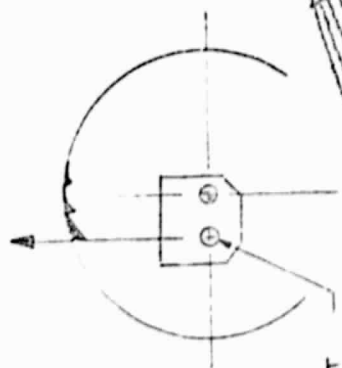
(COCKPIT FRAME OCCLUSION TO PROJECTORS -

AS SEEN BY #1 PILOT LOCATED AT SCREEN CENTER -


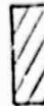
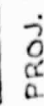
(PD-102 REF.)

FIGURE 4.6.2-3

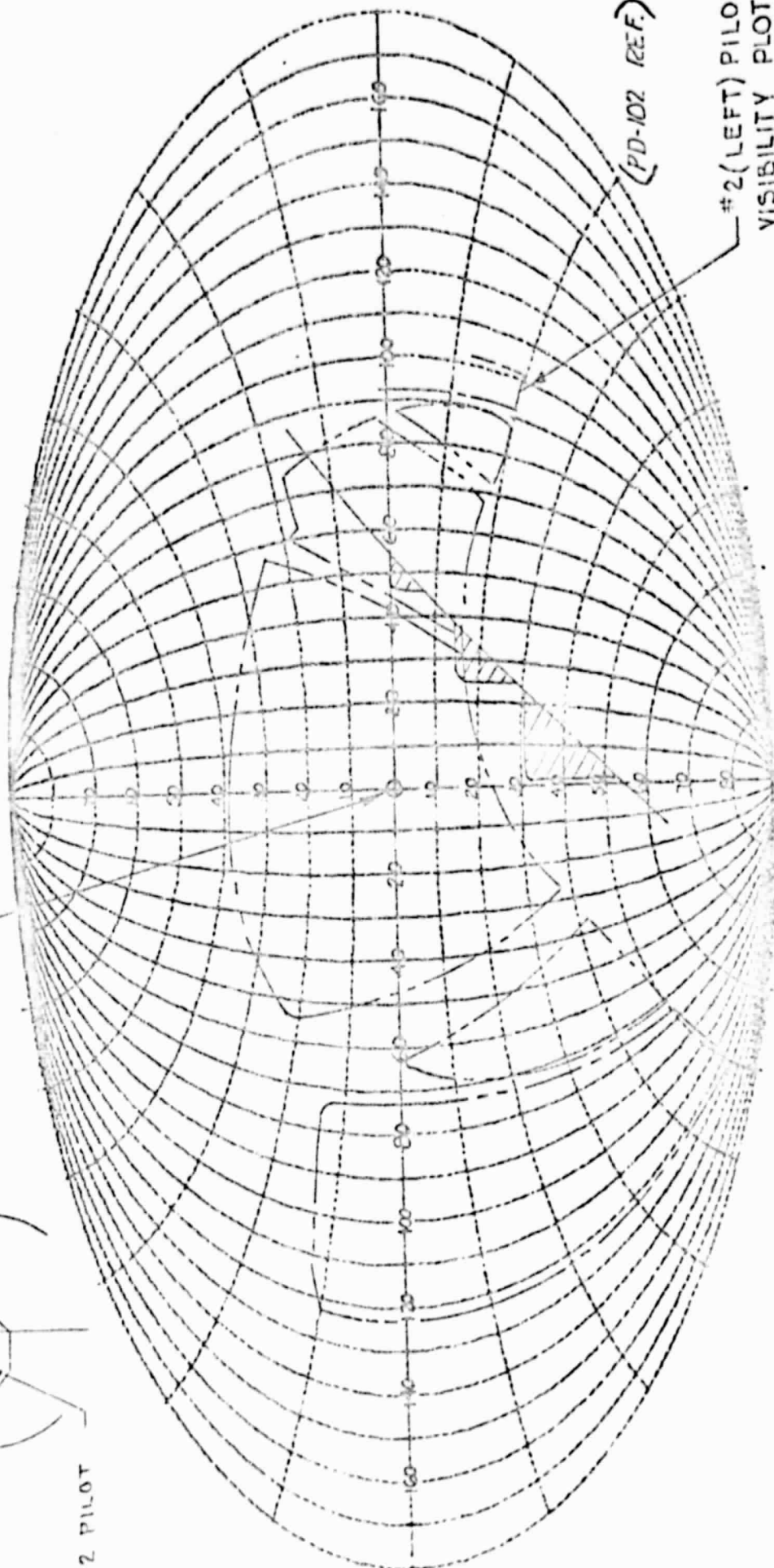
ORIGINAL PAGE IS  
OF POOR QUALITY



#2 PILOT

-  NO OCCLUSION
-  LOWER LENS ONLY
-  PROJ. LENS OCCLUDED BY CKPT FRAME (CANOPY)

#2 PILOT'S EYE POSITION  
(LOCATED 32" TO LEFT OF  
SCREEN CENTER)



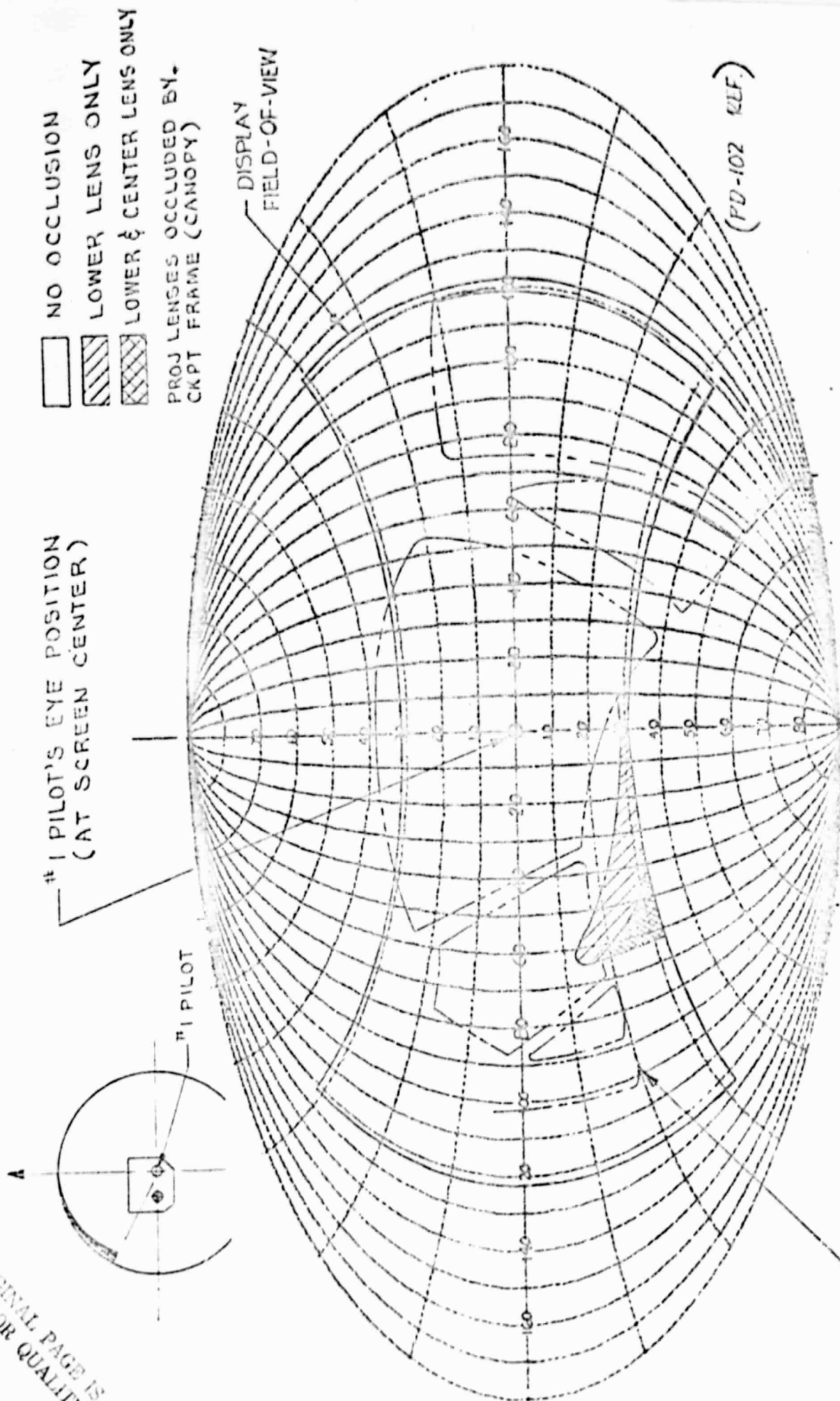
#2 (LEFT) PILOT'S  
VISIBILITY PLOT  
(UH-1H REF)

(PD-102 REF)

VISIBILITY AND OCCLUSION PLOT  
(COCKPIT FRAME OCCLUSION TO PROJECTORS -  
AS SEEN BY #2 PILOT LOCATED 32" LEFT OF SCREEN CENTER  
WORST CASE PROJECTORS ROLLED LEFT)

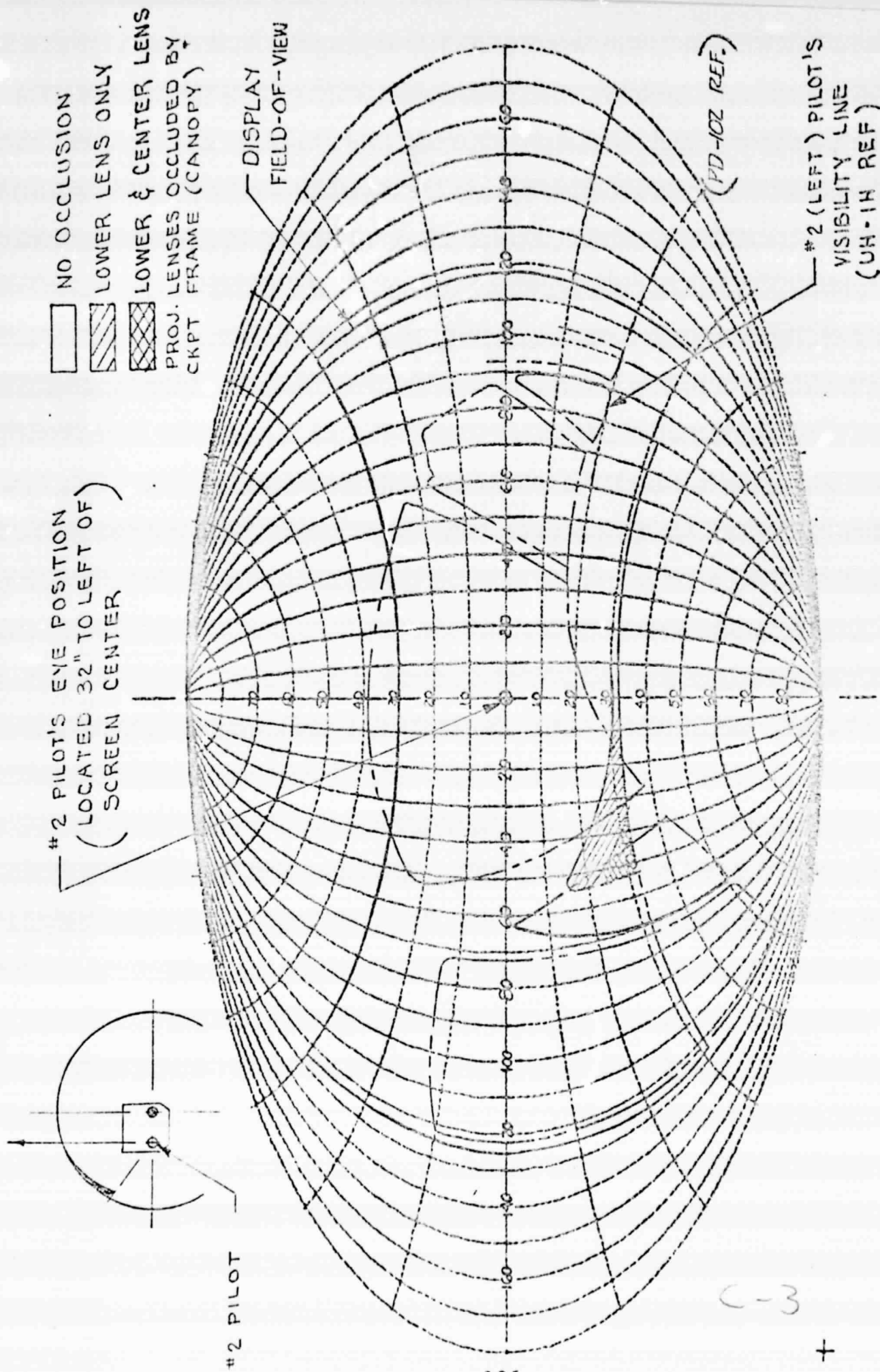
FIGURE 4.6.2-4

ORIGINAL PAGE IS  
OF POOR QUALITY



UH-1H HELICOPTER  
1" PILOT VISIBILITY PLOT  
REF FIG 3.3.5-7A  
TECH REPORT 73-1  
VISIBILITY AND OCCLUSION PLOT  
(COCKPIT FRAME OCCLUSION TO PROJECTORS -  
AS SEEN BY 1 PILOT LOCATED AT SCREEN CENTER)

FIGURE 4.6.2-5



# VISIBILITY AND OCCCLUSION PLOT

(COCKPIT FRAME OCCULSION TO PROJECTORS -  
AS SEEN BY #2 PILOT LOCATED 32" LEFT OF SCREEN CENTER)

- NO ROLL -

FIGURE 4.6.2-6

#### 4.7 Head Slaved Yaw

Some NOE and hovering flight tasks require that the pilot(s) be provided with detailed information to at least  $\pm 90$  degrees. Because of the field-of-view (FOV) constraints imposed by the probe, this is not feasible with a fixed display FOV. This constraint has resulted in the decision to pursue the Head-Slaved-Area-Of-Interest (HSAOI) approach. This approach requires that the look point line-of-sight (LOS) of the probe and display be positioned simultaneously with respect to the pilot's LOS. This permits the displayed FOV window and the information within the FOV to be correctly orientated with respect to the pilot's LOS.

The following approaches that could provide this capability were considered.

- (1) Dynamic continuous servo positioning of the probe and projector LOS
- (2) Continuous servo positioning of the probe LOS and continuous translation of video information between contiguous up display segments.
- (3) Servo positioning of the probe LOS in discrete steps and switching the video information between contiguous displays.

The first approach was studied in some detail prior to this study. Laboratory investigations were conducted on LAMARS at Northrop, and implementation of the technique was integrated into a simulator program at WPAFB. The most significant observations and conclusions from this work are listed below.

- (1) Synchronization - The probe and display control systems synchronization must be extremely precise. If precise synchronization is not achieved, unwanted and distracting movements of the image will occur.
- (2) Image Matching - Matching of the probe and display FOV and distortion characteristics is an important requirement. Lack of accurate matching will result in unwanted movement of some parts of the image with other parts being stable.

#### 4.7 (continued)

- (3) Dynamic Resolution - Resolution is reduced when the probe FOV and display window are moving. This is primarily dependent on the camera tube lag and the field rate of the video system. This is most critical for search and target detection and identification tasks. For these tasks the maximum resolution capability of the display system is required.

Considering the above, it is apparent that degradation of the display can occur during head movements beyond the small hysteresis band. This may not be too serious for the primary pilot (pilot with head slaving) as he may not be fixating on objects during head movement, however, the secondary pilot will receive the full effect of any image degradation as he is free to fixate on any part of the display FOV.

Another potential problem with this approach for the helicopter simulator is the practicability of providing the projector yaw control system power and control system performance required. For this reason a second approach is discussed in the following paragraphs.

In the second approach the probe is positioned the same as previously described. The five display projectors are used to provide the total head slaved FOV. The detailed information normally displayed by the central projectors would be continuously translated from one display to another through video processing. Although this eliminates the requirement of rotating the projector hardware, the video processing is complicated and may produce objectionable discontinuities. The image degradations previously discussed are essentially the same for this approach.

After considering the potential problems associated with the previous techniques a third approach was considered. This approach requires rapid displacement of the probe LOS and at the same time switching of the display video of each projector to the adjacent projector. The advantages of this approach over those previously discussed are as follows.

#### 4.7 (continued)

- (1) The image quality is not compromised or degraded, except when head slaving is actually required, and then only for milli-seconds.
- (2) Head slaving is only initiated when the pilot is required to see past 120 degrees. This permits head movement of  $\pm 45$  degrees before head slaving is required. Therefore, movement of the display window is held to an absolute minimum.
- (3) Mechanization of this approach is simple and does not require expensive video electronics or control system equipment.

Laboratory investigations of the discrete stepping approach were conducted. The probe roll and heading slew rate, for 40 degrees displacement was measured on an older design Farrand probe. The slew rate was found to be  $200^{\circ}/\text{sec}$  or  $40^{\circ}$  in 200 ms which corresponds to 6 TV frames. The current design probes use higher performance D.C. servos which should result in a significant improvement in the attainable slew rate.

#### 4.8 Conclusions and Recommendations

The analyses presented in Section 4.0 establishes a reasonable confidence level that in most areas, the predicted performance for the wide-angle visual system design is achievable. In some cases, where high risk components are combined into a subsystem design, system performance is more difficult to predict. Further analysis in these cases, is recommended prior to the preliminary design phase and is discussed in this section as related to the following categories.

- (1) Areas which do not represent a high technical risk, but require additional analysis to provide a more definitive preliminary design specification.
- (2) Components currently in development stage which represent a high technical risk and require further evaluation.
- (3) Laboratory test and additional analysis to substantiate that the predicted performance is attainable.

##### Modelboard/Probe

Additional analysis in this area should not be required since current modelboard designs are compatible with the physical characteristics of wide-angle optical probes currently in use and adequately provide the surface detail, terrain gradient, and stability required for helicopter simulation. However, as related to category 3, a cost effective method of mapping the modelboard at the time of fabrication should be analysed. The recommended computer-controlled probe protection concept requires that this map be provided in a digital form to be compatible with the probe protection computer. A procedure has been outlined by Piper Model Ltd. in conjunction with Hunting Surveys Ltd. that appears to provide this capability.

The procedure involves taking stereoscopic pairs of photographs and digitizing the features in a photogrammetric stereo-plotter which provides an output on digital tape. This procedure also falls into category 3 and validation by a vendor test is recommended.

### Control Systems and Structural Dynamics

The control system and structural design of the image generation and display system utilizes conventional components and materials. Simulator control systems currently in use have performance characteristics comparable with the wide-angle visual system of the study. As related to category 1, it is recommended that the projector support structure be analyzed during the preliminary design phase for off-zero roll angles. This is required to insure that the support structure design will meet the natural frequency requirements of the wide-angle visual system. The impact of using heavier projection optics should also be considered at the same time.

### Probe Protection

It is concluded that software and hardware requirements for probe protection have been adequately defined. The effectiveness of this approach is primarily dependent on obtaining an accurate map of the modelboard as previously discussed.

### Final Display Image Quality

A critical part of the visual system affecting the image quality of the final display is the probe/camera subsystem. Probe mapping distortion must be corrected in the camera using complex raster shaping. Resolution of the optical probe is much lower than high quality camera lenses and has a significant effect on the system MTF. A wide angle segmented probe and three camera chainicon TV system being developed by Farrand and SRL is nearly operational. The performance requirements of this equipment are similar to the requirements of the wide angle visual system of the study. The SRL Farrand system should be evaluated as related to category 2, during the preliminary design phase. Measured data should be obtained for the camera/probe combination. This should include on-axis and off-axis MTF, distortion, contrast, and dynamic resolution.

The display system affects image quality in a manner similar to the image pickup system, and is required to provide a wide angle display produced by mosaicked real image TV projectors. High brightness, high resolution CRT and compatible optics are required to produce good image quality. Raster shaping is necessary

to edge match these displays. A system using similar components with similar display requirements is being developed at Northrop. This system should be evaluated and measured data should be used to validate predicted display system performance.

Availability of performance data for the image pickup and display subsystems should make it possible to predict end-to-end display performance with a high level of confidence.

#### Cockpit Visibility

Cockpit related visibility studies appear adequate to establish the display field-of-view and occlusions as seen by the pilot. Additional study should only be required if a tandem cockpit arrangement is considered.

#### Head Slaved Yaw

Feasibility of head slaved yaw has only been demonstrated with a minimal laboratory test. A relatively simple test could be implemented prior to the preliminary design phase which would better demonstrate this concept. Head position could be sensed and the display as seen by the pilot could be slaved to the pilot head motion.

#### System Accuracy

Absolute accuracy of all current model/camera systems is questionable. Determining the position of a point on the model from position commands or feedback signals will probably not be better than 0.3 degrees. The principal source of this error is runout in the probe roll prism or mirror. Other errors that contribute to system accuracy are gantry positioning, video stability, and projector pointing. A system accuracy of 0.3 to 0.5 degrees is acceptable for certain tasks. However, for weapon delivery scoring an accuracy of three arc, min. is usually desirable. Providing this level of system accuracy improvement is probably not practical. It is recommended that for weapon delivery scoring, a system be utilized which determines mis-distance of the displayed target relative to the sight pipper at the time of weapon release.